Learning Power Flow Models and Constraints from Time-Synchronised Measurements: A Review

Rahul K. Gupta*, Paolo Attilio Pegoraro†, Ognjen Stanojev‡, Ali Abur§, Carlo Muscas†
Gabriela Hug‡, Mario Paolone**

***Abstract*—Key operational and protection functions of power systems (e.g., optimal power flow scheduling and control, state estimation, protection, and fault location) rely on the availability of models to represent the system's behavior under different operating conditions. Power systems models require knowledge of the components' electrical parameters and the system topology. However, these data may be inaccurate for several reasons (e.g., inaccurate information of components datasheets and/or outdated topological information). The deployment of time synchronization in phasor measurement units (PMUs) and remote terminal units (RTUs) enables the collection of large datasets of synchronised measurements to infer power systems models and learn associated power flow constraints. Within this context, this paper presents a comprehensive review of measurement-based estimation methods for power flow models using time-synchronised measurements. It begins by exploring advancements in time dissemination technologies and the characterization of uncertainties in PMUs and instrument transformers, along with their implications for parameters estimation. The paper then examines the power system parameter estimation problem, highlighting key techniques and methodologies. In the following, the paper focuses on measurement models for state-independent power flow model estimation, including line parameters, admittance matrices, topology, and joint state-parameter estimation. Finally, the review discusses recent approaches for estimating state-dependent power flow models, with particular reference to linearized power flow approximations in view of their large use in control applications.**

***Index Terms*—Power system parameter estimation, Admittance estimation, Line-parameters, Synchrophasor measurements**

I. Introduction

Fundamental operational and protection functions of the power system rely on the availability of reliable models enabling the characterization of the grid behavior under different operating conditions [1], [2]. These models are used in a number of applications such as: state estimation [3], [4], optimal power flow (OPF)-based scheduling and control (e.g. [5], [6]), fault location (e.g. [7]), protection (e.g. [8]) but often require the accurate knowledge of the system's topology and parameters of the connected devices. Usually, these parameters are derived from manufacturers' datasheets [9]. However, the actual parameters can be quite different from the nominal values due to various reasons, such as: inaccurate information on the datasheet, miscalibration, or outdated parameters due to aging (e.g. shunt capacitance of coaxial power cables), influence of weather and environmental conditions, etc. The inaccurate information on the grid parameters leads to erroneous modelling of the grid causing inaccuracy in the estimates of grid analysis tools such as power-flow, state-estimation [10]–[12], etc. Specifically, incorrect parameters could lead to sub-optimal or incorrect control actions, which might destabilize the grid under certain conditions. This is particularly critical in applications such as state estimation, dynamic stability control, and real-time operation, where accurate parameters are essential for reliable operational decisions. Ensuring parameter accuracy is thus a key aspect of maintaining grid stability and operational reliability. A survey of different issues caused by power system's parameters inaccuracies is given in [13].

In this context, measurement-based estimation of the grid parameters is widely proposed and discussed in the literature with the objective to infer reliable power grid models. Indeed, various functions relying on power flow analysis and/or state estimation, are generally carried out by transmission and distribution systems operators on specialized SCADA (Supervisory Control and Data Acquisition) platforms. These platforms depend on the availability of an accurate and up-to-date grid model to perform these analyses effectively. The methods reviewed in this paper are designed to enhance these computational processes by enabling their implementation in SCADAs as parallel routines. These routines can run alongside other SCADA processes, optimizing resource utilization and reducing computational delays. They can be initiated either manually, in response to a specific request from an operator, or automatically by the system itself when certain conditions, or triggers, are detected. Once a computational routine is completed, the results, including updated grid parameters, are automatically relayed to the operator. This step allows the operator to review and validate the output before applying any changes or taking further action, ensuring that the grid's operational integrity is maintained.

In general, measurement-based schemes for estimating the power-flow models can be broadly categorized into two types. The first type focuses on the estimation of the true physical branch/line parameters of the network to be used to formulate power-flow equations; these are referred to as *state-independent models* as they can be used for describing any power system operating state e.g., [14]–[19]. In the second type, the estimation schemes focus on estimating approximated linearized models, which are, by construction, *state dependent*

*School of Electrical Engineering & Computer Science, Washington State University, Pullman, 99163, USA (e-mail: rahul.k.gupta@wsu.edu).

†Department of Electrical and Electronic Engineering, University of Cagliari, 09123 Cagliari, Italy (e-mail: paolo.pegoraro@unica.it and carlo.muscas@unica.it).

‡Power Systems Laboratory, ETH Zürich, CH-8092 Zürich, Switzerland (e-mail: stanojev@eeh.ee.ethz.ch and hug@eeh.ee.ethz.ch).

§Department of Electrical and Computer Engineering, Northeastern University, Boston, MA 02151 USA (e-mail: abur@ece.neu.edu).

**Distributed Electrical Systems Laboratory, École Polytechnique Fédérale de Lausanne, 1015 Lausanne, Switzerland (e-mail: mario.paolone@epfl.ch).

models, e.g., [20]–[22].

Depending on the characterized uncertainty of the measurement, the choice of a suitable *estimation technique* also influences the estimation performance. Measurement-based parameter estimation schemes in power systems can rely on either Phasor Measurement Units (PMUs) or Remote Terminal Units (RTUs) providing, respectively, measurements of voltage and current synchrophasors or moduli of voltages, currents, and powers. Due to the accelerated deployment of RTUs and PMUs time synchronisation technologies, (synchronised) measurements are increasingly available from these devices which offer the possibility to derive advanced data-driven estimation schemes. At present, PMUs and RTUs are largely deployed in the transmission grid, however, multiple applications related to the monitoring and control of "active" distribution grids are emerging [23]. The power system parameters' estimation problem using time-synchronised measurements has several aspects that directly influence the estimation performance, mainly associated with the *uncertainty models* of the PMUs/RTUs measurements as well as their placement. The uncertainty may arise from different processes involved in the measurement, such as the adopted *time dissemination technology* or the *uncertainty characteristic* of the sensing infrastructure. Regarding the placement of PMUs and RTUs for state estimation problems under low-observability conditions, they have been extensively analyzed in the literature to guarantee a sufficient number of synchronised measurements ensuring full observability (e.g. [24]–[31]). Furthermore, optimal placement strategies may also aim to improve the system's resilience against leverage measurements[1] (e.g. [35], [36]) and potential cyberattacks (e.g. [37]), as well as to optimize the investments associated with deploying the measurement infrastructure (e.g. [38], [39]). In this respect, this review paper assumes that the system under study is equipped with a sufficient number of synchronised measurements to ensure full observability.

In this context, the paper reviews the state-of-the-art of measurement-based estimation methods of power flow models using time-synchronised measurements. The paper is organized as follows:

- Section II reviews the recent developments in the area of *time-synchronised measurements in power systems* starting from time dissemination technologies. Then, it discusses the *uncertainty characterization* of PMUs and instrument transformers (IT) and the associated models used in parameters estimation algorithms.
- Section III introduces the power system parameter estimation problem and reviews the most relevant *estimation techniques*.

[1]In state estimation, it is standard practice to distinguish between outliers and leverage points. Outliers are measurements that deviate from the statistical distribution of the other data, often caused by significant errors during acquisition, resulting in values inconsistent with the known properties of measurement noise (commonly referred to as "bad data"). Leverage points, on the other hand, are measurements that strongly influence the state estimator, causing the residuals to align closely with those values [32]. While leverage points may not inherently represent erroneous data, their impact on estimation becomes pronounced if they coincide with bad data, leading to significant deviations in the results [4], [33], [34].

- Section IV reviews the measurement models and their use in relation to the estimation of *state-independent power-flow models*, i.e., the estimation of the line parameters, admittance matrix, topology estimation, joint estimation of state and parameters, etc.
- Section V reviews the most recent approaches related to the estimation of the *state-dependent power-flow models* with particular reference to the linearized power flow approximation.

Finally, Section VI concludes the paper by summarizing the review, stating the open questions and directions for future works.

II. Time-Synchronised Measurements in Power Systems

Time synchronization is a key feature in modern power systems enabling the time alignment of measurements generated by geographically distant devices. These devices can be either RTUs providing measurements of moduli of voltages, currents, and powers, or PMUs providing measurements of voltage and current synchrophasors. For PMUs, time synchronization is also used to generate a unique reference for the measurement of the synchrophasors phase angle.

Without loss of generality, we recall the architecture of a synchrophasor network since similar characteristics also apply to time-synchronised RTUs-based measurement systems. The two main international standards for synchrophasor networks in power systems are IEC/IEEE 60255-118-1:2018 [40] and IEEE C37.118.2 [41]. On the basis of the content of these two standards, the architecture of a synchrophasor network is composed of four main layers whose specific function(s) are given as follows:

- *Time dissemination layer:* it provides to the PMU/RTU a reference time (clock) synchronised to the Coordinated Universal Time (UTC).
- *Sensing layer:* it includes the current/voltage sensors providing signals to PMUs and/or RTUs to estimate complex phasors of voltages/currents and/or other real quantities. The absolute time provided by the time dissemination layer is used to condition the internal clock of the PMU/RTU to time/phase align the measurements of electrical quantities.
- *Data communication layer:* it is responsible for encapsulating and streaming the PMU/RTU measurements according to a given standard data format (e.g., IEEE C37.118.2 [41]).
- *Data processing layer:* it collects and time-aligns the PMUs/RTUs data streams according to their time stamps and forwards them to the various applications.

In the following, we describe the first two layers as they are the main sources of errors in the measurements and affect the measurement-based estimation process the most.

A. Time dissemination technologies in power systems

RTUs and PMUs usually rely on the UTC made available by various time dissemination infrastructures. A Global Navigation Satellite System (GNSS), like the Global Positioning

System (GPS), is among the most adopted systems as it is characterized by a good cost vs. performance tradeoff [42]. However, the inherent vulnerability of the GNSS-GPS (e.g., [43]), the use of underground stations, time propagation from a master UTC-synchronised clock to multiple instruments, etc. may require redundant systems to be deployed over the legacy power systems telecommunication infrastructure [44] such as the Precision Time Protocol (PTP) [45] or the Synchronous-Ethernet based systems like the White Rabbit (WR) Time Protocol [46]. We briefly recall the general principles and performance of these two-time dissemination technologies.

GNSS-based systems rely on the availability of primary time sources available in satellites with known position in space. Each satellite streams to receivers specific messages containing the satellite's position (with respect to an arbitrary reference system) and the absolute time of the primary time source installed in the satellite. The receiver is capable of reading and parsing these messages to determine: (i) the receiver's position on the Earth's surface and (ii) the UTC time. Algorithms that receivers use to determine these quantities are generally based on the method first proposed by Bancroft in 1985 [47]. The typical time accuracy (3σ) of commercial GNSS-GPS receivers is in the order of ± 100 ns or higher.

PTP-based systems rely on a two-way communication layer where a "follower" clock is aligned to a "leader" clock. The leader clock periodically streams time-synch messages to the followers that reply with a delay request message. Subsequently, the leader's clock replies with a delay response message that, along with the time-synchronization and delay request messages, allows each follower's clock to compute its time offset and message propagation delay. The process relies on the fundamental hypothesis of symmetrical time delays of the above-listed messages. The main PTP standard is the IEEE Std. 1588 [45] and the so-called PTP version 2 (PTPv2) is characterised by a typical time accuracy (3σ) better than ± 1 µs. The evolution of the PTPv2 is the so-called WR that, thanks to time-deterministic Ethernet-based systems (i.e., the Synchronous Ethernet SyncE), can reach accuracy levels of ± 1 ns.

B. Measurements, sensing and uncertainty models

Every model and parameter estimation algorithm relies on input data represented by measurements provided by instruments installed in the field. All measurements are unavoidably affected by uncertainty that can be described by studying possible error sources associated with each measured value.

1) Measurement Chain: When dealing with a value that is the result of a measurement process, it is important to analyze the whole measurement chain leading to such value in order to quantify the associated uncertainty. A general scheme for a single synchronised phasor measurement is represented in Fig. 1 (a similar scheme is also valid for any synchronised measurement), where the analog signal x_p from the field (voltage or current of system phase p) is transduced through an instrument transformer (IT) and then, after analog conditioning, it is sampled and converted to digital values so that processing can take place to compute the measured synchrophasor $\bar{x}_p$ (which is produced at every reporting rate interval T_{RR} by the PMU[2]). Synchronisation is also the pervasive task that can be used to define the acquisition rate, the measurement instant definition and thus the timestamp associated with each measured value.

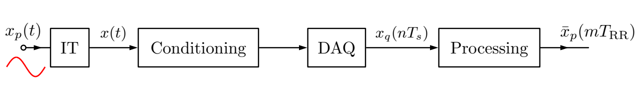

Fig. 1. Measurement chain for synchrophasors.

The different stages of the acquisition, conversion and measurement computation can be performed by different devices. For instance, there could be a stand-alone PMU with different channels, each connected to the output of a Voltage Transformer (VT) or Current Transformer (CT), but there could also be a Stand-Alone Merging Unit (SAMU) that acquires and digitises in a synchronised way the IT output to send "time-located" samples (sampled values) to a separate processing unit (distributed PMU architecture). Synchronisation can rely on internal modules only or on external connected devices (e.g., GPS receivers, PTP servers, etc.) as described in the previous section.

Independent of the specific design of the instrument, each of the functional modules are always present and every element in the chain contributes to the overall measurement uncertainty. Understanding the origin of the possible different error sources in each of these elements is useful to understand their impact on the overall synchrophasor uncertainty.

From another viewpoint, since ITs and PMUs must comply with their relevant product standards, it is important to understand how the accuracy specifications that characterize the different performance classes defined in such standards can be correctly translated into suitable uncertainty models to be used in the estimation procedures.

The most frequently adopted PMU standard for measurement specification is [40]. It is the result of significant changes over the years, starting from the IEEE 1344 standard [48] in 1995 and passing through the standards IEEE C37.118 [49], IEEE C37-118-1 [50] and the amendment IEEE C37.118.1a [51] in 2005, 2011 and 2014, respectively. These standards define the prescribed limits under different test conditions considering two classes: P, for protection applications, and M, conceived for operation in presence of wider variability ranges of relevant signal parameters and stronger disturbances. In particular, the limits for synchrophasor measurement are provided in terms of total vector error (TVE), i.e., of relative vector error magnitude for all the considered test cases. For instance, $1\,\%$ is the reference TVE limit for almost all the stationary

[2]The use of multi-channel PMUs is a common practice among grid operators to optimize the costs associated with deploying this technology. Regarding the identification problems discussed in this review, the single- or multi-channel nature of a PMU does not affect significantly the formulation and characterization of the various estimation problems. Indeed, the number of measured synchrophasors and the noise model of each individual measurement remains unchanged, as they are mainly determined by the current transformers (CTs) and voltage transformers (VTs) available in the substation and the measurement chain as shown in Fig. 1 remains unchanged in case of using a single- or multiple- channel PMU. Therefore, the considerations made regarding the measurement noise models made in this section are not affected by this aspect.

test conditions. This index mixes magnitude and phase angle errors, but further information on the individual contribution to measurement uncertainty can be typically found in PMU datasheets. In IEEE C37.242 [52], useful details are also provided on PMU installation, testing, calibration and possible error sources.

IT specifications are on the other hand covered by the IEC 61869 standards family [53]. In particular, the standards [54] and [55] give the limits of ratio and phase-angle errors for VTs and CTs, respectively, considering different accuracy classes and different ranges of the primary voltage or current. For example, Class 0.5 considers $0.5\,\%$ as the maximum magnitude error at rated voltage and current, while the maximum VT and CT phase-angle error in the same conditions are $0.6\,\mathrm{crad}$ ($1\,\mathrm{crad} = 10^{-2}\,\mathrm{rad}$) and $0.9\,\mathrm{crad}$, respectively.

When dealing with synchronised measurements performed by RTUs or meters, the complexity of the uncertainty description increases. Indeed, while synchronised instruments, such as Power Quality Meters (PQMs) at critical points of the networks, can provide timestamped measurements, their synchronisation accuracy is not as high as in PMUs. For instance, in the standard IEC 61000-4-30 [56] the most accurate class is Class A and requires a time-clock uncertainty that shall not exceed one nominal cycle, consequently phase-angle measurements cannot be provided. Commercial meters and RTUs based on Intelligent Electronic Devices may feature more accurate synchronisation systems, but there is another important aspect related to the measurement instant. RTUs and PQMs usually provide averaged quantities, such as root mean square (rms) measurements, and are not designed to measure dynamic signals. For this reason, the adopted observation window and the position of the measurement time instant within it are not always known or defined according to a standard, thus leading to higher uncertainty. In literature, this is tackled by increasing the nominal uncertainty [57] or by trying to mitigate the time skew [58], [59].

In [60], the impact of the entire measurement chain including ITs on the direct estimation (from voltage drop and current balance equations) of line parameters from PMU measurements is investigated. In the next section, the different types of errors and their influences are discussed.

2) Error models: relying on the aforementioned measurement chain, it is possible to give an error model for synchrophasor measurements that includes all the main sources. Focusing on voltage PMU output and separately considering the error contributions of IT and PMU, we have, for a generic measurement $\tilde{v}_h$[3]:

$$\begin{aligned}\tilde{v}_h &= \tilde{V}_h e^{j\tilde{\theta}_h} = \tilde{V}_h^r + j\tilde{V}_h^x = \\ &= (1+a_h^{\mathrm{IT}})(1+a_h^{\mathrm{PMU}})V_h^R e^{j(\theta_h^R + \Delta\theta_h^{\mathrm{IT}} + \Delta\theta_h^{\mathrm{PMU}})}\end{aligned} \tag{1}$$

where $\tilde{V}_h$ and $\tilde{\theta}_h$ are the magnitude and phase-angle measurements of the synchrophasor, while V_h^R and θ_h^R are the reference values (the sought "true" values). Parameters a_h^{IT} and a_h^{PMU} represent the ratio error, i.e., the magnitude relative errors introduced by IT and PMU, respectively. Phase-angle errors are better represented by the corresponding phase displacements $\Delta\theta_h^{\mathrm{IT}}$ and $\Delta\theta_h^{\mathrm{PMU}}$. A similar model can be adopted also for a generic current measurement. Considering, for instance, a branch current $i_{hk} = I_{hk}e^{j\phi_{hk}}$, with the same modelling approach, ratio and phase-angle errors for both CT and PMU current channel (b_{hk}^{IT}, $\Delta\phi_{hk}^{\mathrm{IT}}$, b_{hk}^{PMU}, and $\Delta\phi_{hk}^{\mathrm{PMU}}$, respectively) can be introduced.

[3] ~ indicates a measured value from here on.

When dealing with a realistic measurement chain under normal conditions, all the errors should be small and thus the ratio errors can be considered to sum up without second order effects. While this model does not provide any insights into the actual origin of each contribution (e.g., PMU synchronization errors are absorbed by $\Delta\theta_h^{\mathrm{PMU}}$ and $\Delta\phi_{hk}^{\mathrm{PMU}}$), it has the merit to distinguish between the errors induced by the instrument and the transducer that are typically from different manufacturers and have different specifications.

In the context of parameter estimation, these errors play a fundamental role. However, another distinction needs to be made between the nature of these errors, namely between random and systematic errors. Random errors are those that vary across repeated measurements of the same quantity under the same conditions, whereas systematic errors are constant (representing the average of the error). It is interesting to highlight that randomness is an abstraction of unpredictability and variability of errors with time and thus is just a model of uncertainty depending on the available knowledge. In the remainder of this paper, and in line with relevant power systems literature, the random contributions are also referred to as measurement noise.

Both ITs and PMUs can introduce both random and systematic errors. As a consequence, the errors can be decomposed as:

$$a_h^{\mathrm{IT}} = a_h^{\mathrm{IT,sys}} + a_h^{\mathrm{IT,rnd}} \tag{2a}$$

$$\theta_h^{\mathrm{IT}} = \theta_h^{\mathrm{IT,sys}} + \theta_h^{\mathrm{IT,rnd}} \tag{2b}$$

$$a_h^{\mathrm{PMU}} = a_h^{\mathrm{PMU,sys}} + a_h^{\mathrm{PMU,rnd}} \tag{2c}$$

$$\theta_h^{\mathrm{PMU}} = \theta_h^{\mathrm{PMU,sys}} + \theta_h^{\mathrm{PMU,rnd}} \tag{2d}$$

Hence, four error contributions are distinguished for magnitude and phase-angle measurements (superscripts *sys* and *rnd* refer to systematic and random contributions, respectively).

Some assumptions can be made to simplify the above expressions [61], [62]. For example, in ITs, systematic effects are typically prevailing. On the other hand, in the high quality PMUs currently available on the market, systematic contributions are often significantly smaller than the corresponding contributions in ITs, whereas their random contributions can be more significant.

The different nature of the errors leads to a different impact on the parameter estimation. Random errors are zero mean and are characterized by their probability distribution. Their influence on the estimates is reduced when multiple measurements corresponding to the same or similar conditions are used and random errors can be thus "averaged" or "filtered" to a given extent. Systematic errors are instead persistent and typically represent unknown quantities that affect the constraints used in the estimation algorithm. Indeed, Kirchhoff's current and voltage laws are the basis of the network model. They hold true only if reference phasors are considered and thus, when dealing with measured values, a mismatch is introduced that can be significant.

The model in (1), even if including all the main contributions, does not account for second order effects, like those depending on the actual measurand and on the operating conditions. For instance, inductive ITs undergo nonlinear effects that can become significant, particularly for CTs that are designed to deal with higher input variations. Since the current magnitude can vary significantly, $b_{hk}^{\text{IT,sys}}$ and $\phi_{hk}^{\text{IT,sys}}$ should be considered as a function of I_{hk}/I_{hk}^{0}, i.e., of the percentage of current on the rated value that is flowing at the measurement instant [63].

When dealing with measurements from synchronised RTUs or meters, for the aforementioned reasons, the model in (1) is still valid if the analysis is limited to the magnitude or rms measurement. Furthermore, while the IT impact is the same, the PMU ratio error is replaced with a_h^{RTU}, which is typically significantly larger.

Focusing on error distributions, PMU errors were usually assumed as having a Gaussian distribution, which is very common in instrument characterisation and is realistic in the presence of several error sources. For instance, in [64], errors of PMUs installed in the field were found to be Gaussian for both magnitudes and phase angles. Recently, this hypothesis has been questioned and new models were proposed. In [65], based on field measurements, voltage magnitude and phase-angle errors are shown to follow non-Gaussian distributions by analysing error differences between two similar PMUs installed at adjacent buses. Following a similar approach, analogous results were obtained for voltage magnitude and phase-angle errors of PMUs installed in distribution systems [66]. As a consequence, Gaussian Mixture Models (GMMs) are proposed for error modelling. In [67], both voltage and current field measurements are also analysed and statistically manipulated to extract PMU random errors and find their distribution, which is fitted through GMM. It is important to highlight that such results rely on a statistical assessment of errors corresponding to different operating conditions and non-stationary signals. In [68], voltage synchrophasor error analysis is performed based on a calibrator. The generated signals are dynamic and correspond to amplitude and phase modulation or frequency ramp tests as described in [40]. The results prove that errors are non-Gaussian, as expected for time varying and off-nominal conditions.

The works in [62] and [69] try to reconcile the most recent results with classic instrument error modelling, for voltage and current synchrophasor measurements, respectively. Through experimental results conducted on commercial PMUs in a controlled laboratory environment and under steady-state conditions, it is proven that magnitude errors can be considered as Gaussian as long as the same operating conditions hold. Non-Gaussianity arises from non-stationarity and/or anomalous ("bad") data. As for phase-angle measurements, the statistical behaviour and thus the validity of errors normality depend on the PMU model, the configured full-scale range and the accuracy, since synchronisation mechanisms, when prevailing, can introduce complex error patterns.

Another element to consider when representing uncertainties of synchrophasors measured by PMUs is related to the system of coordinates adopted for their representation. Indeed, (synchro)phasors can be expressed in both polar or rectangular coordinates. However, as shown in (1), the preferential system of coordinates to represent uncertainties is the polar system since it allows to decouple the uncertainties of the magnitude from those of the phase. As illustrated in the next sections, many identification problems in power systems, such as those related to state estimation, rely on the use of rectangular coordinates for measurement integration as it allows to write simplified measurement functions (e.g. linear ones, depending on the problem at hand). Regardless the exact optimization problem definition, this approach may help both formulation and computation. Indeed, in several cases, like those discussed in Sections IV-B–IV-D, a system of real-valued equations is obtained from the measurement constraints expressed in rectangular coordinates. Therefore, there is the need to project the uncertainties distributions of magnitude and phase from polar to rectangular coordinates. This projection, in general, does not preserve Gaussian normality unless the standard deviations of the original magnitude and phase errors are small [70]. Therefore, in order to properly build the measurements error covariance matrix of any estimation model, the modeler should, in principle, perform such a projection (e.g. using the process in [70]) in order to: (i) correctly estimate the measurements error covariance matrix in rectangular coordinates and (ii) verify the hypotheses on the normality of the measurements uncertainties distributions in rectangular coordinates.

As a final remark on the measurement errors, we can highlight that the error model is crucial for designing, validating and characterizing the estimation techniques discussed in this paper, but there is no universally applicable or accepted model and this is one of the open problems in model estimation research.

III. Overview of Power-flow Models and Estimation Techniques

Power-flow models play a pivotal role in the operational and protection functions of power systems (e.g., optimal power flow, scheduling and control, state estimation, protection, fault location, stability, and contingency analysis, planning and expansion, electricity markets, real-time operation), as they are used to represent the system's behavior under different operating conditions [1], [71]. Hence, in this section, we provide a general description of the considered power flow model before then discussing different estimation techniques and a performance metric.

A. Power-flow Model

The power-flow analysis aims at determining the voltage and current phasors at different nodes/lines in the power system for fixed boundary conditions (such as power injections and module of voltages imposed on the system's nodes). These power flow models can be represented by a generic mathematical formulation given by

$$\mathbf{x} = \Phi(\boldsymbol{\beta}, \mathbf{p}) \tag{3}$$

where, $\mathbf{x}$ refers to the system state (such as phase-to-ground voltage phasors or other quantities such as branch current phasors, etc.), $\boldsymbol{\beta}$ refers to the fixed boundary conditions (such as power injections and voltage phasors imposed on the boundary nodes of the power system), Φ represents the non-linear power flow model. The symbol $\mathbf{p}$ denotes the parameters of the power system electrical circuit (for example, line/transformer impedances, shunt admittances, etc.).

In reality, parameters $\mathbf{p}$ may not be accurately known or are completely unavailable due to several reasons (e.g., inaccurate information of components in the available data sheets and/or outdated topological information). Therefore, measurement-based algorithms are developed for learning the parameter $\mathbf{p}$, referred to as the *parameter estimation problem*. The techniques proposed to solve this problem can be broadly categorized in two groups:

1) *State-independent power-flow models:* refer to the identification of the non-approximated non-linear model of the power system (that is not dependent on the operating state). In this case, the typical parameters to estimate are the line/transformer impedance, shunt admittance, and topology of the network. These estimation models are reviewed in Sec. IV.
2) *State-dependent power-flow models:* refer to the identification of an approximated power system model that is valid in the proximity of a given operating state. They represent approximate models of the power system and their formulation depends on the specific application. One such example is the linearized power flow model modeled by the power-flow sensitivity coefficients (PFSCs) given by the first-order Taylor's approximation of the original non-linear power flow equations. These estimation models are reviewed in Sec. V.

B. Estimation Techniques

In the following, we review different solution techniques that are widely used for solving the power system parameter estimation problem.

With respect to the parameter estimation problem, the model in (3) is often transformed to

$$\mathbf{z} = \mathbf{h}(\mathbf{x}, \mathbf{p}) \tag{4}$$

where $\mathbf{z} \in \mathbb{R}^m$ refer to measurable quantities, $\mathbf{x} \in \mathbb{R}^s$ to the system states, and $\mathbf{h}$ refers to a non-linear measurement function that relates $\mathbf{z}$ and $\mathbf{x}$. The symbol $\mathbf{p} \in \mathbb{R}^n$ is the vector of parameters to be estimated.

Often the estimation model in (4) is transformed into a linearized measurement model, leveraging algebraic manipulations chosen by the modeler. Consequently, the estimation model is expressed as

$$\mathbf{z} = \mathbf{H}(\mathbf{x})\mathbf{p} = \mathbf{H}\mathbf{p} \tag{5a}$$

where $\mathbf{H}(\mathbf{x})$ or $\mathbf{H} \in \mathbb{R}^{m \times n}$ refers to the so-called measurement matrix which is a function of $\mathbf{x}$.

In a parameter estimation problem where the objective is to estimate $\mathbf{p}$, the vectors $\mathbf{z}$ and $\mathbf{x}$ in (5a) are obtained from measurements that are characterized by measurement errors. Denoting the measured quantities for $\mathbf{x}$ and $\mathbf{z}$ as $\tilde{\mathbf{x}}$ and $\tilde{\mathbf{z}}$, respectively, and by modeling the error distributions as independent white Gaussian distributions, $\tilde{\mathbf{x}}$ and $\tilde{\mathbf{z}}$ can be expressed as

$$\tilde{\mathbf{z}} = \mathbf{z} + \delta_{\mathbf{z}}, \qquad \delta_{\mathbf{z}} \sim \mathcal{N}(\mathbf{0}, \mathcal{Q}_{\mathbf{z}}) \tag{5b}$$

$$\tilde{\mathbf{x}} = \mathbf{x} + \delta_{\mathbf{x}}, \qquad \delta_{\mathbf{x}} \sim \mathcal{N}(\mathbf{0}, \mathcal{Q}_{\mathbf{x}}) \tag{5c}$$

where, $\delta_{\mathbf{z}}, \delta_{\mathbf{x}}$ denote the measurement errors on $\mathbf{z}, \mathbf{x}$, respectively, and $\mathcal{Q}_{\mathbf{z}}, \mathcal{Q}_{\mathbf{x}}$ denote the error covariance matrices of $\delta_{\mathbf{z}}, \delta_{\mathbf{x}}$, respectively.

In the following, we review different estimation approaches that are used to estimate $\mathbf{p}$ based on the linear equations in (5) and different assumptions on the measurements errors.

1) Maximum Likelihood Estimator (MLE) – Weighted Total Least Squares (WTLS): here, it is assumed that matrices $\mathcal{Q}_{\mathbf{z}}, \mathcal{Q}_{\mathbf{x}}$ are heteroscedastic, i.e., their diagonal elements are not equal. The unknown parameter $\mathbf{p}$ can be estimated by formulating it as an MLE problem by maximizing the log-likelihood function i.e.,

$$[\widehat{\mathbf{p}}] := \arg\max_{\mathbf{p}} \log\big(\Gamma(\mathbf{x}, \mathbf{z}, \mathbf{p} | \tilde{\mathbf{x}}, \tilde{\mathbf{z}})\big) \tag{6a}$$

subject to

$$\mathbf{z} = \mathbf{H}(\mathbf{x})\mathbf{p} \tag{6b}$$

$$\tilde{\mathbf{z}} = \mathbf{z} + \boldsymbol{\delta}_{\mathbf{z}}, \qquad \boldsymbol{\delta}_{\mathbf{z}} \sim \mathcal{N}(\mathbf{0}, \mathcal{Q}_{\mathbf{z}}) \tag{6c}$$

$$\tilde{\mathbf{x}} = \mathbf{x} + \boldsymbol{\delta}_{\mathbf{x}}, \qquad \boldsymbol{\delta}_{\mathbf{x}} \sim \mathcal{N}(\mathbf{0}, \mathcal{Q}_{\mathbf{x}}). \tag{6d}$$

where, $\Gamma(\mathbf{x}, \mathbf{z}, \mathbf{p} | \tilde{\mathbf{x}}, \tilde{\mathbf{z}}) =$

$$\begin{aligned} &\frac{1}{(2\pi)^{s/2}\sqrt{\det(\mathcal{Q}_{\mathbf{x}})}} \exp\Big(-\frac{1}{2}(\mathbf{x} - \tilde{\mathbf{x}})^\top \mathcal{Q}_{\mathbf{x}} (\mathbf{x} - \tilde{\mathbf{x}})\Big) \times \\ &\frac{1}{(2\pi)^{m/2}\sqrt{\det(\mathcal{Q}_{\mathbf{z}})}} \exp\Big(-\frac{1}{2}(\mathbf{z} - \tilde{\mathbf{z}})^\top \mathcal{Q}_{\mathbf{z}} (\mathbf{z} - \tilde{\mathbf{z}})\Big) \end{aligned} \tag{6e}$$

The above problem can be simplified as follows:

$$\begin{aligned} \min_{\mathbf{p}} \min_{\mathbf{x}} &(\tilde{\mathbf{x}} - \mathbf{x})^\top \mathcal{Q}_{\mathbf{x}}^{-1} (\tilde{\mathbf{x}} - \mathbf{x}) \\ &+ (\tilde{\mathbf{z}} - \mathbf{H}(\mathbf{x})\mathbf{p})^\top \mathcal{Q}_{\mathbf{z}}^{-1} (\tilde{\mathbf{z}} - \mathbf{H}(\mathbf{x})\mathbf{p}) \end{aligned} \tag{6f}$$

It should be noted that the optimization problem in (6f) is non-convex, and only local solutions can be obtained. The work in [72] proposed an iterative scheme to obtain a solution to the Weighted Total Least Squares (WTLS) problem, where the least square solution is used to initialize the estimation process.

2) Ordinary Total Least Squares: by assuming the error covariance matrix in (5b) to be diagonal and homoscedastic, the estimation problem can be approximated by using the ordinary total least squares (OTLS or TLS) (i.e., $\mathcal{Q}_{\mathbf{z}} = \sigma_z^2 \mathbf{I}$ and $\mathcal{Q}_{\mathbf{x}} = \sigma_x^2 \mathbf{I}$) where σ_z^2 and σ_x^2 are the noise variances on $\tilde{\mathbf{z}}$ and $\tilde{\mathbf{x}}$ respectively, and $\mathbf{I}$ is the identity matrix. The parameter estimation problem can be formulated as error-in-variables (EIV) regression [73] given by

$$[\widehat{\mathbf{H}}, \widehat{\mathbf{p}}, \widehat{\mathbf{z}}] := \arg\min_{\mathbf{H}, \mathbf{p}, \mathbf{z}} \| [\mathbf{H}(\mathbf{x}) \ \mathbf{z}] - [\mathbf{H}(\tilde{\mathbf{x}}) \ \tilde{\mathbf{z}}] \|_F \tag{7a}$$

$$\text{subject to} \quad \mathbf{z} = \mathbf{H}(\mathbf{x})\mathbf{p} \tag{7b}$$

where $\|.\|_F$ refers to the Frobenius norm. In OTLS, it is assumed that the error distributions in $[\mathbf{H}(\mathbf{x}) \ \mathbf{z}]$ are zero mean and normally distributed with a covariance matrix that is a multiple of the identity matrix. This problem is often reformulated as a matrix low-rank approximation problem given by

$$[\widehat{\mathbf{H}}, \widehat{\mathbf{p}}, \widehat{\mathbf{z}}] := \arg\min_{\mathbf{H},\mathbf{p},\mathbf{z}} \|[\mathbf{H}(\mathbf{x})\ \mathbf{z}] - [\mathbf{H}(\tilde{\mathbf{x}})\ \tilde{\mathbf{z}}]\|_F \tag{8}$$

$$\text{subject to} \quad \operatorname{rank}([\mathbf{H}(\mathbf{x})\ \mathbf{z}]) \leq n \tag{9}$$

This problem is solved using the singular value decomposition (SVD). Let the SVD of $[\mathbf{H}(\tilde{\mathbf{x}})\ \tilde{\mathbf{z}}]$ be

$$[\mathbf{H}(\tilde{\mathbf{x}})\ \tilde{\mathbf{z}}] = \mathcal{U}\boldsymbol{\Sigma}\mathcal{V}^\top \tag{10}$$

$$\text{where, } \mathcal{V} = \begin{bmatrix} \mathcal{V}_{\mathbf{H},\mathbf{H}} & \mathcal{V}_{\mathbf{H},\mathbf{z}} \\ \mathcal{V}_{\mathbf{z},\mathbf{H}} & \mathcal{V}_{\mathbf{z},\mathbf{z}} \end{bmatrix}, \text{ and } \boldsymbol{\Sigma} = \operatorname{diag}(\overline{\sigma}, \dots, \underline{\sigma}). \tag{11}$$

The TLS solution [74], [75] is then given as:

$$\widehat{\mathbf{p}}_{\text{TLS}} = -\mathcal{V}_{\mathbf{H},\mathbf{z}}\mathcal{V}_{\mathbf{z},\mathbf{z}}^{-1}. \tag{12}$$

3) Ordinary Least Squares (LS) and Weighted Least Squares (WLS) Estimators: if the noise on $\mathbf{x}$ can be neglected (i.e, $\tilde{\mathbf{x}} = \mathbf{x}$), the estimation problem in (6f) is simplified to the estimation of the parameter $\mathbf{p}$ as

$$\min_{\mathbf{p}} \ (\tilde{\mathbf{z}} - \mathbf{H}(\mathbf{x})\mathbf{p})^\top \mathcal{Q}_{\mathbf{z}}^{-1}(\tilde{\mathbf{z}} - \mathbf{H}(\mathbf{x})\mathbf{p}) \tag{13}$$

It can be expressed as the following closed-form solution

$$\widehat{\mathbf{p}}_{\text{WLS}} = (\mathbf{H}(\tilde{\mathbf{x}})^\top \mathcal{Q}_{\mathbf{z}}^{-1}\mathbf{H}(\tilde{\mathbf{x}}))^{-1}\mathbf{H}(\tilde{\mathbf{x}})^\top \mathcal{Q}_{\mathbf{z}}^{-1}\tilde{\mathbf{z}} \tag{14}$$

In the case of ordinary least squares, the $\mathcal{Q}_{\mathbf{z}}$ is replaced by the identity matrix, i.e,

$$\widehat{\mathbf{p}}_{\text{LS}} = (\mathbf{H}(\tilde{\mathbf{x}})^\top\mathbf{H}(\tilde{\mathbf{x}}))^{-1}\mathbf{H}(\tilde{\mathbf{x}})^\top\tilde{\mathbf{z}} \tag{15}$$

4) Ridge and Lasso Regression: two regularized variants of least squares are commonly used in power system identification problems, known as ridge and lasso regressions. The ridge regression (RR), also known as Tikhonov regularization [76], helps addressing the issue of multicollinearity in data, whereas the lasso regression [77] promotes sparse estimates. These regression problems can generically be represented by

$$\widehat{\mathbf{p}}_{\text{REG}} = \min_{\mathbf{p}} \|\tilde{\mathbf{z}} - \mathbf{H}(\tilde{\mathbf{x}})\mathbf{p}\|_2^2 + \lambda\|\mathbf{p}\|_\ell, \tag{16}$$

where $\ell = 2$ for the RR, $\ell = 1$ for the lasso one and λ is a suitable positive regularization parameter. RR admits a closed-form solution given by

$$\widehat{\mathbf{p}}_{\text{REG}} = (\mathbf{H}(\tilde{\mathbf{x}})^\top\mathbf{H}(\tilde{\mathbf{x}}) + \lambda\mathbf{I})^{-1}\mathbf{H}(\tilde{\mathbf{x}})^\top\tilde{\mathbf{z}}, \tag{17}$$

whereas lasso does not have, in general, a closed-form solution and is typically solved iteratively. It is important to note that introducing a regularization term unavoidably introduces bias in the estimate. Therefore, it is crucial to carefully select λ to find a balance between the ridge and lasso goals and the introduced bias.

5) Support Vector Regression (SVR): is capable to handle outliers and multicollinearity in the input data. The regression scheme can be expressed as $\epsilon-$ SVR [78] as

$$\min_{\mathbf{p}} \ \frac{1}{2}\|\mathbf{p}\|_2^2 \tag{18a}$$

$$\text{subject to } \tilde{\mathbf{z}} - \mathbf{H}(\tilde{\mathbf{x}})\mathbf{p} \leq \epsilon\mathbf{1}_m \tag{18b}$$

$$-\tilde{\mathbf{z}} + \mathbf{H}(\tilde{\mathbf{x}})\mathbf{p} \leq \epsilon\mathbf{1}_m, \tag{18c}$$

where ϵ is a parameter. The regression in problem (18) means that the estimated $\mathbf{p}$ allows all the estimation errors below ϵ but not larger than this. In order to handle infeasible cases, this problem is modified by the introduction of a "soft margin" loss function [79], i.e. slack variables $\boldsymbol{\xi}_1, \boldsymbol{\xi}_2 \in \mathbb{R}^m$ are introduced and the problem is expressed as

$$\min_{\mathbf{p},\boldsymbol{\xi}_1,\boldsymbol{\xi}_2} \ \frac{1}{2}\|\mathbf{p}\|_2^2 + \alpha\mathbf{1}_m^\top(\boldsymbol{\xi}_1 + \boldsymbol{\xi}_2) \tag{19a}$$

$$\text{subject to } \tilde{\mathbf{z}} - \mathbf{H}(\tilde{\mathbf{x}})\mathbf{p} \leq \epsilon\mathbf{1}_m + \boldsymbol{\xi}_1, \tag{19b}$$

$$-\tilde{\mathbf{z}} + \mathbf{H}(\tilde{\mathbf{x}})\mathbf{p} \leq \epsilon\mathbf{1}_m + \boldsymbol{\xi}_2, \tag{19c}$$

$$\boldsymbol{\xi}_1, \boldsymbol{\xi}_2 \leq 0, \tag{19d}$$

where $\mathbf{1}_m \in \mathbb{R}^m$ is a vector of ones. The parameter α is decided based on a trade-off between the two objectives. The optimization problem in (19) is often solved by its dual reformulation as detailed in [80].

Another variant of SVR is Kernel-based SVR which is capable of tackling non-linearity in the model by projecting the input data $\mathbf{z}$ and $\mathbf{x}$ through a Kernel function as proposed in [81].

6) Linear Minimum Mean Square Estimation: we here review the stochastic least squares method, also known as Linear Minimum Mean Square Estimation (LMMSE) [82], where the aim is to estimate $\mathbf{z}$ from $\mathbf{x}$ using a (Wiener) filter $\widehat{\mathbf{p}}_{\text{WF}}$ such that the estimate $\widehat{\mathbf{p}}_{\text{WF}}$ minimizes the mean square error $\mathbb{E}[\|\mathbf{H}(\tilde{\mathbf{x}})\mathbf{p}_{\text{WF}} - \tilde{\mathbf{z}}\|_2^2]$. The solution admits a simple closed-form solution (the Wiener-Hopf equation) given by

$$\widehat{\mathbf{p}}_{\text{WF}} := \boldsymbol{\Sigma}_{\mathbf{z},\mathbf{H}}{\boldsymbol{\Sigma}_{\mathbf{H}}}^{-1}, \tag{20}$$

where $\boldsymbol{\Sigma}_{\mathbf{H}}$ and $\boldsymbol{\Sigma}_{\mathbf{z},\mathbf{H}}$ are the covariance of the system state and the cross-covariance of $\mathbf{z}$ and $\mathbf{H}(\mathbf{x})$.

7) Well-Conditioned LMMSE: Often, large condition numbers of $\boldsymbol{\Sigma}_{\mathbf{H}}$ are encountered in network identification problems, thus hindering the numerical computation of $\boldsymbol{\Sigma}_{\mathbf{H}}^{-1}$. The work in [83] proposed a well-conditioned approximate solution to (20), presented in the following. Let us define $\tilde{\mathbf{y}} := (\tilde{\mathbf{z}}, \mathbf{H}(\tilde{\mathbf{x}}))$, with the corresponding joint covariance matrix given by

$$\boldsymbol{\Sigma}_{\mathbf{y}} = \begin{bmatrix} \boldsymbol{\Sigma}_{\mathbf{z}} & \boldsymbol{\Sigma}_{\mathbf{z},\mathbf{H}} \\ {\boldsymbol{\Sigma}_{\mathbf{zH}}}^\top & \boldsymbol{\Sigma}_{\mathbf{H}} \end{bmatrix} = \begin{bmatrix} \mathbf{X}_{\mathbf{z}} \\ \mathbf{X}_{\mathbf{H}} \end{bmatrix} \mathbf{S}_{\mathbf{y}} \begin{bmatrix} \mathbf{X}_{\mathbf{z}} \\ \mathbf{X}_{\mathbf{H}} \end{bmatrix}^\top, \tag{21}$$

with the second equality defining the eigendecomposition of $\boldsymbol{\Sigma}_{\mathbf{y}}$. Now let us partition the eigenvector matrices into an $n \times L$ and an $n \times M$ matrix such that

$$\mathbf{X}_{\mathbf{z}} = \begin{bmatrix} \mathbf{X}_{\mathbf{z},L} & \mathbf{X}_{\mathbf{z},M} \end{bmatrix}, \ \mathbf{X}_{\mathbf{H}} = \begin{bmatrix} \mathbf{X}_{\mathbf{H},L} & \mathbf{X}_{\mathbf{H},M} \end{bmatrix},$$

with $L + M = 2n$, and L being a design parameter. An approximate filter can now be given as

$$\widehat{\mathbf{p}}_{\text{WCWF}} = \mathbf{X}_{\mathbf{z},L}(\mathbf{X}_{\mathbf{H},L}^\top\mathbf{X}_{\mathbf{H},L})^{-1}\mathbf{X}_{\mathbf{H},L}^\top, \tag{22}$$

where all the matrix inverses are $L \times L$ and can be selected to be well-conditioned by choosing an appropriate L.

8) Recursive Estimation Schemes: in cases when the parameters are observed to be varying over time, recursive estimation algorithms can be utilized and the estimations are updated whenever there are new measurements available. These schemes also propagate information from the previous estimations using some forgetting factors.

a) Recursive least squares (RLS): is an approach that solves LS in a recursive way. Usually, to give less importance to previous estimates, an exponential forgetting factor is applied to the observations [84]. The forgetting factor $0 < \mu \leq 1$ is reflected in the covariance matrix update. The varying nature of the measuring quantities and parameters are represented by subscript index k. The estimates are updated according to the following recursive updates:

$$\widehat{\mathbf{p}}_{k,\mathrm{RLS}} = \widehat{\mathbf{p}}_{k-1,\mathrm{RLS}} + \mathbf{K}_k \mathbf{e}_k \tag{23a}$$

where $\widehat{\mathbf{p}}_{k-1,\mathrm{RLS}}$ refers to the previous estimate and $\mathbf{K}_k$ and $\mathbf{e}_k$ are defined as

$$\mathbf{e}_k = \tilde{\mathbf{z}}_k - \mathbf{H}_k \widehat{\mathbf{p}}_{k-1} \tag{23b}$$

$$\mathbf{K}_k = \frac{\boldsymbol{\mathcal{P}}^{\mathrm{cov}}_{t-1} \mathbf{H}_k^\top}{\mu + \mathbf{H}_k \boldsymbol{\mathcal{P}}^{\mathrm{cov}}_{k-1} \mathbf{H}_k^T} \tag{23c}$$

$$\boldsymbol{\mathcal{P}}^{\mathrm{cov}}_k = (\mathbf{I} - \mathbf{K}_k \mathbf{H}_k) \boldsymbol{\mathcal{P}}^{\mathrm{cov}}_{k-1} / \mu \tag{23d}$$

where $\mathbf{K}_k$ is the estimated gain, $\boldsymbol{\mathcal{P}}^{\mathrm{cov}}_k$ is the covariance matrix and $\mathbf{e}_k$ the residual.

As reported in [84], the RLS algorithm with exponential forgetting may suffer from the so-called windup problem of the covariance matrix and may lead to very large covariances resulting in large variances in estimates. Several heuristics approaches are proposed in the literature to solve this issue. For example, a *selective forgetting* strategy was proposed in [84] where forgetting factors are decided as a function of the eigenvalues of the covariance matrix. In another approach, a *constant-trace* algorithm [85] was proposed where an upper bound is imposed on the maximum eigenvalue of $\boldsymbol{\mathcal{P}}^{\mathrm{cov}}_k$. In [86]–[88], a *directional forgetting* algorithm was proposed where $\boldsymbol{\mathcal{P}}^{\mathrm{cov}}_k$ is split into two matrices: the first containing information orthogonal to $\mathbf{H}_k$ and the second part must be forgotten. It allows to only forget the part of the covariance matrix that changes by the newer information.

b) Kalman-filter: the Kalman filter is also a recursive estimation scheme. In power systems, this method has been primarily used for state estimation [4]. In some cases, it has also been used for parameter estimation, for example, [89]–[94]. The Kalman filter (KF) aims at obtaining the system state, or a set of parameters, at a given time by taking into account information available from both measurements and a *process model*. There are different versions of the KF method presented in the literature. The Discrete Kalman Filter (DKF) is used for linear systems, whereas the Extended Kalman Filter (EKF) and the Iterated Kalman Filter (IKF) are used when the process and/or the measurement models are non-linear. The KF consists of a "predictor-measurement update" process that minimizes the estimates error covariance, provided that some specific conditions are met. The objective is to estimate the state of a discrete-time controlled process, governed by the linear stochastic process model given by:

$$\mathbf{p}_k = \mathbf{A}_k \mathbf{p}_{k-1} + \mathbf{B}_k \mathbf{u}_{k-1} + \boldsymbol{\delta}_{\mathbf{p},k-1} \tag{24}$$

where $\mathbf{p}_k$ and $\mathbf{p}_{k-1}$ represent the unknown parameters in correspondence of discrete time steps k and $k-1$, respectively; $\mathbf{u}_{k-1}$ represents a set of control variables (independent from the system state) of the system at time step $k-1$; $\boldsymbol{\delta}_{\mathbf{p},k-1}$ represents the system process noise assumed white and with a normal probability distribution ($\boldsymbol{\delta}_{\mathbf{p}} \sim \mathcal{N}(\mathbf{0}, \mathbf{Q}_{\mathbf{p}})$); $\mathbf{A}_k$ is a matrix that links that state of the system at time step $k-1$ with the one of the current time step k for the case of null control variables and process noise; $\mathbf{B}_k$ is a matrix that links the time evolution of the state of the system with the controls at time step $k-1$ for the case of null process noise.

The measurement model is assumed to be the one in (5a) with the same hypotheses (5b) regarding the error models. Now, it is reasonable to assume that the parameters do not change over time and the prediction model can be simplified as follows:

$$\mathbf{p}_k = \mathbf{p}_{k-1} + \boldsymbol{\delta}_{\mathbf{p},k-1} \tag{25}$$

In the case of unbiased estimation, the Kalman filter estimation equation is obtained as

$$\widehat{\mathbf{p}}_{k,\mathrm{KF}} = \breve{\mathbf{p}}_k + \mathbf{K}_k (\tilde{\mathbf{z}}_k - \mathbf{H}_k \breve{\mathbf{p}}_k) \tag{26}$$

where $\mathbf{K}_k$ is the so-called Kalman gain. In [95], the *optimal Kalman gain* is derived by minimizing the expected value of the square of the magnitude of the estimation error $\mathbb{E}[\|\widehat{\mathbf{p}}_{k,\mathrm{KF}} - \mathbf{p}_k\|^2]$. This is equivalent to minimizing the trace of error covariance matrix $\widehat{\boldsymbol{\mathcal{P}}}_k$ as $\widehat{\boldsymbol{\mathcal{P}}}_k$ given by

$$\widehat{\boldsymbol{\mathcal{P}}}_k = \mathrm{cov}(\widehat{\mathbf{p}}_k - \mathbf{p}_k) \tag{27}$$

As derived in [95], the *optimal Kalman gain* is given by

$$\mathbf{K}_k = \breve{\boldsymbol{\mathcal{P}}}_k \mathbf{H}_k^\top (\mathbf{H}_k \breve{\boldsymbol{\mathcal{P}}}_k \mathbf{H}_k^\top + \boldsymbol{\mathcal{Q}}_{\mathbf{z}})^{-1} \tag{28}$$

where

$$\breve{\boldsymbol{\mathcal{P}}}_k = \widehat{\boldsymbol{\mathcal{P}}}_{k-1} + \boldsymbol{\mathcal{Q}}_{\mathbf{p}} \tag{29}$$

where $\boldsymbol{\mathcal{Q}}_{\mathbf{p}}$ is the process covariance matrix.

To summarize, KF is composed of two steps. The *prediction step* is given by

$$\breve{\mathbf{p}}_k = \widehat{\mathbf{p}}_{k-1} \tag{30a}$$

$$\breve{\boldsymbol{\mathcal{P}}}_k = \widehat{\boldsymbol{\mathcal{P}}}_{k-1} + \boldsymbol{\mathcal{Q}}_{\mathbf{p}} \tag{30b}$$

and the *estimation update* is given by

$$\widehat{\mathbf{p}}_{k,KF} = \breve{\mathbf{p}}_k + \mathbf{K}_k (\tilde{\mathbf{z}}_k - \mathbf{H}_k \breve{\mathbf{p}}_k) \tag{30c}$$

$$\mathbf{K}_k = \breve{\boldsymbol{\mathcal{P}}}_k \mathbf{H}_k^\top (\mathbf{H}_k \breve{\boldsymbol{\mathcal{P}}}_k \mathbf{H}_k^\top + \boldsymbol{\mathcal{Q}}_{\mathbf{z}})^{-1} \tag{30d}$$

$$\widehat{\boldsymbol{\mathcal{P}}}_k = (\mathbf{I} - \mathbf{K}_k \mathbf{H}_k) \breve{\boldsymbol{\mathcal{P}}}_k \tag{30e}$$

9) Iterative Estimation Methods: the estimation problem in (6f) is inherently bi-linear as it estimates the measurement matrix $\mathbf{H}$ as well as $\mathbf{p}$. This non-convexity has been tackled by iterative estimation methods with particular reference to joint estimation problems such as state and parameter estimation (Sec. IV-A1b), topology and line parameter estimation (Sec. IV-D6), systematic error and parameter estimation (Sec. IV-C2) that can be cast into iterative optimization schemes as discussed later in detail.

C. Performance Metric: Cramér-Rao Lower Bound

The majority of the estimation models in power systems fall into the category of so-called *Minimum Variance Unbiased Estimator (MVU)* unless there is a presence of a systematic error in the measurement model. A MVU estimator must satisfy the condition

$$\mathbb{E}(\widehat{\mathbf{p}}) = \mathbf{p}^{\text{true}} \tag{31}$$

i.e., the average of all the estimates converges to its "true" value ($\mathbf{p}^{\text{true}}$) [96]. A biased estimator does not satisfy (31) and the biasedness can be defined as how far the average is from the true value.

For an MVU estimator, a lower bound on the variance of the estimator can be defined by the *Cramér-Rao Lower Bound (CRLB)* that can be used to benchmark the performance against any estimator. The performance of such MVU can be evaluated by evaluating the Fisher Information Matrix (FIM) [96] which quantifies the information that the measurements carry about an unknown parameters vector.

According to the Cramér-Rao theorem (Chapter. 3 in [96]), the trace of the inverse of the FIM gives a lower bound on the variance of any unbiased estimator, referred to as the CRLB. It is given by

$$\text{var}(\widehat{\mathbf{p}}) \geq \frac{1}{\boldsymbol{\mathcal{I}}(\mathbf{p})} \tag{32}$$

where $\boldsymbol{\mathcal{I}}(\mathbf{p})$ denotes FIM. Using the log-likelihood function in (6e), FIM is expressed as

$$\boldsymbol{\mathcal{I}}(\mathbf{p}) = -\mathbb{E}\Big[\frac{\partial^2 \log\, \Gamma(\mathbf{x},\mathbf{z},\mathbf{p})}{\partial \mathbf{p}^2}\Big] \tag{33}$$

The CRLB can be used to benchmark different estimation models; the one achieving the closest variance to the CRLB is the best estimator.

For linear estimation models (e.g., Sec. III-B3), the MVU estimator is given by

$$\widehat{\mathbf{p}} = (\mathbf{H}^\top \mathbf{H})^{-1}\mathbf{H}\mathbf{z}. \tag{34}$$

Using the expressions defined in (6e), (33), FIM is given by

$$\boldsymbol{\mathcal{I}}(\widehat{\mathbf{p}}) = \mathbf{H}^\top \mathbf{H} \tag{35}$$

Therefore, in this case, the CRLB is

$$\text{var}(\widehat{\mathbf{p}}) \geq (\mathbf{H}^\top \mathbf{H})^{-1} \tag{36}$$

As a final remark, power flow identification problems often exhibit nonlinearity and nonconvexity depending on the nature of the problem, meaning that the objective function, over the feasible solution region, contains multiple local optima. This arises due to the nonlinear relationships between inputs and outputs, measurement noise, and the coupling of system states/parameters to be identified. This requires the modeler to use convexification techniques, such as linearization and convex relaxations. The choice of estimation schemes and their estimation accuracy often depend on the inputs to the parameter estimation problem and on the exactness of the assumptions. A key challenge in parameter estimation is to verify the accuracy of the estimated parameters as the true parameters may not be known. In this respect, statistical methods such as CRLB in Sec. III-C are useful for benchmarking the estimation methods, and future research may enhance such bounds with domain-specific knowledge of power system physics. Future research will also benefit from the use of machine learning enhanced techniques (e.g. [97]–[101]) in combination with conventional mathematical solvers to enhance estimation performance.

With the comprehensive overview over parameters estimation methods given in this section, we now review the approaches which use these methods to estimate state-dependent and state-independent power flow models.

IV. Estimating State-independent Grid Models

As described before, state-independent models are models that are used for the exact representation of the power system and can be applied to describe any steady-state operating point. These models are typically composed of circuit representations of the power network such as lines, transformers, shunt admittances, grid topology, compound admittance matrices, etc. This section aims to review different schemes for estimating these state-independent parameters and discusses the key challenges, and potential ways to tackle them. It is organized as follows: in Section IV-A, we review methods for identifying erroneous parameters among the already-known grid parameters and topologies. Then, in Section IV-B, we present models and methods for the estimation of line/shunt parameters. In Section IV-C, we review methods in which line parameters are estimated jointly with grid states or systematic errors, and then in Section IV-D, we review methods for the estimation of the compound admittance matrix.

A. Identification of Erroneous Parameters and Topology

1) Identification of Erroneous Parameters: the function of a power system state estimator is to provide the real-time operating state of the system while detecting and identifying sources of errors. Errors may originate from wrong measurements, wrong network model topology, or inaccurate network parameters. Under normal operating conditions when generation matches the slowly changing bus loads, static state estimators perform this function quite well based on SCADA measurements. Measurements are received from substations every few seconds and the state estimator is executed every few minutes and the system is said to be operating in a pseudo steady-state. Based on these assumed conditions, error processing is commonly carried out post-estimation based on the measurement residuals, i.e. the differences between the estimated and measured values. In order to account for the differences in measurement accuracy, network topology, and measurement configuration, residuals are normalized to yield a set of values that are supposed to have a standard normal distribution. Significant deviations from this distribution are flagged as bad data. Historically, network models and parameters are considered to be perfectly known, and bad data are blamed on gross errors in analog measurements. This assumption is unfortunately not valid for large power grids where parameters of lines, transformers, capacitors, and reactors may vary under ambient conditions, may be incorrectly entered into the database, or may not be properly updated after scheduled or required maintenance. Detecting, identifying, and correcting network parameter errors improves the accuracy and reliability of not only the state estimator but also all the network applications relying on state estimator results.

In the following, we review two different approaches to detect parameter errors. The first one is an offline approach, whereas the second is an online approach.

a) Non-robust offline approach for detecting parameter errors: Initial attempts to process parameter errors used sensitivity analysis to identify the parameter responsible for large residuals, implicitly assuming that measurement errors are insignificant [102]–[105]. Alternative approaches were proposed by augmenting the state vector with suspect parameters and simultaneously estimating the states and suspect parameters [89], [106]–[108]. While quite effective for cases where the suspect set was reasonably small and contained all incorrect parameters, the problem would rapidly become prohibitively large when the suspect set contained large sets of parameters. A major shortcoming of both types of methods is that they do not differentiate between gross errors in measurements and parameter errors.

The problem of parameter error detection can be addressed by incorporating the parameter errors $\mathbf{p}_e = \mathbf{p} - \mathbf{p}^{\text{true}}$ as unknown variables in the measurement equations (4) as in [109]:

$$\mathbf{z} = \mathbf{h}\left(\mathbf{x}, \mathbf{p}_e\right) + \mathbf{e} \tag{37}$$

where $\mathbf{p}$ is the assumed parameter vector, $\mathbf{p}^{\text{true}}$ is the true but unknown parameter vector and $\mathbf{e}$ the measurement error. Using (37) as the measurement equation, the state estimation problem takes the following form:

$$\begin{aligned} \min_{\mathbf{p_e}} \quad & J\left(\mathbf{x}, \mathbf{p}_e\right) = \tfrac{1}{2}\mathbf{r}^\top \mathbf{R}\mathbf{r} \\ \text{subject} \quad \text{to} \quad & \mathbf{p}_e = 0 \end{aligned} \tag{38}$$

where $\mathbf{R} = \mathcal{Q}_{\mathbf{z}}^{-1}$ is the inverse of the measurement error covariance matrix, and $\mathbf{r} = \tilde{\mathbf{z}} - \mathbf{h}(\tilde{\mathbf{x}}, \mathbf{p}_e)$ is the measurement residual vector.

The optimization problem (38) can be solved by forming the Lagrangian:

$$\mathcal{L}\left(\mathbf{x}, \mathbf{p}_e, \boldsymbol{\lambda}\right) = \frac{1}{2}\mathbf{r}^\top \mathbf{R}^{-1}\mathbf{r} - \boldsymbol{\lambda}^\top \mathbf{p}_e \tag{39}$$

Applying the first-order optimality conditions yields:

$$\frac{\partial \mathcal{L}}{\partial \mathbf{p}} = \mathbf{H}_{\mathbf{p}}^\top \mathbf{R}^{-1}\mathbf{r} + \boldsymbol{\lambda} = 0 \tag{40}$$

where $\mathbf{H_p} = \frac{\partial \mathbf{h}(\mathbf{x}, \mathbf{p}_e)}{\partial \mathbf{p}}$ is the measurement jacobian with respect to the parameter errors $\mathbf{p}$. At the solution, the Lagrange multipliers $\boldsymbol{\lambda}$ can be recovered using (40) as in [109]:

$$\boldsymbol{\lambda} = -\mathbf{H}_{\mathbf{p}}^\top \mathbf{R}^{-1}\mathbf{r} \tag{41}$$

As shown in [110] using the linear approximation, where $\mathbf{H_x} = \frac{\partial \mathbf{h}(\mathbf{x}, \mathbf{p}_e)}{\partial \mathbf{x}}$ is the measurement jacobian with respect to states $\mathbf{x}$, measurement residuals can be expressed as a linear combination of measurement and parameter errors:

$$\mathbf{r} = (\mathbf{I} - \mathbf{H_x}\mathbf{G}^{-1}\mathbf{H}_{\mathbf{x}}^\top \mathbf{R}^{-1})\mathbf{e} - (\mathbf{I} - \mathbf{H_x}\mathbf{G}^{-1}\mathbf{H}_{\mathbf{x}}^\top \mathbf{R}^{-1})\mathbf{H_p}\mathbf{p}_e \tag{42}$$

Substituting (42) into (41) yields:

$$\boldsymbol{\lambda} = \boldsymbol{\Lambda}\mathbf{p}_e + \mathbf{A}\mathbf{e} \tag{43}$$

where:

$$\mathbf{A} = -\mathbf{H}_{\mathbf{p}}^\top \mathbf{R}^{-1}(\mathbf{I} - \mathbf{H_x}\mathbf{G}^{-1}\mathbf{H}_{\mathbf{x}}^\top \mathbf{R}^{-1}) \tag{44}$$

$$\boldsymbol{\Lambda}\boldsymbol{\Lambda} = \mathbf{H}_p^\top \mathbf{R}^{-1}(\mathbf{I} - \mathbf{H}_x\mathbf{G}^{-1}\mathbf{H}_{\mathbf{x}}^\top \mathbf{R}^{-1})\mathbf{H_p} \tag{45}$$

$$\mathbf{G} = \mathbf{H}_{\mathbf{x}}^\top \mathbf{R}^{-1}\mathbf{H_x} \tag{46}$$

In order to evaluate the significance of the entries in $\boldsymbol{\lambda}$, its statistical properties are used to normalize their values. Assuming that $\mathbb{E}(\mathbf{e}) = 0$, the expected value and covariance of $\boldsymbol{\lambda}$ can be derived as:

$$\mathbb{E}\left(\boldsymbol{\lambda}\right) = \mathbb{E}\left(\boldsymbol{\Lambda}\mathbf{p}_e\right) \tag{47}$$

$$\boldsymbol{\Lambda} = \operatorname{cov}\left(\boldsymbol{\lambda}\right) = \mathbf{H}_{\mathbf{p}}^\top \mathbf{R}^{-1}(\mathbf{I} - \mathbf{H_x}\mathbf{G}^{-1}\mathbf{H}_{\mathbf{x}}^\top \mathbf{R}^{-1})\mathbf{H_p} \tag{48}$$

Note that $\boldsymbol{\Lambda}$ not only represents the sensitivity of $\boldsymbol{\lambda}$ to parameter errors $\mathbf{p}_e$, but it is also the covariance matrix of $\boldsymbol{\lambda}$. The entries of $\boldsymbol{\lambda}$ can thus be normalized to yield:

$$\lambda_i^{\mathcal{N}} = \frac{\lambda_i}{\sqrt{\Lambda_{ii}}} \tag{49}$$

where λ_i is the $i-$th element of $\boldsymbol{\lambda}$ and Λ_{ii} is $i-$th diagonal element of $\boldsymbol{\Lambda}$.

In the absence of measurement errors, i.e. $\mathbf{e} \approx \mathbf{0}$, $\lambda_i^{\mathcal{N}}$ has a standard normal distribution:

$$\lambda_i^{\mathcal{N}} \sim \mathcal{N}\left(0,\ 1\right)$$

whereas in the presence of parameter errors, its distribution changes to:

$$\lambda_i^{\mathcal{N}} \sim \mathcal{N}\left(\sqrt{\Lambda_{ii}}p_{e,\,i},\ 1\right)$$

A cyclic identification test similar to the well-documented "largest normalized residual test" for bad data [111] can be designed to identify and remove parameter errors. The test is used simultaneously on normalized residuals $r_i^{\mathcal{N}}$ and $\lambda_i^{\mathcal{N}}$ since both are expected to have the same standard normal distribution in the absence of gross errors. Once the state estimator converges, $|r_i^{\mathcal{N}}|$ and $|\lambda_i^{\mathcal{N}}|$ are calculated and ranked in descending order. Starting from the largest, the corresponding measurement or parameter is flagged if the value exceeds the detection threshold which is commonly set equal to 3.0. Flagged parameters or measurements are corrected using the linearized model as follows [112]:

$$p_{\text{corr},i} = p_{\text{bad},i} - \lambda_i/\Lambda_{ii} \tag{50}$$

$$z_{\text{corr},i} = z_{\text{bad},i} - r_i/\mathcal{S}_{ii} \tag{51}$$

where $\mathcal{S}_{ii}$ is $i-$the diagonal element of matrix $\boldsymbol{\mathcal{S}} = (\mathbf{I} - \mathbf{H_x}\mathbf{G}^{-1}\mathbf{H_x^\top}\mathbf{R}^{-1})$ and subscripts "corr" and "bad" refer to "corrected" and "erred" parameters.

The corresponding computational burden is proportional to the number of detected measurements and parameter errors due to the iterative nature of the process. However, parameter errors do not have to be identified online at every state estimation run, they can be tested periodically once every day, week, or season based on the system operator's judgment. More details on the computational shortcuts in calculating $\mathbf{\Lambda}$, detectability and identifiability of parameters, parameters with low sensitivities, and ways of handling such parameters via the use of successive scans can be found in [110], [112], [113].

b) Robust online approach for detecting parameter errors: As discussed in section IV-A1, the parameter error detection and estimation are typically addressed as a post-estimation function either as an off-line procedure [13], [109], [110], [114], [115] or an on-line augmented state approach [116]–[120] with a limited predetermined set of suspect parameters. Those approaches that formulate the problem as an extension of state estimation by augmenting the state vector with unknown parameters are unreliable due to the difficulty in differentiating between measurement and parameter errors which impact the residuals simultaneously.

The use of an inherently robust estimation method such as least absolute value (LAV) may be a possible solution provided that errors in measurements and parameters are simultaneously processed and differentiated. In attempting to formulate this problem, the following observation can be exploited: while measurement errors are widespread, i.e. they are present in all measured quantities with an expected normal distribution, parameter errors are quite sparse affecting only a small subset of the system parameters. This observation can be used to modify the ℓ_1-norm minimization of the absolute values of measurement residuals and add a penalty term that penalizes the ℓ_1-norm of the parameter errors.

Consider the first-order linear approximation of the measurement equation (37):

$$\Delta\mathbf{z} = \mathbf{H_x}\Delta\mathbf{x} + \mathbf{H_p}\Delta\mathbf{p} + \mathbf{e} \tag{52}$$

where $\Delta\mathbf{p}$ is the correction on the parameter vector. At this point, let us exploit the above stated observation that parameter errors typically occur in a small percentage of the network elements and therefore $\Delta\mathbf{p}$ can be considered a sparse vector. Furthermore, parameter errors that remain Gaussian with variances commensurate with measurement error variances can be ignored given the uncertainties in measurements. Hence, the objective of the formulation is to identify and correct gross errors in the "unknown sparse set" of parameters which will appear as significantly large entries in $\Delta\mathbf{p}$. Hence, the penalty term in form of ℓ_1-norm of $\Delta\mathbf{p}$ can be added to the LAV objective function yielding the following modified LAV optimization problem [121]:

$$\min \|\mathbf{r}\|_1 + \|\Delta\mathbf{p}\|_1 \tag{53}$$

$$\text{subject to } \Delta\mathbf{z} = \mathbf{H_x}\Delta\mathbf{x} + \mathbf{H_p}\Delta\mathbf{p} + \mathbf{r} \tag{54}$$

Note that the solution of the above optimization problem yields nonzero entries in $\Delta\mathbf{p}$ only for those parameters which have gross errors. Otherwise, the parameters are not changed and values taken from the existing database are used without change. Consequently, this formulation has the advantage that gross measurement errors are automatically rejected without having any influences of parameter errors, since parameter errors are corrected by the sparse $\Delta\mathbf{p}$ estimate. The incorrect parameters can be identified and their corrected values recovered by inspecting $\Delta\mathbf{p}$ once the optimization solution is obtained.

An important detail which should be addressed is the fact that in the augmented objective function (53) measurement residuals and parameter error corrections are assigned equal weights. Even though both are expressed in per unit, depending on the type of parameters residuals and parameter errors may not be compatible leading to implicit bias in the optimization. To address this issue, proper weights can be assigned to $\Delta\mathbf{p}$ terms using normalization among measurement residuals and parameter errors. Note that in case of an error in parameter i, Δp_i's impact is magnified by $\mathbf{H_p}(\cdot, i)$ (ith column) on the measurement residuals. $\mathbf{H_p}$ being a sparse matrix, the expected magnification of Δp_i is given by the expected value of the absolute nonzero entries of the corresponding column in $\mathbf{H_p}$:

$$d_i = \mathbb{E}\{|\mathbf{H_p}(\cdot, i)| \ \text{ for } \mathbf{H_p}(\cdot, i) \neq 0\} \tag{55}$$

where $\mathbb{E}$ represents the mean (expected) value.

Defining the diagonal matrix $\mathbf{D}$ whose elements are given by d_i, (53) can be replaced by the following formulation removing the implicit bias from the objective function:

$$\min_{\Delta\mathbf{p}} \|\mathbf{r}\|_1 + \|\mathbf{D}\Delta\mathbf{p}\|_1 \tag{56}$$

$$\text{subject to } \Delta\mathbf{z} = \mathbf{H_x}\Delta\mathbf{x} + \mathbf{H_p}\Delta\mathbf{p} + \mathbf{r} \tag{57}$$

The solution of this optimization problem can be obtained by first converting it into an equivalent linear programming (LP) problem and then using any of the existing efficient LP solvers. Note that $\Delta\mathbf{p}$ is expected to be sparse since only a small percentage of the network parameters' errors will be significantly large. In this respect, the second term in the objective function facilitates the removal of only such gross parameters errors while the first term enables bad measurement rejection simultaneously. This optimization problem can be readily formulated as an equivalent LP problem and solved efficiently by commonly available sparse LP solvers. More details can be found in [121].

2) Identification of Erroneous Topology: Network connectivity is commonly established by the topology processor (TP) which receives the status of switches and circuit breakers represented by detailed node-breaker (NB) models of substations and builds the bus-branch (BB) model of the power system. While electrically equivalent, NB and BB models do not carry the same information since the flow measurements through closed breakers are not usable. If a closed breaker is opened during a fault or planned substation reconfiguration, a topology error is created until its new status is reported to the TP.

Such errors are difficult to identify by the state estimator's traditional bad data processing function since it is designed to suspect only measurement errors assuming perfect knowledge of network topology.

Early works in detecting topology errors have been limited to incorrect branch status cases using the BB models [122], [123]. This limitation is later removed by using the NB models and augmenting the state vector by flows through breakers as introduced and described in [124]–[126]. While quite effective, this approach results in a heavy computational burden due to the significantly increased size of the augmented state vector. The computational complexity could be addressed by first localizing the suspect area and then applying the NB model to a small subsystem enclosing the suspect area as discussed in [127]–[131]. Formulation of the state and topology estimation based on the NB model of the network is described below.

a) Augmented SE Using Node-Breaker (NB) Model: Use of power flows through breakers as additional system states [124], [125] modifies the measurement equations by introducing a $(m \times l)$ measurement to breaker incidence[4] matrix ($\mathbf{H}_m$), m and l being the number of measurements and breakers, respectively:

$$\mathbf{H}_{m,i,j} = \begin{cases} 1 & \text{if measurement } i \text{ is incident to} \\ & \text{from-bus of breaker } j \\ -1 & \text{if measurement } i \text{ is incident to} \\ & \text{to-bus of breaker } j \\ 0 & \text{otherwise} \end{cases} \tag{58}$$

Let the vector of newly added breaker flow variables be denoted by $\mathbf{f}$. Then, the measurement equations of (4) can be re-written as:

$$\mathbf{z} = \mathbf{h}(\mathbf{x}, \mathbf{f}) + \mathbf{e} \tag{59}$$

where, $\mathbf{z} \in \mathbb{R}^m$, $\mathbf{x} \in \mathbb{R}^s$, $\mathbf{f} \in \mathbb{R}^l$ and $\mathbf{e} \in \mathbb{R}^m$ are the measurements, bus voltages, breaker flows and measurement errors, respectively. The following first order approximation of the measurement equations (59) around $(\mathbf{x}_0, \mathbf{f}_0)$ can be used to iteratively solve for the augmented states:

$$\Delta\mathbf{z} = \left[\mathbf{H}_\mathbf{x}\, \mathbf{H}_m\right] \begin{bmatrix} \Delta\mathbf{x} \\ \Delta\mathbf{f} \end{bmatrix} + \mathbf{e} \tag{60}$$

where, $\Delta\mathbf{z} = \mathbf{z} - \mathbf{h}(\mathbf{x}_0, \mathbf{f}_0)$, $\dfrac{\partial \mathbf{h}}{\partial \mathbf{x}} = \left[\mathbf{H}_\mathbf{x}\, \mathbf{H}_m\right]$ at $\mathbf{x}_0$, $\Delta\mathbf{x} = \mathbf{x} - \mathbf{x}_0$, and $\Delta\mathbf{f} = \mathbf{f} - \mathbf{f}_0$.

Using a typical substation example modeled by NB models as shown in Fig. 2, a number of virtual measurements can be created from equality constraints. The voltage magnitude and phase angle across a closed breaker between nodes s and t denoted by $|v_s|, |v_t|$ and θ_s, θ_t, respectively satisfies:

$$|v_s| - |v_t| = 0 \text{ and } \theta_s - \theta_t = 0 \tag{61}$$

Similarly, for an open breaker zero flows for the active (P) and reactive (Q) power can be included as:

$$P_{st} = 0 \text{ and } Q_{st} = 0 \tag{62}$$

[4] The incidence matrix is very useful in formulating multiple functions (including fault locations as in [132], [133]) due to its capability to compactly defining buses-to-branches connectivity.

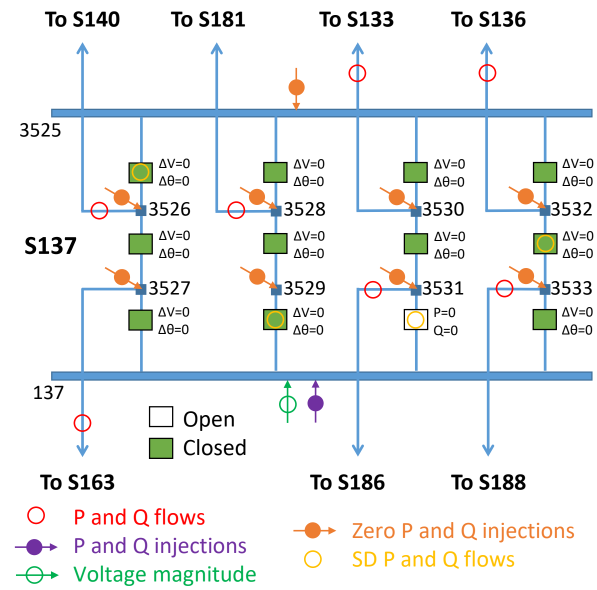

Fig. 2. Node breaker model of a typical substation

For example, applying (61) and (62) to the substation shown in Fig. 2, results in 22 constraints for the closed breakers and 2 null (active and reactive) power flow constraints for one open breaker that can be added to the existing measurement set. Similarly, 9 zero injections[5] are available at the newly created nodes within the substation.

All of these additional equality constraints can be compactly written in terms of the augmented set of states:

$$\mathbf{c}(\mathbf{x}, \mathbf{f}) = 0 \tag{63}$$

The final estimation problem is composed of (60), (61), (62) and (63) can be cast into a constrainted WLS regression problem where the objective is to estimate $\mathbf{f}$. This can be accomplished via several different computationally efficient implementations, a detailed description of one possible alternative can be found in [134].

B. Line Parameter Estimation

1) Transmission and Distribution Systems Models: For distribution networks, the three-phase π and T-circuit representations are the most adopted models in order to capture the common lack of conductors transposition. In some cases, a single-phase model may be considered in the presence of conductors transposition or as an approximated model when the conductors electromagnetic coupling is neglected [61], [135]–[141].

[5] Substation node-branch diagram will contain several nodes which are incident to breakers and lines without any external source or loads connected to them. Such nodes will constitute the so called "zero injection nodes" since the net injections are known to be zero without requiring explicit injection measurements to be taken at those nodes. Such zero injections are referred in the literature as "virtual" measurements and they boost measurement redundancy as well as accuracy since they do not carry any measurement errors. They are error-free measurements to be used by the state estimator in the form of true equalities.

The classical π-model representation of a power system line is shown in Fig. 3. It provides an exact circuit representation of the solution of the telegraphers equations for a fixed frequency. In a three-phase system, the line impedances and shunt admittances are represented by 3×3 matrices.

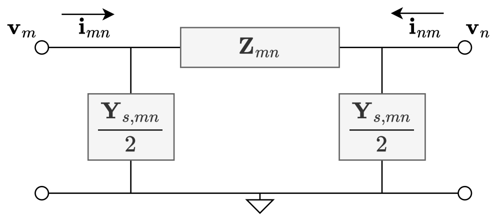

Fig. 3. Generic multi-phase $\pi-$ line model.

Moreover, the $T-$ model simplification of a power-line is shown in Fig. 4 which relates the voltages to the currents through impedance.

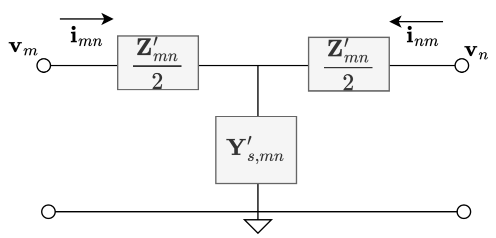

Fig. 4. Generic multi-phase $T-$ line model.

The longitudinal impedance matrix $\mathbf{Z}_{mn}, \mathbf{Z}'_{mn} \in \mathbb{C}^{3\times3}$ and the shunt elements matrix $\mathbf{Y}_{s,mn}, \mathbf{Y}'_{s,mn} \in \mathbb{C}^{3\times3}$ can be represented as

$$\mathbf{Z}_{mn} = \mathbf{R}_{mn} + j\omega\mathbf{L}_{mn} \tag{64}$$

$$\mathbf{Y}_{s,mn} = \mathbf{G}_{s,mn} + j\omega\mathbf{C}_{s,mn} \tag{65}$$

where $\mathbf{R}_{mn} \in \mathbb{R}^{3\times3}$ and $\mathbf{L}_{mn} \in \mathbb{R}^{3\times3}$ are longitudinal resistance and inductance matrices, respectively, and $\mathbf{G}_{s,mn} \in \mathbb{R}^{3\times3}$ (often assumed negligible as in the positive-sequence model) and $\mathbf{C}_{s,mn} \in \mathbb{R}^{3\times3}$ are shunt conductance and capacitance matrices, respectively. The impedance and admittance matrices in π and $T-$ model representation are equal for the case of short-line approximation i.e., when $\mathbf{Z}_{mn}\mathbf{Y}_{s,mn} \approx \mathbf{0}$ holds true.

Here, $\omega = 2\pi f$, f being the system frequency. Figure 3 also reports the quantities of interest to be measured, which are the voltage phasors at the nodes and the branch current phasors as seen from the sending and receiving line terminals (or nodes). The three-phase node voltage phasors (indicated by vectors $\mathbf{v}_m \in \mathbb{C}^3$ and $\mathbf{v}_n \in \mathbb{C}^3$ at two ends) relate to the three-phase current phasors ($\mathbf{i}_{mn} \in \mathbb{C}^3$ and $\mathbf{i}_{nm} \in \mathbb{C}^3$) by using these admittances as in [142]–[148] and in [149].

Typically, the shunt admittance can be neglected in low-voltage distribution systems as well as for short overhead lines in medium voltage systems [150]–[152]. However, in the case of long medium voltage overhead and/or coaxial cable lines, the shunt elements should be taken into account.

For transmission lines, the π-model can be reduced to its equivalent single-phase model as they are typically transposed. The single-phase model corresponds to the positive sequence component [60], [153]–[169] and the elements $\mathbf{R}_{mn}, \mathbf{L}_{mn}, \mathbf{G}_{s,mn}, \mathbf{C}_{s,mn}$ reduce to scalar quantities. In this case, the positive sequence measurements from the measurement units (which can be computed in the post-processing from phase measurements) can be used for the estimation. Shunt conductance can be typically neglected in transmission systems.

In a case where more than three conductors are present, for instance, due to the presence of a neutral conductor, Kron reduction can be applied to reduce the generic impedance/admittance matrices to 3×3 matrices. A frequently adopted circuital model is represented in Fig. 5, where, in the case of a three-phase system with neutral conductor, the mutual resistances, $R_{mn,pq}$, and reactances, $X_{mn,pq}$, with $p, q \in \{a, b, c\}$, allow to consider also the effects of current circulation in the neutral conductor on the other phases of the system.

In some research works, the π-model with concentrated parameters for longer lines is rewritten in terms of distributed parameters and in particular of the characteristic impedance and propagation constant of the line [19], [170]–[173].

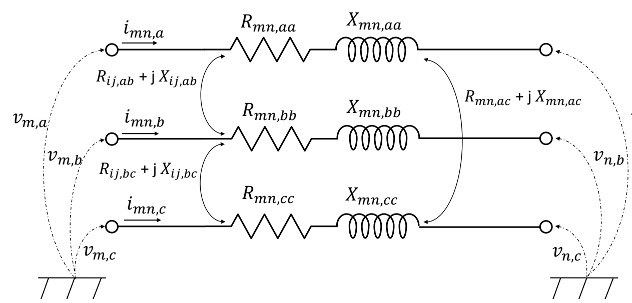

Fig. 5. A circuital model in the case of a three-phase system with neutral conductor.

2) Admittance, Impedance and Transmittance Matrices for a Line: based on the aforementioned matrices defining the general line model, i.e. $\mathbf{Z}_{mn}$ and $\mathbf{Y}_{s,mn}$, different specific estimation models have been used, depending also on the available measurements. These are reviewed below.

a) Admittance-line model: relies on the $\pi-model$ representation of the power line as shown in Fig. 3; the line current synchrophasors at the two ends can be expressed as

$$\begin{bmatrix} \mathbf{i}_{mn} \\ \mathbf{i}_{nm} \end{bmatrix} = \begin{bmatrix} \mathbf{Z}_{mn}^{-1} + \dfrac{\mathbf{Y}_{s,mn}}{2} & -\mathbf{Z}_{mn}^{-1} \\ -\mathbf{Z}_{mn}^{-1} & \mathbf{Z}_{mn}^{-1} + \dfrac{\mathbf{Y}_{s,mn}}{2} \end{bmatrix} \begin{bmatrix} \mathbf{v}_m \\ \mathbf{v}_n \end{bmatrix} \tag{66}$$

In [14]–[19], [143], [144], [174], the line currents and nodal voltage measurements from the PMUs are used for the estimation of the line and shunt parameters, i.e., $\mathbf{Z}_{mn}$ and $\mathbf{Y}_{s,mn}$. In this case, (66) can be expressed as follows

$$\begin{bmatrix} \mathbf{i}_{mn}^\top \\ \mathbf{i}_{nm}^\top \end{bmatrix} = \begin{bmatrix} \mathbf{v}_m^\top - \mathbf{v}_n^\top & \dfrac{\mathbf{v}_m^\top}{2} \\ \mathbf{v}_n^\top - \mathbf{v}_m^\top & \dfrac{\mathbf{v}_n^\top}{2} \end{bmatrix} \begin{bmatrix} (\mathbf{Z}_{mn}^{-1})^\top \\ \mathbf{Y}_{s,mn}^\top \end{bmatrix} \tag{67}$$

The proposed approaches in [135], [136], [158], [175]–[178] utilize power injections and voltage measurements from RTUs [179], [180] instead of voltages and current phasor measurements whereas [181], [182] uses smart meter data on nodal power injections and voltages for the estimation. In some cases, both the power and current measurements are used for parameter estimation [183] along with the nodal voltage phasor measurements.

b) Impedance-line model: relies on $T-$ model of a power-line as illustrated in Fig. 4. The relation between voltage and currents can be also expressed in terms of the impedances given by

$$\begin{bmatrix}\mathbf{v}_m\\ \mathbf{v}_n\end{bmatrix} = \begin{bmatrix}\dfrac{\mathbf{Z'}_{mn}}{2}+\mathbf{Y'}^{-1}_{s,mn} & \mathbf{Y'}^{-1}_{s,mn}\\ \mathbf{Y'}^{-1}_{s,mn} & \dfrac{\mathbf{Z'}_{mn}}{2}+\mathbf{Y'}^{-1}_{s,mn}\end{bmatrix}\begin{bmatrix}\mathbf{i}_{mn}\\ \mathbf{i}_{nm}\end{bmatrix}. \tag{68}$$

This line model can be used for estimating the line and shunt admittances by rewriting (68) as

$$\begin{bmatrix}\mathbf{v}_m^\top\\ \mathbf{v}_n^\top\end{bmatrix} = \begin{bmatrix}\dfrac{\mathbf{i}_{mn}^\top}{2} & \mathbf{i}_{mn}^\top+\mathbf{i}_{nm}^\top\\ \dfrac{\mathbf{i}_{nm}^\top}{2} & \mathbf{i}_{mn}^\top+\mathbf{i}_{nm}^\top\end{bmatrix}\begin{bmatrix}\mathbf{Z'}^\top_{mn}\\ (\mathbf{Y'}^{-1}_{s,mn})^\top\end{bmatrix}. \tag{69}$$

Such a scheme is used in [144] and compared against the admittance estimation model.

c) Transmittance model: Sending-end currents and voltages can be linked to the corresponding values at the receiving end as follows [184]

$$\begin{bmatrix}\mathbf{v}_m\\ \mathbf{i}_{mn}\end{bmatrix} = \begin{bmatrix}\mathbf{I}+\dfrac{\mathbf{Z}_{mn}\mathbf{Y}_{s,mn}}{2} & -\mathbf{Z}_{mn}\\ \mathbf{Y}_{s,mn}\left(\mathbf{I}+\dfrac{\mathbf{Z}_{mn}\mathbf{Y}_{s,mn}}{4}\right) & -\left(\mathbf{I}+\dfrac{\mathbf{Z}_{mn}\mathbf{Y}_{s,mn}}{2}\right)\end{bmatrix}\begin{bmatrix}\mathbf{v}_n\\ \mathbf{i}_{nm}\end{bmatrix} \tag{70}$$

where $\mathbf{I}\in\mathbb{R}^{3\times3}$ is identity matrix. This model is also referred to as the two-port network model and transmittance model [144].

In (70), the term $\mathbf{Z}_{mn}\mathbf{Y}_{s,mn}$ can be approximated as null matrix $\mathbf{0}\in\mathbb{C}^{3\times3}$ for electrically short lines [185], i.e., $\mathbf{Z}_{mn}\mathbf{Y}_{s,mn}\approx\mathbf{0}$. Then, (70) results in

$$\begin{bmatrix}\mathbf{v}_m\\ \mathbf{i}_{mn}\end{bmatrix} \approx \begin{bmatrix}\mathbf{I} & -\mathbf{Z}_{mn}\\ \mathbf{Y}_{s,mn} & -\mathbf{I}\end{bmatrix}\begin{bmatrix}\mathbf{v}_n\\ \mathbf{i}_{nm}\end{bmatrix} \tag{71}$$

This approximation is often referred to as the "short-line approximation" and it has been observed that this approximation holds accurate even for electrically medium length lines [185], operating at very high rated voltages (e.g., 380 kV).

For this, the estimation model can be expressed as

$$\begin{bmatrix}\mathbf{v}_m^\top\\ \mathbf{i}_{mn}^\top\end{bmatrix} = \begin{bmatrix}-\mathbf{i}_{nm}^\top & \mathbf{0}\\ \mathbf{0} & \mathbf{v}_{nm}^\top\end{bmatrix}\begin{bmatrix}\mathbf{Z}_{mn}^\top\\ \mathbf{Y}_{s,mn}^\top\end{bmatrix} + \begin{bmatrix}\mathbf{v}_n^\top\\ -\mathbf{i}_{nm}^\top\end{bmatrix} \tag{72}$$

This model is widely used for transmission line parameter estimation, e.g. in [14], [18], [171], [186]–[190].

When dealing with network model identification, in addition to line parameter models, network branches equipped with tap-changing transformers also need to be modeled. Tap changer ratios cannot be perfectly known and uncertainty is inevitable [191] although the knowledge of the transformer's tap changers ratio is essential for different monitoring tools, including state estimation [192]. Several papers tackle the problem of the estimation of the transformer tap changer ratio by considering an equivalent single-phase model like the one reported in Fig. 6 (i.e., an impedance in series $y^{\mathrm{off}}_{\mathrm{sc},sr}$ with off-nominal turn ratio) in contexts like state estimation [193]–[196] and line parameters estimation [170], [171]. The model in Fig. 6 is included in the estimators through its equivalent π-model. It is interesting to note that in such model the off-nominal short circuit admittance $y^{\mathrm{off}}_{\mathrm{sc}_{sr}}$ should be defined more generally considering also the ratio between the impedance of the winding without the tap changer and one of the tapped winding through an additional parameter k [197], which impacts parameters and tap ratio estimation [198].

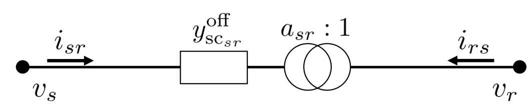

Fig. 6. Tap-changing transformer model with short circuit impedance at the off-nominal turns side.

A single-phase equivalent model of the transformer is used in [172] which estimates only the positive-sequence component. However, other papers (e.g., [146], [199]) have considered the three-phase transformer's model.

These network models from Sec. IV-B can be integrated into the measurement functions in the estimation model given in (6f), where the quantities on voltages, currents and powers are obtained from PMUs or RTUs and the parameters to estimate are the line admittances and impedances. This is often achieved by separating the complex equations into their real and imaginary components and stacking them (for example [144]). In the following, we discuss different estimation methods, differing by how the estimation is carried out, i.e. offline or online, and if measurement noise is taken into account.

3) Offline Estimation Methods: it is assumed that the parameters remain constant over time, therefore, in such a case the estimations can be conducted offline. Offline estimation approaches leverage historical measurements that are stacked together to obtain an over-determined system to improve the accuracy of the estimates. In the following, we review different works in the literature grouped based on the assumptions made on the measurement noise.

a) Negligible Measurement Noise: the basic regression-based schemes such as OLS and WLS [135], [143], [179] are the most adopted estimation methods for line parameter estimation. In these estimation methods, the measurement noise is ignored [17], [175], [181], [200]–[202], although, this assumption is not representative of a real-life scenario. The OLS and WLS estimation methods are described briefly in Sec.III-B3. As stated before, these methods suffer from several issues such as unrealistic noise hypothesis, multi-collinearity, etc.

b) Realistic Measurement Noise Models, Homoscedastic Covariance Matrix: as shown in [144], OLS and WLS-based estimation methods fail when the measurement noise is significant leading to non-negligible noise on the matrix $\mathbf{H}$ violating the assumption made in the OLS and WLS methods. In such a case, error-in-variables (EIV) schemes such as TLS [136] (briefly discussed in Sec. III-B2) are proposed. These schemes consider the noise on both $\mathbf{z}$ and $\mathbf{H}$ but it is assumed that the noise covariance matrix is homoscedastic. It should be noted that when TLS is fed with a large number of measurements (with non-negligible noise), it attempts to estimate a large number of variables, namely the measurement errors along with the line parameters. This results in poor estimates as reported in [203]. One way to overcome this problem is by pre-filtering the measurement data in order to reduce the noise as proposed in [183], [204].

c) Realistic Measurement Noise Models, Heteroscedastic Covariance Matrix: in real life, the covariance matrices $\mathcal{Q}_{\mathbf{z}}, \mathcal{Q}_{\mathbf{x}}$ may be heteroscedastic, i.e., their diagonal elements are not equal. Consequently, the ordinary TLS scheme cannot be applied as it violates the homoscedastic noise assumption. Alternatively, the estimation scheme can be formulated as a Maximum Likelihood Estimation (MLE) problem, i.e. it is expressed as an optimization problem to maximize the log-likelihood function as given in (6). The optimization problem is inherently non-convex, and only local solutions can be obtained. In [72], methods to obtain solutions for this problem are presented. In [136], [182], an MLE-based approach is proposed by deriving a WTLS problem that is solved using the stochastic gradient descent (SGD) algorithm. As expected, however, a global optimum solution cannot be guaranteed.

4) Online Estimation Methods: traditionally it is assumed that the line parameters are constant as they are determined based on conductor size, type and tower geometry [205], [206]. Calculated values are stored in databases and usually remain unchanged for long periods despite the fact that parameters change due to ambient conditions, line maintenance, or changes in tower configurations. Thus, it is preferable to monitor and track line parameters using online SCADA or PMU measurements.

Most of the work done in online estimation involves positive sequence model parameters [207]–[218]. Methods to track untransposed line parameters have also been investigated [14], [219]–[222]. The main issue of rank deficiency of the measurement-parameter coefficient matrix is commonly addressed by multi-scan measurements [14], [209]–[211], [220]–[223] assuming that parameters remain unchanged for the multi-scan duration. This raises numerical issues since voltages also remain nearly unchanged during this period. A better alternative is to implement a dynamic estimator as done in [212], [213], [224] with state augmentation. However, this approach is vulnerable to convergence issues when applied to non-transposed lines. In [18], [19], [183], the OLS and WLS are solved repeatedly with new measurements, however without using the previous estimates of the line parameters. In such schemes, estimations are performed with measurements in a moving window fashion. In many cases, the recursive estimation algorithms are utilized where the previous estimates and new measurements are used per estimation iteration. These schemes propagate information from the previous estimations using some forgetting factor. For example in [19], a recursive least squares (RLS) algorithm (Sec. III-B8a) is used for the estimation of transmission line parameters. In [89]–[94], [188], Kalman filtering (Sec. III-B8b) is used for the estimation of the line parameters.

C. Joint Estimation Methods

The problem of joint state and parameter estimation appears when both the states and unknown parameters of a system must be estimated simultaneously from available measurements. This task is particularly challenging due to two major factors: observability and correlation between states and parameters. Regarding the former challenge, in many cases, the combined estimation of the system of states and parameters lacks sufficient measurement redundancy, making the estimation difficult or even infeasible. Regarding the latter, states and parameters are often interdependent, creating correlated estimation errors where inaccuracies in one can propagate into the other, leading to poor overall estimation performance. Effective strategies, such as staged or sequential estimation techniques, are therefore essential to manage these challenges by decoupling the estimation processes and improving the adverse effects of correlations on estimation accuracy.

In the following, we discuss two different joint estimation techniques. In the first, state and parameter estimation problems are tackled jointly, whereas in the second, systematic errors and parameter estimation problems are tackled jointly.

1) Joint State Estimation and Parameter Tracking: Joint estimation of state and line parameters allows accounting for the varying nature of the line parameter in the state estimation problem [212]–[218] and is numerically robust and computationally viable as shown in [225] for a fully coupled three-phase transmission line. This algorithm alternates between state estimation, which relies on the most recent parameter estimates and filters the voltage and current measurement noise, and parameter tracking, which relies on the most recent state estimates and filters the current measurement noise. Thus, the mismatch between the actual and estimated parameters is minimized.

Considering the varying nature of the parameters, the measurement model of (4) can be written with subscript k as

$$\mathbf{z}_k = \mathbf{h}(\mathbf{x}_k, \mathbf{p}_k) + \mathbf{e}_k \tag{73}$$

The estimation of state $\mathbf{x}_k$ and $\mathbf{p}_k$ in (73) is carried out iteratively by iterating between a static estimation to determine $\mathbf{x}_k$ assuming $\mathbf{p}_k$ is known and parameter estimation using the previously determined values for $\mathbf{x}_k$. Iterations are terminated upon convergence to the desired state and parameter estimates. In the following, we describe in more detail these steps.

a) State estimation: The process starts with the formulation of the measurement equations

$$\mathbf{z}_k = \mathbf{H}_{\mathbf{p},k}\, \mathbf{x}_k + \boldsymbol{\delta}_{x,k} \tag{74}$$

where $\boldsymbol{\delta}_{x,k}$ is measurement noise with zero mean and covariance $\mathbf{R}_x$ and $\mathbf{H}_{\mathbf{p},k}$ is the measurement jacobian at time k defined as $\mathbf{H}_{\mathbf{p},k} = \begin{bmatrix} \mathbf{I}_{4n_p \times 4n_p} \\ \breve{\mathbf{H}}_{\mathbf{p},k} \end{bmatrix} \in \mathbb{R}^{8n_p \times 4n_p}$ where $\mathbf{I}_{4n_p \times 4n_p}$ indicates an identity matrix and $\breve{\mathbf{H}}_{\mathbf{p},k} \in \mathbb{R}^{4n_p \times 4n_p}$ is constructed by the most recent parameter estimates $\widehat{\mathbf{p}}_k$. The WLS estimator for $\mathbf{x}_k$ as described in section III-B3 can be used to estimate the state. If there is a wide-area linear state estimator, raw PMU measurements at line terminals can be replaced by their estimated values improving the estimator.

b) Parameter estimation: Current flows measured at line terminals are used to track the parameters leveraging

$$\mathbf{i}_k = \mathbf{H}_{\mathbf{x},k}\ \mathbf{p}_k + \boldsymbol{\delta}_{\mathbf{p},k} \tag{75}$$

where $\boldsymbol{\delta}_{\mathbf{p},k}$ is the measurement noise with zero mean and covariance $\mathbf{R}_{\mathbf{p}}$.

We further assume that parameters have a prediction model that leaves the values unchanged except for the zero-mean disturbance:

$$\mathbf{p}_k = \mathbf{p}_{k-1} + \mathbf{w}_{\mathbf{p},k} \tag{76}$$

where $\mathbf{w}_{\mathbf{p},k}$ is the noise due to ambient conditions distributed with zero mean and covariance $\mathcal{Q}_{\mathbf{p}}$. The well documented recursive steps of the Kalman filter described also in section III-B8b using the state dynamics (76) and measurement model (75) are carried out iteratively at each measurement scan yielding an online parameter tracking tool for all line elements (i.e., real and imaginary parts of $\mathbf{Z}_{mn}$).

2) Joint Parameter and Systematic Errors Estimation: Considering the error model in (1) and (2), systematic error contributions can strongly affect parameters estimation and therefore need to be compensated. The methods illustrated in Section IV typically rely on multiple measurement sets corresponding to different snapshot of the monitored quantities, i.e., to different timestamps, which however consistently include the systematic errors. Hence, methods have been proposed to reduce their impact on the estimation of the network model or to estimate them together with the model. The systematic errors estimation leads also to the favourable side-effect of computing compensation factors or offsets to improve the measurement chain and, in particular, the IT effects.

In [142], voltage and current synchrophasor calibration factors are introduced and the availability of pre-calibrated ITs and PMU at a bus of the network is assumed as a starting point for the estimation procedure which is based on ordinary LS and Newton-Raphson iterations. Similarly, in [156] complex calibration factors for positive-sequence synchrophasors at the end node of a transmission line are estimated together with the line parameters through LS, starting from a calibrated measurement chain at the start node. A bias error detection test to identify major systematic errors in ITs is also introduced. In [226], the errors are attributed to the positive sequence voltage and current synchrophasor measurements at the beginning of a line. The systematic phase error of the voltage and systematic magnitude error of the current are neglected, thus addressing the simultaneous line parameters estimation and the compensation of the other systematic measurement errors. The method relies on the minimisation of the sum of the squared correlation coefficients between the line parameters obtained directly from measurements and the sum of the squared current magnitudes measured at the ends of the line. Using one calibrated end as reference, [150] introduces lump compensation factors with equivalent effects on the three-phase PMU measurements at the other end before estimating them through LS together with the line parameters. In [157], positive-sequence equivalent line parameters including IT errors are estimated with multiple applications of LS using different sets of PMU measurements and then, starting from a node with calibrated measurements, the calibration is propagated to a portion of the network. In [161], a detection method for significant systematic errors in VTs is proposed and, assuming VTs and CTs at the sending node as calibrated, positive sequence transmission line parameters are estimated through LS together with correction factors for the end node.

A different approach is proposed in [61] and [152] for distribution networks (single-phase and three-phase model, respectively) and in [163] for transmission networks. Including all the systematic errors as additional unknowns in the estimation process, an improved estimation of line parameters on multiple network branches is accompanied by the estimation of magnitude and phase-angle systematic errors. The method leverages prior knowledge on ITs and PMUs accuracy (within a WLS framework in [61] and [152] and a Tikhonov regularisation of the WLS in [163]) and allows computing compensation factors for all the measured quantities. It is robust with respect to measurement error model mismatch and can exploit correlations in PMU measurement channels [227]. In [146], this approach is extended also to tap changer ratio estimation. In [63], the complex behaviour of CTs systematic errors under varying current levels in distribution lines is considered through an extension of the estimation framework.

D. Compound Admittance Matrix Estimation Models

1) Compound Admittance Matrix: the admittance matrix plays a pivotal role in power systems research due to its use in numerous applications and strong relation to the underlying network parameters and topology. Here, we review the problem and the proposed solutions for estimating the parameters of the admittance matrix of single- and three-phase power networks using phasor measurements of bus voltages and nodal current injections.

We consider the generic case of an unbalanced, polyphase power network composed of N_b polyphase nodes $\mathcal{N}_b = \{1, \ldots, N_b\}$, a node $\{0\}$ which represents the common electrical ground, and N_e undirected edges $\mathcal{E} \subseteq \mathcal{N}_b \times \mathcal{N}_b$. A polyphase node consists of N_p different terminals (phases) collected in the set $\mathcal{F} = \{1, 2, \ldots, N_p\}$. The network can thus be represented by a connected undirected graph $\mathcal{G} := (\mathcal{N}_b, \mathcal{E})$ with edges weighted by complex $N_p \times N_p$ matrices $\mathbf{y}_{ij}$. Reciprocity of the electromagnetic effects renders $\mathbf{y}_{ij}$ symmetric for all $(i, j) \in \mathcal{E}$. Admittances connected to the ground node $\mathbf{y}_{i0}$ may also exist at nodes $i \in \mathcal{N}_b$ and possess the same properties as the series admittances. Three matrices associated with the weighted graph model can now be introduced, namely the primitive compound admittance matrix $\mathbf{Y}_{\mathcal{L}}$, the primitive compound shunt admittance matrix $\mathbf{Y}_{\mathcal{T}}$, and the polyphase incidence matrix $\mathbf{A}_{\mathcal{P}}$, defined by [228]:

$$\begin{aligned}\mathbf{Y}_{\mathcal{L}} &= \operatorname{blkdiag}(\{\mathbf{y}_e\}_{e=1}^{N_e}),\\ \mathbf{Y}_{\mathcal{T}} &= \operatorname{blkdiag}(\{\mathbf{y}_{i0}\}_{i=1}^{N_b}),\\ \mathbf{A}_{\mathcal{P}} &= \mathbf{A} \otimes \mathbf{I}_{N_p},\end{aligned}$$

where $e \in \{1, \ldots, N_e\}$ is a unique identifier assigned to each edge, and $\mathbf{A} \in \{-1, 0, 1\}^{N_b \times N_e}$ is an incidence matrix of $\mathcal{G}$.

Each node $i \in \mathcal{N}_b$ in the network is associated with a polyphase nodal current injection $\mathbf{i}_i := (i_i^1, i_i^2, \ldots, i_i^{N_p}) \in \mathbb{C}^{N_p}$, and a polyphase nodal bus voltage $\mathbf{v}_i := (v_i^1, v_i^2, \ldots, v_i^{N_p}) \in \mathbb{C}^{N_p}$, collecting current injections and bus voltages of different phases defined with respect to the common electrical ground. Applying Kirchhoff's and Ohm's laws leads to the following model of polyphase networks:

$$\mathbf{i} = \mathbf{A}_{\mathcal{P}} \mathbf{Y}_{\mathcal{L}} \mathbf{A}_{\mathcal{P}}^{\top} \mathbf{v} + \mathbf{Y}_{\mathcal{T}} \mathbf{v} = \mathbf{Y} \mathbf{v}, \tag{77}$$

where $\mathbf{i} := (\mathbf{i}_1, \ldots, \mathbf{i}_{N_b})$ and $\mathbf{v} := (\mathbf{v}_1, \ldots, \mathbf{v}_{N_b})$ collect the current injections and bus voltages of all polyphase nodes. As can be seen from above, the compound admittance matrix $\mathbf{Y}$ is a complex block symmetric matrix with a graph Laplacian structure, whose diagonal $N_p \times N_p$ blocks are given by $\mathbf{Y}_{ii} = \sum_{j=1, j\neq i}^{n} \mathbf{y}_{ij} + \mathbf{y}_{i0}, \forall i \in \mathcal{N}_b$, and the off-diagonal blocks by $\mathbf{Y}_{ij} = -\mathbf{y}_{ij}, \forall \{i, j\} \in \mathcal{E}$ and $\mathbf{Y}_{ij} = \mathbf{0}_{N_p \times N_p}$ otherwise. We refer the reader to [228], [229] for a detailed analysis of the admittance matrix properties.

2) Formulating the Regression Problem: to apply the regression methods introduced in previous sections, the model in (77) needs to be transformed such that the parameters of the admittance matrix are the independent variables, as in (5a). First, as admittance matrices $\mathbf{y}_{ij}$ modeling lines $(i, j) \in \mathcal{E}$ and shunts $i \in \mathcal{N}_b, j = 0$ are symmetric, the lower-triangular entries entirely determine the parameters of each $N_p \times N_p$ block $\mathbf{Y}_{ij}$ of the admittance matrix, and therefore

$$\operatorname{vec}(\mathbf{Y}_{ij}) = \mathbf{D}_{N_p} \mathbf{p}_{ij},\ i = \{1, \ldots, N_b\},\ j = \{1, \ldots, N_b\}, \tag{78}$$

with $\mathbf{D}_{N_p}$ being the ${N_p}^2 \times N_p(N_p + 1)/2$ duplication matrix, and $\mathbf{p}_{ij} := \operatorname{vech}(\mathbf{Y}_{ij})$. Considering that $\mathbf{Y}$ is block-symmetric, we can apply block-vectorization[6] on (77) to obtain

$$\mathbf{i} = (\mathbf{v}^{\top} \otimes \mathbf{I}_{N_b \times N_p})(\mathbf{D}_{N_b} \otimes \mathbf{I}_{N_p^2})(\mathbf{I}_{N_b(N_b+1)/2} \otimes \mathbf{D}_{N_p})\mathbf{p}, \tag{79}$$

where $\mathbf{p}$ stacks the half-vectorized blocks $\mathbf{p}_{ij}$, collecting the admittance matrix parameters. The above equation brings the admittance matrix estimation problem into the desired form (5a).

3) Estimation Challenges: given measurements of nodal voltages and currents, estimation of the admittance matrix reduces to solving a (deceptively simple) linear regression problem (79). However, obtaining an estimate of $\mathbf{Y}$ is faced with several challenges. These challenges are either data-related or related to the admittance matrix structure and properties. As discussed previously, the admittance matrix is symmetric and, additionally, if the shunt admittances are neglected, or nonexistent, $\mathbf{Y}$ has zero row-sums. Furthermore, the admittance matrices are commonly sparse since most power systems are characterized by a large number of buses and low incidence. These properties are not guaranteed to hold for generic linear regression estimates and therefore need to be imposed or promoted in the regression problem. On the other hand, the data-related challenges are caused by the attributes of electrical measurements and their placement, i.e., measurement errors, multicollinearity, and incomplete network observability. Since the current injections/flows and bus voltages are obtained via synchrophasor measurements, both the dependent and the independent variables in (77) are corrupted by measurement noise. Moreover, measurements collected on different buses are observed to be highly correlated with each other due to the structure of the network and the low phase differences between nodes. Finally, not all the nodes in the network may be observed, and recovery of the unobserved nodes and line connections to or between them.

4) Solution methods: the OLS regression (15) is the most common and the most straightforward method considered in the literature [230]–[234]. In [230], a technique for estimating the admittance matrix by applying matrix least squares estimation to phasor measurements is presented. To enforce the Laplacian matrix structure in the least squares estimate, a constrained least squares approach is developed in [232]. A recursive least squares method (23) is introduced in [233] to enable frequent online updates instead of using batch processing. To enhance the least squares estimation when the admittance matrix is known to be sparse, [234] introduces a sparsity promoting ℓ_1-norm regularizer (16). However, these approaches assume noise-free measurements of the independent variables, which can lead to biased estimates when using realistic data with errors in all measurements.

To overcome this limitation, error-in-variables methods have been proposed [83], [204], [235], [236]. The work in [204] employs TLS (7) and demonstrates the performance improvement compared to OLS. A WTLS method (6) is introduced in [235], and then extended in [236] to a Bayesian framework that allows for exploiting different forms of prior knowledge of the admittance matrix. Finally, a well-conditioned Wiener filter method (22) was introduced in [83] to address the measurement multicollinearity.

The work in [232] shows that the Kron-reduced admittance matrix can be determined even if some nodes in the system are unobserved. An algorithm based on graph theory is proposed to uncover the actual admittance matrix of systems with unobserved nodes. Furthermore, it is shown that the recovery of unobserved nodes is unique only in the case of radial networks and not for general meshed systems. The work in [237] proposed a scheme to estimate topology using limited set of measurements. It uses a graph-theoretical approach where the network is partitioned into observable islands. It then presents a scheme for strategic sensor placement for recovery of the network topology.

5) Pre- and post-processing techniques: as discussed in [204], the estimation quality deteriorates with high measurement uncertainty, especially with the IT class above 0.5 and 1.0. In such a case, pre-processing of the measurements is

[6] Transforms $np \times m$ matrix into $npm \times 1$ vector by stacking $p \times 1$ blocks row by row through all m columns and for all n rows.

proposed which is designed to reduce the noise, therefore enhancing the estimation performance. The pre-processing schemes also help to remove repeated measurements, hence improving the conditionality of the measurement matrix. In [14], a moving window averaging on the raw data is proposed for improving TLS-based line parameter estimation by reducing the noise level. The method was proposed for the estimation of a transposed and balanced line and used measurements of nodal powers along with currents and voltages. In [204], another averaging approach using a k-means clustering method was proposed. In this case, the measurements are first clustered into different groups based on the features defined beforehand, then, in each of the clusters, the measurements are averaged (i.e., taking the centroid of each cluster as measurements). Such pre-processing scheme enhances the estimation performance by two to three orders of magnitude. It should be noted that such averaging schemes preserve the mathematical structure of the original formulation, provided that the parameter estimation model is linear (for example the line parameter models in Sec. IV-B.).

Post-filtering of the obtained admittance matrix estimate is also considered in the literature to refine the estimate. In [83], it is demonstrated that Laplacianity properties can be enforced *a posteriori* by applying a post-filter. The postfilter is constructed from the pseudoinverse of a duplication matrix and the pseudoinverse of a matrix enforcing zero row-sums. A post-filtering heuristic to yield sparse estimates of $\mathbf{Y}$ is considered in [238]. After estimating the admittance matrix, the lines whose estimated conductances are relatively small are progressively removed, therefore promoting network sparsity.

6) Joint Estimation of Topology and Parameters: the admittance estimation problem corresponds to the estimation of the network topology and the line parameters. This approach has been followed in [17], [136], [175], [176], [181], [200], [238], [239]. The problem is usually solved in an iterative way (see also Sec. III-B9) where the line parameter is estimated first based on initial topology information, then the topology is estimated using the estimated line parameters and finally parameters are estimated again.

In [136], [238], first the line parameters are estimated assuming an initial topology (such as all the lines are assumed to be connected), then lines with the least conductance are removed, iteratively with some thresholds. It is based on a heuristic rule such that the likelihood of the re-estimated EIV model should not go lower than the likelihood of the model with all lines assumed to be connected. The work in [176] proposed a two-stage numerical approach. First, a data-driven regression method is used to estimate a preliminary model whose objective is to estimate *proxy* conductance and susceptance matrices. In the preliminary state, it assumes the voltage angle to be near zero, therefore approximating the *sines* and *cosines* of the angle correspondingly. It simplifies the power flow relations where the active and reactive powers are expressed proportionally to the voltage multiplication of two nodes. This first estimation is then used to identify the topology which is then used in the second stage for better estimation of the line parameters with a much more rigorous power-flow model. This problem is solved by a numerical approach, the Newton-Raphson method. In [175], [200], topology is estimated first using statistical analysis (correlation) of the nodal voltage and power injection measurements. Then, the branch parameters are estimated in the second stage. In [181], the network topology is estimated by reconstructing a weighted Laplacian matrix of distribution networks. In the second stage, a least absolute deviations (LAD) regression model is developed for estimating the line impedance of a single branch based on the nonlinear (inverse) power flow model, wherein a conductor library is leveraged to narrow down the solution space. The LAD regression model is originally a mixed-integer nonlinear program whose continuous relaxation is still non-convex. In [17], effective impedances are estimated via the reduced Laplacian form of the Kron reduced admittance matrix, termed the “subKron” form. It uses the complex recursive grouping algorithm to reconstruct radial networks from effective impedances. The work in [239] formulates the associated constrained maximum likelihood (CML) estimator as the solution of a constrained optimization problem with Laplacian and sparsity constraints. It develops an efficient solution using the associated alternating direction method of multipliers (ADMM) algorithm with an $l1-$ relaxation.

E. Future Directions

The key challenges that need to be addressed in the parameter estimation literature are summarized here below.

- *Estimation under limited observability:* the majority of existing literature assumes full observability for the admittance and topology estimation problem. However, in practical situations, achieving full observability is unrealistic due to various factors such as communication issues, missing data or lack of sensors, etc. Limited observability renders the estimation problem challenging. Advanced signal processing techniques, machine learning approaches, compressed sensing or optimization methods to infer missing information may be useful in improving the estimation accuracy.
- *Non-normal noise distributions:* realistic measurements are often characterized by noise distributions that are not normal. Processing raw time-domain samples to extract phasor quantities requires the application of signal processing algorithms that, to ensure compliance with existing international standards (e.g., [40], [41]), may produce non-normal noise distributions with a potentially discrete nature. This characteristic necessitates the adoption of alternative estimation approaches, such as particle filters, which are inherently capable of handling nonlinear measurement models and non-Gaussian noise distributions although they are characterized by a very high computational cost. Additionally, the measurement error characterization requires further investigation, particularly under real operating conditions, since distinguishing truly non-normal distributions from the effects of non-stationarity is crucial for an accurate model.
- *Systematic errors:* as mentioned before, systematic errors in the measurement chain can jeopardize estimation results. Particular attention is needed in IT compensation and/or PMU calibration. A significant research effort is required in

designing compensation instruments and tools that can help reducing the systematic errors directly on the field, reducing as much as possible downtimes and increasing the usability of the measurements. It is also worth highlighting that ITs evolution is ongoing and new generation ITs will provide lower uncertainty intervals, but the impact of influencial quantities (like frequency or temperature [240], [241]) is still to be assessed. A more punctual characterization of the instrumentation under various and non-standard conditions would be of great help in improving the uncertainty description and in ruling out unreliable measurement data from the estimation.
- *Providing estimation error guarantees:* To enable deployment of the newly developed estimation algorithms, it is necessary to provide error bounds on the estimated parameters as function of the measured quantities and associated noise. Such error bounds can be integrated in optimization schemes and can help quantifying the uncertainty associated with estimated values.
- *Model parameters at non-fundamental frequencies:* PMU design is under constant evolution and harmonic PMUs are emerging as a powerful tool to measure harmonic phasors. An evolution of model estimation relying on non-fundamental frequency synchronised measurements emerges as an interesting and challenging research direction. It is important to notice that accurate absolute phase-angle measurements are even more crucial in this regard, with new challenges in time-synchronization accuracy.
- *Integration with conventional measurements:* Synchronised measurements are the key tool for parameter estimation in advanced monitoring infrastructures, but a full integration with information available from already existing measuring infrastructure is still missing. Conventional measurements are not time-synchronised and their accuracy is usually far from that needed for the discussed estimation algorithms, but they are often already available and could be used as prior information to limit the exploration space in the estimation process. However, associating them with meaningful uncertainty models, which can support an estimation based on synchronised measurements in an effective and efficient way, is still a research direction to be further investigated.

V. Estimating State-dependent Grid Models

In contrast to the estimation of the state-independent models such as admittance parameters (line, shunt, and topology) of the power networks that can be used for their exact representation, several methods in the literature propose estimating an approximated representation of the power-flow equations. One such example is the derivation of approximated power flow models using the first (or multiple) order of Taylor's series expansion of the power flow equations (e.g., [242], [243]). These models are widely used for formulating different control schemes such as voltage control, and lines congestions management [244], [245] etc. These models are valid in the proximity of the considered operating point, hence, they are referred to as state-dependent models.

In the following, first we recap a scheme for power-flow approximation around an operating point, then we review different methods proposed in the literature for measurement-based estimation of such approximated power-flow models.

A. Power-flow Approximation around an Operating Point

Let the nodal apparent power injections be denoted as $\mathbf{S} = [\mathbf{S}_1, \cdots, \mathbf{S}_{N_b}]$, with $\mathbf{S}_i \in \mathbb{C}^{N_p} = \mathbf{P}_i + j\mathbf{Q}_i$ where $\mathbf{P}_i \in \mathbb{R}^{N_p}$ and $\mathbf{Q}_i \in \mathbb{R}^{N_p}$ are the active and reactive power injections at node $i \in \mathcal{N}_b$. Using the previous notations of multi-phase voltage and admittance matrix, it can be re-written compactly as

$$\mathbf{S}_i = \mathbf{P}_i + j\mathbf{Q}_i = \mathbf{v}_i \circ \sum_{j \in \mathcal{N}_b} \underline{\mathbf{Y}}_{ij}\underline{\mathbf{v}}_j \tag{80}$$

where $\circ$ refers to Hadamard product.

The aim of power flow analysis is to express the nodal voltage phasors $\mathbf{v}_i = |\mathbf{v}_i|\angle\boldsymbol{\theta}_i = \Re\{\mathbf{v}_i\} + j\Im\{\mathbf{v}_i\}$ as a function of the injections i.e., $P_i, Q_i, i \in \mathcal{N}_b$ and the slack-bus voltage phasor $\mathbf{v}_0$, which can be expressed by the following non-linear function

$$\mathbf{v}_i = \mathbf{v}_i(\mathbf{v}_0, \mathbf{P}_1, \ldots, \mathbf{P}_{N_b}, \mathbf{Q}_1, \ldots, \mathbf{Q}_{N_b}) \tag{81}$$

In practical applications, such as for voltage control, the non-linear expression in (81) is often approximated by a linear or quadratic expression. One such approach is using the Taylor's series expansion around a pre-defined operating point. These expansions can be performed considering several higher-order terms, as demonstrated in [242], [246], however, in the majority of the cases, the higher order terms are neglected to obtain a linear approximation. Such Taylor's expansion can be written for polar and rectangular coordinates, as described below.

1) Polar coordinates: Using the polar coordinates, the First-order Taylor's approximation of the power-flow equations in (81) around an operating point, $\mathbf{v}_i^\bullet = |\mathbf{v}_i^\bullet|\angle\boldsymbol{\theta}_i^\bullet$ yields linear expressions for the voltage magnitudes and angles as

$$|\mathbf{v}_i| = |\mathbf{v}_i^\bullet| + \sum_{j \in \mathcal{N}_b} \mathbf{K}^m_{P,ij}(\mathbf{P}_j - \mathbf{P}_j^\bullet) + \sum_{j \in \mathcal{N}_b} \mathbf{K}^m_{Q,ij}(\mathbf{Q}_j - \mathbf{Q}_j^\bullet) \tag{82a}$$

$$\boldsymbol{\theta}_i = \boldsymbol{\theta}_i^\bullet + \sum_{j \in \mathcal{N}_b} \mathbf{K}^\theta_{P,ij}(\mathbf{P}_j - \mathbf{P}_j^\bullet) + \sum_{j \in \mathcal{N}_b} \mathbf{K}^\theta_{Q,ij}(\mathbf{Q}_j - \mathbf{Q}_j^\bullet) \tag{82b}$$

where, $\mathbf{P}_j^\bullet$ and $\mathbf{Q}_j^\bullet$ are operating points for the active and reactive powers, respectively. The symbols $\mathbf{K}^m_{P,ij}, \mathbf{K}^m_{Q,ij}, \mathbf{K}^\theta_{P,ij}, \mathbf{K}^\theta_{Q,ij} \in \mathbb{R}^{N_p \times N_p}$ are the Taylor's coefficients, also referred to as sensitivity coefficients, their elements are defined as,

$$K^m_{P,ij,\psi\psi'} = \frac{\partial |v_i^\psi|}{\partial P_j^{\psi'}} \text{ and } K^m_{Q,ij,\psi\psi'} = \frac{\partial |v_i^\psi|}{\partial Q_j^{\psi'}} \tag{83a}$$

$$K^\theta_{P,ij,\psi\psi'} = \frac{\partial \theta_i^\psi}{\partial P_j^{\psi'}} \text{ and } K^\theta_{Q,ij,\psi\psi'} = \frac{\partial \theta_i^\psi}{\partial Q_j^{\psi'}} \tag{83b}$$

2) Rectangular coordinates: the first-order Taylor's expansion around an operating point in rectangular coordinates $\mathbf{v}_i^\bullet = \Re(\mathbf{v}_i^\bullet) + j\Im(\mathbf{v}_i^\bullet)$ is expressed as

$$\Re\{\mathbf{v}_i\} = \Re\{\mathbf{v}_i^\bullet\} + \sum_{j\in\mathcal{N}_b} \mathbf{K}_{P,ij}^{re}(\mathbf{P}_j - \mathbf{P}_j^\bullet) + \sum_{j\in\mathcal{N}_b} \mathbf{K}_{Q,ij}^{re}(\mathbf{Q}_j - \mathbf{Q}_j^\bullet) \tag{84a}$$

$$\Im\{\mathbf{v}_i\} = \Im\{\mathbf{v}_i^\bullet\} + \sum_{j\in\mathcal{N}_b} \mathbf{K}_{P,ij}^{im}(\mathbf{P}_j - \mathbf{P}_j^\bullet) + \sum_{j\in\mathcal{N}_b} \mathbf{K}_{Q,ij}^{im}(Q_j - Q_j^\bullet) \tag{84b}$$

where, the symbols $\mathbf{K}_{P,ij}^{re}, \mathbf{K}_{Q,ij}^{re}, \mathbf{K}_{P,ij}^{im}, \mathbf{K}_{Q,ij}^{im}$ are the corresponding coefficients defined as

$$K_{P,ij,\psi\psi'}^{re} = \frac{\partial(\Re\{v_i^\psi\})}{\partial P_j^{\psi'}} \text{ and } K_{P,ij,\psi\psi'}^{im} = \frac{\partial(\Im\{v_i^\psi\})}{\partial P_j^{\psi'}} \tag{85a}$$

$$K_{Q,ij,\psi\psi'}^{re} = \frac{\partial(\Re\{v_i^\psi\})}{\partial Q_j^{\psi'}} \text{ and } K_{Q,ij,\psi\psi'}^{im} = \frac{\partial(\Im\{v_i^\psi\})}{\partial Q_j^{\psi'}} \tag{85b}$$

It should be remarked that the sensitivity coefficients, $\mathbf{K}_{P,ij}^m, \mathbf{K}_{Q,ij}^m, \mathbf{K}_{P,ij}^\theta, \mathbf{K}_{Q,ij}^\theta$ and $\mathbf{K}_{P,ij}^{re}, \mathbf{K}_{Q,ij}^{re}, \mathbf{K}_{P,ij}^{im}, \mathbf{K}_{Q,ij}^{im}$ are state-dependent as they are defined for a specific operating point.

In a measurement-based setting, the objective is to estimate the sensitivity coefficients in (83) and (85) by using the measurements of the nodal voltages and active/reactive power injections.

In the following, we review the estimation problem, the key challenges, and different approaches to tackling them.

B. Measurement-based Estimation Models

Given the availability of measurements of nodal voltages and power injections, the coefficients in (82) and 84 can be estimated by formulating a regression-based estimation problem. Assuming that (i) the measurements are available from PMUs or RTUs over a time window of $[t_1, \dots, t_m]$, and (ii) the sensitivity coefficients do not change over this window, the linearized expression in (82) and (84) can be written as ($\sim$ with a symbol is used to indicate measured quantity)

$$\begin{bmatrix} \Delta\tilde{\mathbf{z}}_i(t_1) \\ \vdots \\ \Delta\tilde{\mathbf{z}}_i(t_k) \\ \vdots \\ \Delta\tilde{\mathbf{z}}_i(t_m) \end{bmatrix} = \begin{bmatrix} \Delta\tilde{\mathbf{P}}(t_1) & \Delta\tilde{\mathbf{Q}}(t_1) \\ \vdots & \vdots \\ \Delta\tilde{\mathbf{P}}(t_k) & \Delta\tilde{\mathbf{Q}}(t_k) \\ \vdots & \vdots \\ \Delta\tilde{\mathbf{P}}(t_m) & \Delta\tilde{\mathbf{Q}}(t_m) \end{bmatrix} \begin{bmatrix} \mathbf{K}_{P,i}^\diamond \\ \mathbf{K}_{Q,i}^\diamond \end{bmatrix} \tag{86}$$

where z_i refers to any of the dependent variables corresponding to node i in (82) and (84), i.e., $\mathbf{z}_i = \{|\mathbf{v}_i^\top|, \boldsymbol{\theta}_i^\top, \Re(\mathbf{v}_i^\top), \Im(\mathbf{v}_i^\top)\}$ and $\Delta\mathbf{z}_i = \mathbf{z}_i - \mathbf{z}_i^\bullet$ refer to the deviations with respect to the operating point; the same applies to $\Delta\mathbf{P}$ and $\Delta\mathbf{Q}$. The vectors $\mathbf{K}_{P,i}^\diamond, \mathbf{K}_{Q,i}^\diamond$ are the sensitivity coefficients for node i with respect to the power injections at all nodes, i.e, $\mathbf{K}_{P,i}^\diamond = [\mathbf{K}_{P,i1}^\diamond, \dots, \mathbf{K}_{P,iN_b}^\diamond]$ and $\mathbf{K}_{Q,i}^\diamond = [\mathbf{K}_{Q,i1}^\diamond, \dots, \mathbf{K}_{Q,iN_b}^\diamond]$ and the $\diamond = \{m, \theta, re, im\}$ defines the corresponding sensitivity coefficient of interest in (82) and (84).

With respect to the choice of operating point, two distinct approaches have been reported in the existing literature. The first corresponds to the case, when $\mathbf{z}_i^\bullet$ is chosen as the measurement observed at the previous time step. In this case, $\Delta\tilde{\mathbf{z}}_i(t_k) = \tilde{\mathbf{z}}_i(t_k) - \tilde{\mathbf{z}}_i(t_{k-1})$. Similarly, $\Delta\tilde{\mathbf{P}}(t_k) = \tilde{\mathbf{P}}(t_k) - \tilde{\mathbf{P}}(t_{k-1})$ and $\Delta\tilde{\mathbf{Q}}(t_k) = \tilde{\mathbf{Q}}(t_k) - \tilde{\mathbf{Q}}(t_{k-1})$. Such approach is followed in [20], [245], [247], [248].

In another case, the operating point is chosen as the no-load conditions (e.g., [22], [243], [249]), i.e. $\mathbf{z}_i^\bullet = \mathbf{z}_0, \mathbf{P}^\bullet = 0, \mathbf{Q}^\bullet = 0$. This simplification leads to

$$\begin{bmatrix} \tilde{\mathbf{z}}_i(t_1) - \mathbf{z}_0 \\ \vdots \\ \tilde{\mathbf{z}}_i(t_k) - \mathbf{z}_0 \\ \vdots \\ \tilde{\mathbf{z}}_i(t_m) - \mathbf{z}_0 \end{bmatrix} = \begin{bmatrix} \tilde{\mathbf{P}}(t_1) & \tilde{\mathbf{Q}}(t_1) \\ \vdots & \vdots \\ \tilde{\mathbf{P}}(t_k) & \tilde{\mathbf{Q}}(t_k) \\ \vdots & \vdots \\ \tilde{\mathbf{P}}(t_m) & \tilde{\mathbf{Q}}(t_m) \end{bmatrix} \begin{bmatrix} \mathbf{K}_{P,i}^\diamond \\ \mathbf{K}_{Q,i}^\diamond \end{bmatrix} \tag{87}$$

In reality, the voltage at no load might not be available, then $\mathbf{v}_0$ can be replaced by some pseudo measurements such as the mean of $\mathbf{v}_i$. Such a scheme was proposed in [22].

In (86), (87), the values $\mathbf{z}_i, \Delta\mathbf{P}, \Delta\mathbf{Q}$ are known from the measurements, and the parameters to estimate are $\mathbf{K}_P^\diamond$ and $\mathbf{K}_Q^\diamond$. As long as the number of measurement m is greater than the number of variables to be estimated $2 \times (N_b - 1)$, (86) can be formulated as a standard regression problem and can employ any of the estimation techniques described earlier in Sec. III-B. For simplifaction, the models in (86), (87) can be represented similar to the ones in (5a), as

$$\tilde{\mathbf{z}} = \tilde{\mathbf{H}}\mathbf{p} + \boldsymbol{\epsilon}, \tag{88}$$

where $\tilde{\mathbf{z}} \in \mathbb{R}^{m\times N_p}$ and $\tilde{\mathbf{H}} \in \mathbb{R}^{m\times 2N_pN_b}$ are constructed from the nodal voltage and power measurements, respectively; the symbol $\mathbf{p} = [\mathbf{K}_P^\diamond \ \mathbf{K}_Q^\diamond]^\top \in \mathbb{R}^{2N_pN_b\times N_p}$ is collecting all the sensitivity parameters to be estimated, $\boldsymbol{\epsilon}$ denotes the error vector arising from measurements and model approximation.

Other than the regression-based methods, other approaches, as proposed in [250], [251], involve estimating the sensitivity coefficient through a *perturb and observe* scheme. However, this method requires regular and significant perturbations in nodal injections, making it impractical in real-life scenarios. Therefore, in the following, we mainly review the estimation challenges and potential solutions with respect to the regression-based methods.

C. Estimation Challenges and Solutions

The key challenges in estimating the sensitivity coefficients parameters in state-dependent models are described below.

1) Multicollinearity: this problem is prevalent in estimation schemes where multiple predictors in the regression model are similar or *collinear*, i.e., the several columns of the $\mathbf{H}$ matrix in (88) are correlated to each other. This phenomenon might occur when the power network has similarly varying power injections (such as in Photovoltaic plants), etc. In such a case, the matrix $\mathbf{H}$ becomes ill-conditioned and the inverse $\mathbf{H}^\top\mathbf{H}$ might be ill-defined. It results in estimates which are very sensitive to small changes in the measurement data as the condition number of the ill-conditioned matrix is very high. It results in high variance of the estimates of some coefficients which are highly affected by the multi-collinearity problem.

The problem of multi-collinearity has been recently tackled by several works. For example, [22], [252] proposed using principle component regression (PCR) [253] where the matrix $\mathbf{H}$ is transformed into a reduced dimensional space with independent predictors. This allows the correlated predictors to be removed and only independent predictors are considered in the regression algorithm. This is achieved by carrying out singular value decomposition (SVD) on $\mathbf{H}$ and taking the columns with dominant eigenvalues.

A similar approach has also been followed in [254]–[257] which uses different versions of *partial least squares* (PLS) method. PLS addresses the collinearity problem as well as the lack of enough observations by combining the features from principal component analysis (PCA) and canonical correlation analysis (CCA) [258]. Different approaches has been deployed to implement PLS schemes, for example in [254], [255] utilize a nonlinear iterative partial least squares (NIPALS) method [259], whereas in [256], [257], a statistically inspired modification of the partial least squares (SIMPLS) has been used, and have computational advantage compared to NIPALS.

The works in [254] proposes to use a *Bayesian Learning Regression (BLR)* which is also effective in mitigating the collinearity problem. An advantage of using the BLR is to be able to express the posterior distributions on the estimated parameters as a function of the likelihood of the input data and prior known distribution of parameters [260]. However, a key challenge in using BLR is the characterisation of the likelihood and prior distribution.

Multicollinearity has been also tackled using the ridge-regression (RR) based methods [21], [261]–[263]. As described in (Sec. III-B4), it includes adding a norm term also referred to as Tikhonov–Phillips regularization into the weighted LS (WLS) algorithm allowing sensitivity coefficient estimates to be stable. As shown in [264], the regularization term renders the overall gain matrix $(\mathbf{H}^\top\mathbf{H} + \lambda\mathbf{I})$ well-conditioned, therefore the estimates are stable. In [21], it was proposed to use locally weighted RR (LWRR) to achieve stable estimation in the presence of collinearity. In another variation, [261] proposed a noise-assisted ensemble regression (NAER) scheme which inserts a noise ensemble into the LWLS scheme and uses the mean of LWLS estimates. In [261], it is claimed that NAER gives equivalent estimates as RR, i.e., adding a norm-2 regularization term into the WLS. The work in [262] utilized RR to address the collinearity problem in estimating linearized models for three-phase systems.

2) Low excitation: when the power injections are extremely low (much lower than the nominal values), the change in the grid states may be negligible, which makes it difficult to estimate the sensitivity coefficients. The issue of low excitation has been tackled by pre-filtering approaches. For example, in [20], only the voltage measurement deviations above a certain threshold are used for the estimation, resulting in estimation performance improvement. In [265], this issue is tackled by limiting the measurements to relevant data around the operating point referred to as "sufficient effective data condition" which is defined as a measurement within 5% around the operating point. The work proposed a "resampling" and "compression" procedure to achieve 'sufficient effective data condition". Then, this data is used to formulate a LWLS scheme where the weights are computed as an exponential distance function. Due to low excitation, the inverse of the gain matrix may be too large, therefore the problem of high variance in the estimates may occur; in this context, the RR-based methods are also found to be effective to solve this issue.

3) Adaptability to the Changing Grid Data and Measurement Noise: for adapting to changes in the measurement noise, WLS with appropriate weighting could be effective. The work in [20] derived a correlation matrix by accounting for the correlation between the two consecutive deviations of the measurements. Such a covariance matrix showed better performance compared to ordinary LS.

To adapt to the change in load variation, the work in [266] proposed a piece-wise model where the load is clustered into three different zones: low load, high load, and reverse power flow. For each of these zones, a separate sensitivity coefficient is defined. However, this is carried out offline using historical data and discretizing the load into three different zones may not produce accurate results.

In [267], TLS and WTLS methods are proposed that account for measurement noise in both $\tilde{\mathbf{H}}$ and $\tilde{\mathbf{z}}$. It showed robust estimation performance with different levels of measurement noises.

The works in [268], [269] propose using recursive online estimation methods which update the sensitivity coefficients using recent measurements. RLS schemes are found to be suitable, as they are capable of tracking the changing nature of the sensitivity coefficients recursively with newer grid measurements. These schemes employ exponential forgetting on the past measurements, giving more weight to the most recent measurements. Similarly, in [255], a recursive version of PLS is proposed which is effective in tackling the collinearity problem. In [270], the authors propose using RLS schemes with a *directional forgetting* strategy [88] to avoid the covariance matrix *windup* problem. Different forgetting algorithms are compared against OLS methods in [271], [272], and those with *selective forgetting* [84] and directional forgetting were found to be the most dominant.

4) Tackling Outliers: the standard regression-based schemes are quite sensitive to the outliers, especially for measurement-based schemes. Therefore, the works in [273], [274] proposed using SVR (Sec. III-B5) to achieve good estimation performance in the case of outliers in the measurements. SVR models have been shown to perform better than the LS and PLS schemes against different percentage of outliers in the input data. In addition, due to the regularization term in SVR, it also helps in tackling the multicollinearity issue, as demonstrated in [273], [274].

D. Future Directions

The key challenges that need to be addressed in the parameter estimation literature in addition to challenges mentioned already in the previous section for state-independent grid models are listed here below.

- *Multi-collinearity:* It is a common occurrence in power system parameter estimation as the relevant measurements are usually correlated. This leads to numerical instability, ambiguity in model interpretation, and increased sensitivity of estimated values to small changes in measurements. Techniques such as variable selection, regularization, and pre-processing have been proposed in the existing literature. Mitigating multicollinearity is crucial for obtaining accurate and reliable parameter estimates in power system modeling.

- *Accuracy of Model Approximations:* The power flow equations are inherently non-linear and approximations of linear or quadratic nature induce errors into the estimation process. The accuracy that can be achieved with approximations is dependent on the specific formulation but also the specific system and operating point. Hence, understanding and quantifying under which conditions a chosen model is sufficiently close to an accurate representation provides insights into the achievable accuracy of the estimation process.
- *Adapting to faster changing grid state:* With the increasing level of resources with fast-regulating power outputs, the time interval during which the system is sufficiently "steady", reduces. Consequently, the question of efficient adaptation of the models to varying system states is becoming increasingly important.

VI. Concluding Remarks and Future Directions

In this paper, we reviewed the state-of-the-art measurement-based techniques and solution approaches for estimating the power flow models using time-synchronised measurements, with the goal of providing a summary and suggestions for researchers in this field. First, the paper reviewed recent developments in the area of time-synchronised measurements in power systems, starting from time dissemination technologies to the uncertainty characterization of the measurements from PMUs and instrument transformers. These uncertainty models can serve as a guide for researchers working on parameter estimation. The paper then reviewed different estimation techniques which are widely employed to solve the parameter estimation problem but differ by the noise characterization. The estimation techniques are grouped into state-independent and state-dependent power flow estimation models. The state-independent models include schemes for estimating power line parameters, admittance, and topology, as well as joint estimation models such as the joint estimation of state and line parameter errors, and systematic errors. The state-dependent models included estimation of approximated power-flow models such as First-order Taylor's approximation. The paper highlights several open problems and suggests potential areas for future research.

The future research on parameter estimation must address the evolving needs of power grids, which are increasingly incorporating inverter-based resources. These systems introduce distinct dynamics and transients that are becoming increasingly pronounced. Consequently, monitoring technologies are shifting from static, time-synchronised measurements (e.g., RMS or phasor-based) to the so-called synchro-waveforms (or point-on-wave). This transition is driving the development of network applications into a fundamentally different domain, where PMU or SCADA measurements will be integrated with higher-resolution data. This integration will enable the formulation of estimation problems spanning both the frequency and time domains. The methods reviewed in this paper may be complemented by alternative approaches capable of operating at higher resolutions and handling greater computational demands.

Finally, the current literature lacks experimental and numerical validations of the parameter estimation algorithms and related assumptions on real-life distribution and transmission systems. Therefore, future works should also validate the framework on real-life systems.

References

[1] P. Kundur, N. Balu, and M. Lauby, *Power system stability and control*. McGraw-Hill, 1994.

[2] F. Milano, *Power system modelling and scripting*. Springer Science & Business Media, 2010.

[3] F. C. Schweppe and E. J. Handschin, "Static state estimation in electric power systems," *Proc. of the IEEE*, vol. 62, no. 7, pp. 972–982, 1974.

[4] A. Abur and A. G. Exposito, *Power system state estimation: theory and implementation*. CRC press, 2004.

[5] P. Mercier, R. Cherkaoui, and A. Oudalov, "Optimizing a battery energy storage system for frequency control application in an isolated power system," *IEEE Trans. Power Syst.*, vol. 24, no. 3, pp. 1469–1477, 2009.

[6] G. Celli, E. Ghiani, S. Mocci, and F. Pilo, "A multiobjective evolutionary algorithm for the sizing and siting of distributed generation," *IEEE Transactions on power systems*, vol. 20, no. 2, pp. 750–757, 2005.

[7] M. M. Saha, J. Izykowski, and E. Rosolowski, *Fault location on power networks*. Springer, 2010, vol. 2.

[8] L. G. Perez and A. J. Urdaneta, "Optimal computation of distance relays second zone timing in a mixed protection scheme with directional overcurrent relays," *IEEE Trans. Power Del.*, vol. 16, pp. 385–388, 2001.

[9] W. H. Kersting, *Distribution system modeling and analysis*. CRC press, 2012.

[10] M. Pau, P. A. Pegoraro, and S. Sulis, "WLS distribution system state estimator based on voltages or branch-currents: Accuracy and performance comparison," in *I2MTC*. IEEE, 2013, pp. 493–498.

[11] G. D'Antona, "Uncertainty of power system state estimates due to measurements and network parameter uncertainty," in *International Workshop AMPS*. IEEE, 2010, pp. 37–40.

[12] G. Sivanagaraju, S. Chakrabarti, and S. C. Srivastava, "Uncertainty in transmission line parameters: Estimation and impact on line current differential protection," *IEEE Transactions on Instrumentation and Measurement*, vol. 63, no. 6, pp. 1496–1504, 2013.

[13] P. Zarco and A. G. Exposito, "Power system parameter estimation: a survey," *IEEE Transactions on power systems*, vol. 15, no. 1, pp. 216–222, 2000.

[14] D. Shi, D. J. Tylavsky, K. M. Koellner, N. Logic, and D. E. Wheeler, "Transmission line parameter identification using PMU measurements," *Eur. Trans. Elect. Power*, vol. 21, no. 4, pp. 1574–1599, May 2011.

[15] C. Indulkar and K. Ramalingam, "Estimation of transmission line parameters from measurements," *International Journal of Electrical Power & Energy Systems*, vol. 30, no. 5, pp. 337–342, 2008.

[16] K. Dasgupta and S. Soman, "Line parameter estimation using phasor measurements by the total least squares approach," in *2013 IEEE Power & Energy Society General Meeting*. IEEE, 2013, pp. 1–5.

[17] K. Moffat, M. Bariya, and A. Von Meier, "Unsupervised impedance and topology estimation of distribution networks—limitations and tools," *IEEE Transactions on Smart Grid*, vol. 11, no. 1, pp. 846–856, 2019.

[18] X. Zhao, H. Zhou, D. Shi, H. Zhao, C. Jing, and C. Jones, "On-line pmu-based transmission line parameter identification," *CSEE Journal of Power and Energy Systems*, vol. 1, no. 2, pp. 68–74, 2015.

[19] Y. Du and Y. Liao, "On-line estimation of transmission line parameters, temperature and sag using pmu measurements," *Electric Power Systems Research*, vol. 93, pp. 39–45, 2012.

[20] C. Mugnier, K. Christakou, J. Jaton, M. De Vivo, M. Carpita, and M. Paolone, "Model-less/measurement-based computation of voltage sensitivities in unbalanced electrical distribution networks," in *2016 Power Systems Computation Conference (PSCC)*. IEEE, 2016, pp. 1–7.

[21] J. Zhang, Z. Wang, X. Zheng, L. Guan, and C. Chung, "Locally weighted ridge regression for power system online sensitivity identification considering data collinearity," *IEEE Transactions on Power Systems*, vol. 33, no. 2, pp. 1624–1634, 2017.

[22] G. Valverde, T. Zufferey, S. Karagiannopoulos, and G. Hug, "Estimation of voltage sensitivities to power injections using smart meter data," in *2018 IEEE International Energy Conference (ENERGYCON)*. IEEE, 2018, pp. 1–6.

[23] NASPI Distribution Task Team, "Synchrophasor monitoring for distribution systems technical foundations and applications [white paper]," 2018.

[24] R. Nuqui and A. Phadke, "Phasor measurement unit placement techniques for complete and incomplete observability," *IEEE Transactions on Power Delivery*, vol. 20, no. 4, pp. 2381–2388, 2005.

[25] S. Chakrabarti and E. Kyriakides, "Optimal placement of phasor measurement units for power system observability," *IEEE Transactions on Power Systems*, vol. 23, no. 3, pp. 1433–1440, 2008.

[26] B. Gou, "Generalized integer linear programming formulation for optimal pmu placement," *IEEE Transactions on Power Systems*, vol. 23, no. 3, pp. 1099–1104, 2008.

[27] S. Chakrabarti, E. Kyriakides, and D. G. Eliades, "Placement of synchronized measurements for power system observability," *IEEE Transactions on Power Delivery*, vol. 24, no. 1, pp. 12–19, 2009.

[28] R. Emami and A. Abur, "Robust measurement design by placing synchronized phasor measurements on network branches," *IEEE Transactions on Power Systems*, vol. 25, no. 1, pp. 38–43, 2010.

[29] E. Caro, I. Arévalo, C. García-Martos, and A. J. Conejo, "Power system observability via optimization," *Electric Power Systems Research*, vol. 104, pp. 207–215, 2013.

[30] N. M. Manousakis and G. N. Korres, "An advanced measurement placement method for power system observability using semidefinite programming," *IEEE Systems Journal*, vol. 12, no. 3, pp. 2601–2609, 2018.

[31] G. N. Korres, N. M. Manousakis, T. C. Xygkis, and J. Löfberg, "Optimal phasor measurement unit placement for numerical observability in the presence of conventional measurements using semi-definite programming," *IET Generation, Transmission & Distribution*, vol. 9, no. 15, pp. 2427–2436, 2015.

[32] J. O. Rawlings, S. G. Pantula, and D. A. Dickey, Eds., *Problem Areas in Least Squares*. New York, NY: Springer New York, 1998, pp. 325–340.

[33] L. Mili, M. Cheniae, N. Vichare, and P. Rousseeuw, "Robust state estimation based on projection statistics [of power systems]," *IEEE Transactions on Power Systems*, vol. 11, no. 2, pp. 1118–1127, 1996.

[34] J. Zhao and L. Mili, "Vulnerability of the largest normalized residual statistical test to leverage points," *IEEE Transactions on Power Systems*, vol. 33, no. 4, pp. 4643–4646, 2018.

[35] A. Abur, F. Magnago, and F. Alvarado, "Elimination of leverage measurements via matrix stretching," *International Journal of Electrical Power & Energy Systems*, vol. 19, no. 8, pp. 557–562, 1997. [Online]. Available: https://www.sciencedirect.com/science/article/pii/S014206159700029X

[36] M. Dorier, G. Frigo, A. Abur, and M. Paolone, "Leverage point identification method for lav-based state estimation," *IEEE Transactions on Instrumentation and Measurement*, vol. 70, pp. 1–10, 2021.

[37] E. Shereen and G. Dán, "Network topology-aware mitigation of undetectable pmu time synchronization attacks," *IEEE Transactions on Control of Network Systems*, pp. 1–12, 2024.

[38] A. Pal, A. K. S. Vullikanti, and S. S. Ravi, "A pmu placement scheme considering realistic costs and modern trends in relaying," *IEEE Transactions on Power Systems*, vol. 32, no. 1, pp. 552–561, 2017.

[39] M. H. F. Wen, J. Xu, and V. O. K. Li, "Optimal multistage pmu placement for wide-area monitoring," *IEEE Transactions on Power Systems*, vol. 28, no. 4, pp. 4134–4143, 2013.

[40] IEC/IEEE, *IEEE/IEC International Standard - Measuring relays and protection equipment - Part 118-1: Synchrophasor for power systems - Measurements*, IEEE/IEC 60255-118-1:2018, Dec 2018.

[41] IEEE, *IEEE Standard for Synchrophasor Data Transfer for Power Systems*, IEEE Std C37.118.2-2011 (Revision of IEEE Std C37.118-2005), 2011.

[42] "Application of phasor measurement units for monitoring power system dynamic performance," Cigré WG C4.34, Tech. Rep., Sept. 2017.

[43] X. Jiang, J. Zhang, B. J. Harding, J. J. Makela, and A. D. Dominguez-Garcia, "Spoofing gps receiver clock offset of phasor measurement units," *IEEE Transactions on Power Systems*, vol. 28, no. 3, pp. 3253–3262, 2013.

[44] "Time synchronization in the electric power system," NASPI Task Force on Time Synchronization, Tech. Rep., March 2018.

[45] IEC/IEEE, *IEC/IEEE International Standard - Precision Clock Synchronization Protocol for Networked Measurement and Control Systems*, IEEE/IEC 61588-2021, 2021.

[46] J. Serrano, P. Alvarez, M. Cattin, E. Garcia Cota, J. Lewis, P. Moreira, T. Wlostowski, and et al., "The white rabbit project," in *Proc. of the ICALEPCS TUC004*, 2009.

[47] S. Bancroft, "An algebraic solution of the gps equations," *IEEE Transactions on Aerospace and Electronic Systems*, vol. AES-21, no. 1, pp. 56–59, 1985.

[48] IEEE, *IEEE Standard for Synchrophasors for Power Systems*, IEEE Std 1344-1995, 1995.

[49] ——, *IEEE Standard for Synchrophasors for Power Systems*, IEEE Std C37.118-2005 (Revision of IEEE Std 1344-1995), 2006.

[50] ——, *IEEE Standard for Synchrophasor Measurements for Power Systems*, IEEE Std C37.118.1-2011 (Revision of IEEE Std C37.118-2005), 2011.

[51] ——, *IEEE Standard for Synchrophasor Measurements for Power Systems – Amendment 1: Modification of Selected Performance Requirements*, IEEE Std C37.118.1a-2014 (Amendment to IEEE Std C37.118.1-2011), 2014.

[52] IEEE, *IEEE Guide for Synchronization, Calibration, Testing, and Installation of Phasor Measurement Units (PMUs) for Power System Protection and Control*, IEEE Std C37.242-2021 (Revision of IEEE Std C37.242-2013), 2021.

[53] IEC, *Instrument transformers - Part 1: General requirements*, IEC Std 61869-1:2009, 2009.

[54] ——, *Instrument transformers - Part 3: Additional requirements for inductive voltage transformers*, IEC Std 61869-3:2011, 2017.

[55] ——, *Instrument transformers - Part 2: Additional requirements for current transformers*, IEC Std 61869-2-:2012, 2012.

[56] ——, *Electromagnetic compatibility (EMC) - Part 4-30: Testing and measurement techniques - Power quality measurement methods*, IEC Std 61000-4-30:2015+AMD1:2021 CSV Consolidated version, 2021.

[57] J. Liu, J. Tang, F. Ponci, A. Monti, C. Muscas, and P. A. Pegoraro, "Trade-offs in PMU deployment for state estimation in active distribution grids," *IEEE Transactions on Smart Grid*, vol. 3, no. 2, pp. 915–924, 2012.

[58] A. Angioni, M. Pau, F. Ponci, and A. Monti, "Effect of latency on state estimation uncertainty," in *2019 IEEE 10th International Workshop on Applied Measurements for Power Systems (AMPS)*, 2019, pp. 1–6.

[59] B. A. Alcaide-Moreno, C. R. Fuerte-Esquivel, M. Glavic, and T. Van Cutsem, "Electric power network state tracking from multirate measurements," *IEEE Transactions on Instrumentation and Measurement*, vol. 67, no. 1, pp. 33–44, 2018.

[60] M. Asprou, E. Kyriakides, and M. M. Albu, "Uncertainty Bounds of Transmission Line Parameters Estimated From Synchronized Measurements," *IEEE Transactions on Instrumentation and Measurement*, vol. 68, no. 8, pp. 2808–2818, Aug. 2019.

[61] P. A. Pegoraro, K. Brady, P. Castello, C. Muscas, and A. von Meier, "Line impedance estimation based on synchrophasor measurements for power distribution systems," *IEEE Transactions on Instrumentation and Measurement*, vol. 68, no. 4, pp. 1002–1013, 2019.

[62] P. Castello, C. Muscas, and P. A. Pegoraro, "Statistical behavior of PMU measurement errors: An experimental characterization," *IEEE Open Journal of Instrumentation and Measurement*, vol. 1, pp. 1–9, 2022.

[63] C. Laurano, P. A. Pegoraro, C. Sitzia, A. V. Solinas, S. Sulis, and S. Toscani, "Refined modeling and compensation of current transformers behavior for line parameters estimation based on synchronized measurements," *IEEE Open Journal of Instrumentation and Measurement*, vol. 2, pp. 1–11, 2023.

[64] M. Pignati, L. Zanni, P. Romano, R. Cherkaoui, and M. Paolone, "Fault detection and faulted line identification in active distribution networks using synchrophasors-based real-time state estimation," *IEEE Transactions on Power Delivery*, vol. 32, no. 1, pp. 381–392, 2017.

[65] S. Wang, J. Zhao, Z. Huang, and R. Diao, "Assessing gaussian assumption of PMU measurement error using field data," *IEEE Transactions on Power Delivery*, vol. 33, no. 6, pp. 3233–3236, 2018.

[66] C. Huang, C. Thimmisetty, X. Chen, E. Stewart, P. Top, M. Korkali, V. Donde, C. Tong, and L. Min, "Power distribution system synchrophasor measurements with non-gaussian noises: Real-world data testing and analysis," *IEEE Open Access Journal of Power and Energy*, vol. 8, pp. 223–228, 2021.

[67] T. Ahmad and N. Senroy, "Statistical characterization of PMU error for robust wams based analytics," *IEEE Transactions on Power Systems*, vol. 35, no. 2, pp. 920–928, 2019.

[68] D. Salls, J. R. Torres, Antos, C. Varghese, J. Patterson, and A. Pal, "Statistical characterization of random errors present in synchrophasor measurements," in *2021 IEEE Power & Energy Society General Meeting (PESGM)*, 2021.

[69] P. Castello, G. Gallus, C. Muscas, P. A. Pegoraro, D. Sitzia, and S. Sulis, "A statistical investigation of pmu errors in current measurements," in *2023 IEEE International Instrumentation and Measurement Technology Conference (I2MTC)*, 2023, pp. 1–6.

[70] M. Paolone, J.-Y. L. Boudec, S. Sarri, and L. Zanni, *Advanced Techniques for Power System Modelling, Control and Stability Analysis*. IET, 2015, ch. Static and recursive PMU-based state estimation processes for transmission and distribution power grids.

[71] B. Stott, "Review of load-flow calculation methods," *Proceedings of the IEEE*, vol. 62, no. 7, pp. 916–929, 1974.

[72] B. Schaffrin and A. Wieser, "On weighted total least-squares adjustment for linear regression," *Journal of geodesy*, vol. 82, pp. 415–421, 2008.

[73] S. Van Huffel, "Recent advances in total least squares techniques and errors-in-variables modeling," 1997.

[74] S. Van Huffel and P. Lemmerling, *Total least squares and errors-in-variables modeling: analysis, algorithms and applications*. Springer Science & Business Media, 2013.

[75] I. Markovsky and S. Van Huffel, "Overview of total least-squares methods," *Signal processing*, vol. 87, no. 10, pp. 2283–2302, 2007.

[76] A. N. Tikhonov, "On the solution of ill-posed problems and the method of regularization," in *Doklady akademii nauk*, vol. 151, no. 3. Russian Academy of Sciences, 1963, pp. 501–504.

[77] R. Tibshirani, "Regression shrinkage and selection via the lasso," *Journal of the Royal Statistical Society Series B: Statistical Methodology*, vol. 58, no. 1, pp. 267–288, 1996.

[78] V. Vapnik, *The nature of statistical learning theory*. Springer science & business media, 1999.

[79] C. Cortes and V. Vapnik, "Support-vector networks," *Machine learning*, vol. 20, pp. 273–297, 1995.

[80] A. J. Smola and B. Schölkopf, "A tutorial on support vector regression," *Statistics and computing*, vol. 14, pp. 199–222, 2004.

[81] B. Scholkopf and A. J. Smola, *Learning with kernels: support vector machines, regularization, optimization, and beyond*. MIT press, 2018.

[82] T. Kailath, A. Sayed, and B. Hassibi, *Linear Estimation*, ser. Prentice-Hall information and system sciences series. Prentice Hall, 2000.

[83] O. Stanojev, L. Werner, S. Low, and G. Hug, "Tractable identification of electric distribution networks," 2023.

[84] J. Parkum, N. K. Poulsen, and J. Holst, "Recursive forgetting algorithms," *International Journal of Control*, vol. 55, no. 1, pp. 109–128, 1992.

[85] T. Fortescue, L. S. Kershenbaum, and B. E. Ydstie, "Implementation of self-tuning regulators with variable forgetting factors," *Automatica*, vol. 17, no. 6, pp. 831–835, 1981.

[86] T. Hägglund, "The problem of forgetting old data in recursive estimation," *IFAC Proceedings Volumes*, vol. 16, no. 9, pp. 213–214, 1983, iFAC Workshop on Adaptive Systems in Control and Signal Processing 1983, San Francisco, CA , USA, 20-22 June 1983. [Online]. Available: https://www.sciencedirect.com/science/article/pii/S1474667017623863

[87] R. Kulhavý and M. Kárný, "Tracking of slowly varying parameters by directional forgetting," *IFAC Proceedings Volumes*, vol. 17, no. 2, pp. 687–692, 1984, 9th IFAC World Congress: A Bridge Between Control Science and Technology, Budapest, Hungary, 2-6 July 1984. [Online]. Available: https://www.sciencedirect.com/science/article/pii/S1474667017610516

[88] S. Bittanti, P. Bolzern, and M. Campi, "Exponential convergence of a modified directional forgetting identification algorithm," *Systems & Control Letters*, vol. 14, no. 2, pp. 131–137, 1990.

[89] I. W. Slutsker, S. Mokhtari, and K. A. Clements, "Real time recursive parameter estimation in energy management systems," *IEEE Transactions on Power Systems*, vol. 11, no. 3, pp. 1393–1399, Aug 1996.

[90] C. Mishra, V. A. Centeno, and A. Pal, "Kalman-filter based recursive regression for three-phase line parameter estimation using synchrophasor measurements," in *2015 IEEE Power & Energy Society General Meeting*. IEEE, 2015, pp. 1–5.

[91] P. Ren, H. Lev-Ari, and A. Abur, "Tracking three-phase untransposed transmission line parameters using synchronized measurements," *IEEE Transactions on Power Systems*, vol. 33, no. 4, pp. 4155–4163, 2017.

[92] R. F. R. Pereira, F. P. De Albuquerque, L. H. B. Liboni, E. C. M. Costa, and M. C. de Oliveira, "Impedance parameters estimation of transmission lines by an extended kalman filter-based algorithm," *IEEE Transactions on Instrumentation and Measurement*, vol. 71, pp. 1–10, 2022.

[93] P. K. Mansani, A. Pal, M. Rhodes, and B. Keel, "Estimation of transmission line sequence impedances using real pmu data," in *2018 North American Power Symposium (NAPS)*. IEEE, 2018, pp. 1–6.

[94] Y. Zhang and Y. Liao, "Kalman filter based method for tracking dynamic transmission line parameters," *SN Applied Sciences*, vol. 3, pp. 1–11, 2021.

[95] A. Gelb *et al.*, *Applied optimal estimation*. MIT press, 1974.

[96] S. M. Kay, *Fundamentals of statistical signal processing: estimation theory*. Prentice-Hall, Inc., 1993.

[97] L. Pagnier and M. Chertkov, "Embedding power flow into machine learning for parameter and state estimation," *arXiv preprint arXiv:2103.14251*, 2021.

[98] ——, "Physics-informed graphical neural network for parameter & state estimations in power systems," *arXiv preprint arXiv:2102.06349*, 2021.

[99] A. Afonin and M. Chertkov, "Which neural network to choose for post-fault localization, dynamic state estimation, and optimal measurement placement in power systems?" *Frontiers in big Data*, vol. 4, p. 692493, 2021.

[100] D. Cao, J. Zhao, W. Hu, N. Yu, J. Hu, and Z. Chen, "Physics-informed graphical learning and bayesian averaging for robust distribution state estimation," *IEEE Transactions on Power Systems*, vol. 39, no. 2, pp. 2879–2892, 2023.

[101] Q.-H. Ngo, B. L. Nguyen, T. V. Vu, J. Zhang, and T. Ngo, "Physics-informed graphical neural network for power system state estimation," *Applied Energy*, vol. 358, p. 122602, 2024.

[102] D. L. Fletcher and W. O. Stadlin, "Transformer tap position estimation," *IEEE Transactions on Power Apparatus and Systems*, vol. PAS-102, no. 11, pp. 3680–3686, Nov 1983.

[103] W. H. E. Liu, F. F. Wu, and S. M. Lun, "Estimation of parameter errors from measurement residuals in state estimation (power systems)," *IEEE Transactions on Power Systems*, vol. 7, no. 1, pp. 81–89, Feb 1992.

[104] W. H. E. Liu and S.-L. Lim, "Parameter error identification and estimation in power system state estimation," *IEEE Transactions on Power Systems*, vol. 10, no. 1, pp. 200–209, Feb 1995.

[105] M. R. M. Castillo, J. B. A. London, N. G. Bretas, S. Lefebvre, J. Prevost, and B. Lambert, "Offline detection, identification, and correction of branch parameter errors based on several measurement snapshots," *IEEE Transactions on Power Systems*, vol. 26, no. 2, pp. 870–877, May 2011.

[106] E. Handschin and E. Kliokys, "Transformer tap position estimation and bad data detection using dynamic signal modelling," *IEEE Transactions on Power Systems*, vol. 10, no. 2, pp. 810–817, May 1995.

[107] O. Alsac, N. Vempati, B. Stott, and A. Monticelli, "Generalized state estimation," *IEEE Transactions on Power Systems*, vol. 13, no. 3, pp. 1069–1075, Aug 1998.

[108] N. Petra, C. G. Petra, Z. Zhang, E. M. Constantinescu, and M. Anitescu, "A bayesian approach for parameter estimation with uncertainty for dynamic power systems," *IEEE Transactions on Power Systems*, vol. 32, no. 4, pp. 2735–2743, July 2017.

[109] J. Zhu and A. Abur, "Identification of network parameter errors," *IEEE Transactions on Power Systems*, vol. 21, no. 2, pp. 586–592, 2006.

[110] Y. Lin and A. Abur, "A new framework for detection and identification of network parameter errors," *IEEE Transactions on Smart Grid*, vol. 9, no. 3, pp. 1698–1706, May 2018.

[111] A. Monticelli and A. Garcia, "Reliable bad data processing for real-time state estimation," *IEEE Transactions on Power Apparatus and Systems*, vol. PAS-102, no. 5, pp. 1126–1139, May 1983.

[112] Y. Lin and A. Abur, "Fast correction of network parameter errors," *IEEE Transactions on Power Systems*, vol. 33, no. 1, pp. 1095–1096, Jan 2018.

[113] ——, "Enhancing network parameter error detection and correction via multiple measurement scans," *IEEE Transactions on Power Systems*, vol. 32, no. 3, pp. 2417–2425, May 2017.

[114] L. Zhang and A. Abur, "Strategic placement of phasor measurements for parameter error identification," *IEEE Transactions on Power Systems*, vol. 28, no. 1, pp. 393–400, 2013.

[115] W.-H. Liu, F. Wu, and S.-M. Lun, "Estimation of parameter errors from measurement residuals in state estimation (power systems)," *IEEE Transactions on Power Systems*, vol. 7, no. 1, pp. 81–89, 1992.

[116] V. H. Quintana and T. Van Cutsem, "Real-time processing of transformer tap positions," *Canadian Electrical Engineering Journal*, vol. 12, no. 4, pp. 171–180, 1987.

[117] X. Bian, X. R. Li, H. Chen, D. Gan, and J. Qiu, "Joint estimation of state and parameter with synchrophasors—part i: State tracking," *IEEE Transactions on Power Systems*, vol. 26, no. 3, pp. 1196–1208, 2011.

[118] ——, "Joint estimation of state and parameter with synchrophasors—part ii: Parameter tracking," *IEEE Transactions on Power Systems*, vol. 26, no. 3, pp. 1209–1220, 2011.

[119] O. Alsac, N. Vempati, B. Stott, and A. Monticelli, "Generalized state estimation," *IEEE Transactions on Power Systems*, vol. 13, no. 3, pp. 1069–1075, 1998.

[120] N. Petra, C. G. Petra, Z. Zhang, E. M. Constantinescu, and M. Anitescu, "A bayesian approach for parameter estimation with uncertainty for dynamic power systems," *IEEE Transactions on Power Systems*, vol. 32, no. 4, pp. 2735–2743, 2017.

[121] Y. Lin and A. Abur, "Robust state estimation against measurement and network parameter errors," *IEEE Transactions on power systems*, vol. 33, no. 5, pp. 4751–4759, 2018.

[122] K. A. Clements and P. W. Davis, "Detection and identification of topology errors in electric power systems," *IEEE Transactions on Power Systems*, vol. 3, no. 4, pp. 1748–1753, Nov. 1988.

[123] F. F. Wu and W-H. E. Liu, "Detection of topology errors by state estimation (power systems)," *IEEE Transactions on Power Systems*, vol. 4, no. 1, pp. 176–183, Feb. 1989.

[124] M. R. Irving and M. J. Sterling, "Substation data validation," *IEE Proceedings*, vol. 129, no. 3, pp. 119–122, May 1982.

[125] A. Monticelli, "The impact of modeling short circuit branches in state estimation," *IEEE Transactions on Power Systems*, vol. 8, no. 1, pp. 364–370, Feb. 1993.

[126] ——, "Modeling circuit breakers in weighted least squares state estimation," *IEEE Transactions on Power Systems*, vol. 8, no. 3, pp. 1143–1149, Aug. 1993.

[127] A. Abur, H. Kim, and M. K. Celik, "Identifying the unknown circuit breaker statuses in power networks," *IEEE Transactions on Power Systems*, vol. 10, no. 4, pp. 2029–2037, Nov. 1995.

[128] A. Gómez-Expósito and A. de la Villa Jaén, "Reduced substation models for generalized state estimation," *IEEE Transactions on Power Systems*, vol. 16, no. 4, pp. 839–846, Nov 2001.

[129] K. A. Clements and A. S. Costa, "Topology error identification using normalized lagrange multipliers," *IEEE Transactions on Power Systems*, vol. 13, no. 2, pp. 347–353, May 1998.

[130] L. Mili, G. Steeno, F. Dobraca, and D. French, "A robust estimation method for topology error identification," *IEEE Transactions on Power Systems*, vol. 14, no. 4, pp. 1469–1476, Nov. 1999.

[131] O. Alsac, N. Vempati, B. Stott, and A. Monticelli, "Generalized state estimation," *IEEE Transactions on Power Systems*, vol. 13, no. 3, pp. 1069–1075, Aug. 1998.

[132] N. P. Theodorakatos, "Fault location observability using phasor measurement units in a power network through deterministic and stochastic algorithms," *Electric Power Components and Systems*, vol. 47, no. 3, pp. 212–229, 2019.

[133] N. P. Theodorakatos, M. D. Lytras, K. T. Kantoutsis, A. P. Moschoudis, and C. A. Theodoridis, "Optimization-based optimal pmu placement for power state estimation and fault observability," in *AIP Conference Proceedings*, vol. 2872, no. 1. AIP Publishing, 2023.

[134] B. Donmez and A. Abur, "Static state estimation without topology processor," *IEEE Transactions on Power Systems*, vol. 36, no. 5, pp. 4712–4722, 2021.

[135] A. M. Prostejovsky, O. Gehrke, A. M. Kosek, T. Strasser, and H. W. Bindner, "Distribution line parameter estimation under consideration of measurement tolerances," *IEEE Transactions on Industrial Informatics*, vol. 12, no. 2, pp. 726–735, 2016.

[136] J. Yu, Y. Weng, and R. Rajagopal, "Patopaem: A data-driven parameter and topology joint estimation framework for time-varying system in distribution grids," *IEEE Transactions on Power Systems*, vol. 34, no. 3, pp. 1682–1692, 2018.

[137] J. Sun, M. Xia, and Q. Chen, "A classification identification method based on phasor measurement for distribution line parameter identification under insufficient measurements conditions," *IEEE Access*, vol. 7, pp. 158 732–158 743, 2019.

[138] Y. Hou, T. Fang, F. Shi, and H. Zhang, "Parameter estimation method of distribution network based on PMU measurement data," in *2020 5th Asia Conference on Power and Electrical Engineering (ACPEE)*, 2020, pp. 1620–1625.

[139] M. Xiao, W. Xie, C. Fang, S. Wang, Y. Li, S. Liu, Z. Ullah, X. Zheng, and R. Arghandeh, "Distribution line parameter estimation driven by probabilistic data fusion of D-PMU and AMI," *IET Generation, Transmission & Distribution*, vol. 15, no. 20, pp. 2883–2892, 2021.

[140] J. Li, J. Qiao, Z. Zhao, X. Wang, and M. Shi, "A model-data-combined identification approach for distribution grid line parameter," in *2022 4th International Conference on Smart Power & Internet Energy Systems (SPIES)*, 2022, pp. 1596–1601.

[141] P. Shah and X. Zhao, "Network identification using μ-pmu and smart meter measurements," *IEEE Transactions on Industrial Informatics*, vol. 18, no. 11, pp. 7572–7586, 2022.

[142] Z. Wu, L. T. Zora, and A. G. Phadke, "Simultaneous transmission line parameter and pmu measurement calibration," in *2015 IEEE Power & Energy Society General Meeting*, 2015, pp. 1–5.

[143] V. Milojević, S. Čalija, G. Rietveld, M. V. Ačanski, and D. Colangelo, "Utilization of pmu measurements for three-phase line parameter estimation in power systems," *IEEE Transactions on Instrumentation and Measurement*, vol. 67, no. 10, pp. 2453–2462, 2018.

[144] A. Wehenkel, A. Mukhopadhyay, J.-Y. Le Boudec, and M. Paolone, "Parameter estimation of three-phase untransposed short transmission lines from synchrophasor measurements," *IEEE Transactions on Instrumentation and Measurement*, vol. 69, no. 9, pp. 6143–6154, 2020.

[145] H. Goklani, G. Gajjar, and S. A. Soman, "Simultaneous three-phase line parameter estimation and instrument transformer calibration using pmu data," in *2020 21st National Power Systems Conference (NPSC)*, 2020, pp. 1–5.

[146] P. A. Pegoraro, C. Sitzia, A. V. Solinas, and S. Sulis, "PMU-based estimation of systematic measurement errors, line parameters, and tap changer ratios in three-phase power systems," *IEEE Transactions on Instrumentation and Measurement*, vol. 71, pp. 1–12, 2022.

[147] R. Khalili and A. Abur, "Transmission line parameter error identification and estimation in three-phase networks," *IEEE Transactions on Power Systems*, vol. 37, no. 3, pp. 2271–2282, 2022.

[148] M. Cenký, J. Bendík, B. Cintula, P. Janiga, A. Beláň, and v. Eleschová, "Three-phase and single-phase measurement of overhead power line capacitance evaluation," *Electrical Engineering*, Jan. 2023.

[149] F. P. de Albuquerque, R. Nascimento, C. A. Prete, and E. Coelho Marques da Costa, "Phasor measurement unit-driven estimation of transmission line parameters using variable noise model," *Energies*, vol. 17, no. 14, 2024.

[150] R. S. Singh, S. Babaev, V. Cuk, S. Cobben, and H. van den Brom, "Line parameters estimation in presence of uncalibrated instrument transformers," in *2019 2nd International Colloquium on Smart Grid Metrology (SMAGRIMET)*, 2019, pp. 1–8.

[151] C. Roberts, C. M. Shand, K. Brady, E. M. Stewart, A. W. McMorran, and G. A. Taylor, "Improving distribution network model accuracy using impedance estimation from micro-synchrophasor data," in *2016 IEEE Power and Energy Society General Meeting (PESGM)*, 2016, pp. 1–5.

[152] P. A. Pegoraro, K. Brady, P. Castello, C. Muscas, and A. von Meier, "Compensation of systematic measurement errors in a pmu-based monitoring system for electric distribution grids," *IEEE Transactions on Instrumentation and Measurement*, vol. 68, no. 10, pp. 3871–3882, 2019.

[153] D. Ritzmann, P. S. Wright, W. Holderbaum, and B. Potter, "A method for accurate transmission line impedance parameter estimation," *IEEE Transactions on Instrumentation and Measurement*, vol. 65, no. 10, pp. 2204–2213, Oct. 2016.

[154] D. Ritzmann, "A Novel Approach to Noninvasive Measurement of Overhead Line Impedance Parameters," *IEEE Transactions on Instrumentation and Measurement*, vol. 66, no. 6, p. 9, Jun. 2017.

[155] M. Asprou and E. Kyriakides, "Identification and estimation of erroneous transmission line parameters using PMU measurements," *IEEE Transactions on Power Delivery*, vol. 32, no. 6, pp. 2510–2519, 2017.

[156] K. V. Khandeparkar, S. A. Soman, and G. Gajjar, "Detection and correction of systematic errors in instrument transformers along with line parameter estimation using PMU data," *IEEE Transactions on Power Systems*, vol. 32, no. 4, pp. 3089–3098, 2017.

[157] C. Wang, V. A. Centeno, K. D. Jones, and D. Yang, "Transmission lines positive sequence parameters estimation and instrument transformers calibration based on PMU measurement error model," *IEEE Access*, vol. 7, pp. 145 104–145 117, 2019.

[158] H. Zhang, Z. Diao, and Y. Cui, "Identification of power network branch parameters based on state space transformation," *IEEE Access*, vol. 7, pp. 91 720–91 730, 2019.

[159] A. Xue, H. Kong, Y. Lao, Q. Xu, Y. Lin, L. Wang, F. Xu, S. Leng, Z. Yuan, and G. Wei, "A new robust identification method for trans-

mission line parameters based on ADALINE and IGG method," *IEEE Access*, vol. 8, pp. 132 960–132 969, 2020.

[160] A. Xue, F. Xu, K. E. Martin, H. You, J. Xu, L. Wang, and G. Wei, "Robust identification method for transmission line parameters that considers PMU phase angle error," *IEEE Access*, vol. 8, pp. 86 962–86 971, 2020.

[161] H. Goklani, G. Gajjar, and S. Soman, "Instrument transformer calibration and robust estimation of transmission line parameters using pmu measurements," *IEEE Transactions on Power Systems*, vol. 36, no. 3, pp. 1761–1770, 2021.

[162] S. Vlahinić, D. Franković, M. Ž. Đurović, and N. Stojković, "Measurement uncertainty evaluation of transmission line parameters," *IEEE Transactions on Instrumentation and Measurement*, vol. 70, pp. 1–7, 2021.

[163] C. Sitzia, C. Muscas, P. A. Pegoraro, A. V. Solinas, and S. Sulis, "Enhanced PMU-based line parameters estimation and compensation of systematic measurement errors in power grids considering multiple operating conditions," *IEEE Transactions on Instrumentation and Measurement*, vol. 71, pp. 1–12, 2022.

[164] F. P. De Albuquerque, E. C. M. Da Costa, R. F. R. Pereira, L. H. B. Liboni, and M. C. De Oliveira, "Nonlinear analysis on transmission line parameters estimation from noisy phasorial measurements," *IEEE Access*, vol. 10, pp. 1720–1730, 2022.

[165] H. Haiyan, K. He, G. Lei, M. Jing, X. Feiyang, and X. Ancheng, "Steady-state PMU data selection for parameter identification of transmission line considering the influence of measurement error," *IET Gener. Transm. Distrib.*, vol. 16, pp. 4549–4562, 2022.

[166] D. Franković, S. Vlahinić, and M. Ž. Đurović, "Application of different least square methods for transmission line parameter estimation," in *2022 IEEE 12th International Workshop on Applied Measurements for Power Systems (AMPS)*. IEEE, 2022, pp. 1–5.

[167] A. C. Varghese, A. Pal, and G. Dasarathy, "Transmission line parameter estimation under non-gaussian measurement noise," *IEEE Transactions on Power Systems*, pp. 1–16, 2022.

[168] A. Abdolkhalig, "Innovative method to identify the impedance parameters of a three-phase electric power medium-size transmission line," *Electrical Engineering*, Mar. 2023.

[169] E. Saldanha, M. Pacheco, and A. P. Ferreira, "Estimation of transmission line parameters in modern power systems from phasor measurements," in *2024 Mediterranean Smart Cities Conference (MSCC)*, 2024, pp. 1–5.

[170] C. Borda, A. Olarte, and H. Diaz, "Pmu-based line and transformer parameter estimation," in *2009 IEEE/PES Power Systems Conference and Exposition*, 2009, pp. 1–8.

[171] A. S. Dobakhshari, M. Abdolmaleki, V. Terzija, and S. Azizi, "Online non-iterative estimation of transmission line and transformer parameters by scada data," *IEEE Transactions on Power Systems*, vol. 36, no. 3, pp. 2632–2641, 2020.

[172] M. R. Rezaei, S. R. Hadian-amrei, and M. R. Miveh, "Online identification of power transformer and transmission line parameters using synchronized voltage and current phasors," *Electric Power Systems Research*, vol. 203, Feb. 2022.

[173] E. Satsuk, A. Zhukov, D. Dubinin, I. Ivanov, and A. Murzin, "Analytical approach to phasor-based line parameter estimation verified through real PMU data," in *2022 International Conference on Smart Grid Synchronized Measurements and Analytics (SGSMA)*, 2022, pp. 1–6.

[174] H. Goklani, G. Gajjar, and S. Soman, "Instrument transformer calibration and robust estimation of transmission line parameters using pmu measurements," *IEEE Transactions on Power Systems*, vol. 36, no. 3, pp. 1761–1770, 2020.

[175] S. Park, D. Deka, S. Backhaus, and M. Chertkov, "Learning with end-users in distribution grids: Topology and parameter estimation," *IEEE Transactions on Control of Network Systems*, vol. 7, no. 3, pp. 1428–1440, 2020.

[176] J. Zhang, Y. Wang, Y. Weng, and N. Zhang, "Topology identification and line parameter estimation for non-pmu distribution network: A numerical method," *IEEE Transactions on Smart Grid*, vol. 11, no. 5, pp. 4440–4453, 2020.

[177] Z. Shi, Q. Xu, Y. Liu, C. Wu, and Y. Yang, "Line parameter, topology and phase estimation in three-phase distribution networks with non-μPMUs," *International Journal of Electrical Power & Energy Systems*, vol. 155, p. 109658, 2024.

[178] S. Mittal, P. Pareek, and A. Verma, "Distribution line parameters estimation framework with correlated injections using smart meter measurements," *Electric Power Systems Research*, vol. 228, p. 110083, 2024.

[179] R. Dutta, V. S. Patel, S. Chakrabarti, A. Sharma, R. K. Das, and S. Mondal, "Parameter estimation of distribution lines using scada measurements," *IEEE Transactions on Instrumentation and Measurement*, vol. 70, pp. 1–11, 2020.

[180] Y. Wang, W. Xu, and J. Shen, "Online tracking of transmission-line parameters using scada data," *IEEE Transactions on Power Delivery*, vol. 31, no. 2, pp. 674–682, 2015.

[181] Y. Guo, Y. Yuan, and Z. Wang, "Distribution grid modeling using smart meter data," *IEEE Transactions on Power Systems*, vol. 37, no. 3, pp. 1995–2004, 2021.

[182] W. Wang and N. Yu, "Parameter estimation in three-phase power distribution networks using smart meter data," in *2020 International Conference on Probabilistic Methods Applied to Power Systems (PMAPS)*. IEEE, 2020, pp. 1–6.

[183] L. Ding, T. Bi, and D. Zhang, "Transmission line parameters identification based on moving-window tls and pmu data," in *2011 international conference on advanced power system automation and protection*, vol. 3. IEEE, 2011, pp. 2187–2191.

[184] S. Azizi, M. Sanaye-Pasand, and M. Paolone, "Locating faults on untransposed, meshed transmission networks using a limited number of synchrophasor measurements," *IEEE Transactions on Power Systems*, vol. 31, no. 6, pp. 4462–4472, 2016.

[185] C. R. Paul, *Analysis of multiconductor transmission lines*. John Wiley & Sons, 2007.

[186] D. Shi, D. J. Tylavsky, N. Logic, and K. M. Koellner, "Identification of short transmission-line parameters from synchrophasor measurements," in *2008 40th North American Power Symposium*. IEEE, 2008, pp. 1–8.

[187] S. S. Mousavi-Seyedi, F. Aminifar, and S. Afsharnia, "Parameter estimation of multiterminal transmission lines using joint pmu and scada data," *IEEE Transactions on Power Delivery*, vol. 30, no. 3, pp. 1077–1085, 2014.

[188] A. K. Al-Othman, K. M. El-Naggar, and M. E. AlSharidah, "On-line estimation of transmission line parameters using synchronized measurements," *Electric Power Components and Systems*, vol. 44, no. 2, pp. 233–239, 2016.

[189] R. E. Wilson *et al.*, "Calculation of transmission line parameters from synchronized measurements," *Electric Machines & Power Systems*, vol. 27, no. 12, pp. 1269–1278, 1999.

[190] Y. Liao and M. Kezunovic, "Online optimal transmission line parameter estimation for relaying applications," *IEEE Transactions on Power Delivery*, vol. 24, no. 1, pp. 96–102, 2008.

[191] IEC, *IEC/IEEE International Standard- Power transformers - Part 21: Standard requirements, terminology, and test code for step-voltage regulators*, IEC Std 60076-21:2018(E) IEEE Std C57.15-2017, 2018.

[192] G. Korres, P. Katsikas, and G. Contaxis, "Transformer tap setting observability in state estimation," *IEEE Transactions on Power Systems*, vol. 19, no. 2, pp. 699–706, May 2004.

[193] S. G. Ghiocel, J. H. Chow, G. Stefopoulos, B. Fardanesh, D. Maragal, B. Blanchard, M. Razanousky, and D. B. Bertagnolli, "Phasor-measurement-based state estimation for synchrophasor data quality improvement and power transfer interface monitoring," *IEEE Transactions on Power Systems*, vol. 29, no. 2, pp. 881–888, 2014.

[194] R. C. Pires, L. Mili, and F. A. B. Lemos, "Constrained robust estimation of power system state variables and transformer tap positions under erroneous zero-injections," *IEEE Transactions on Power Systems*, vol. 29, no. 3, pp. 1144–1152, May 2014.

[195] E. R. Fernandes, S. G. Ghiocel, J. H. Chow, D. E. Ilse, D. D. Tran, Q. Zhang, D. B. Bertagnolli, X. Luo, G. Stefopoulos, B. Fardanesh, and R. Robertson, "Application of a phasor-only state estimator to a large power system using real PMU data," *IEEE Transactions on Power Systems*, vol. 32, no. 1, pp. 411–420, 2017.

[196] M. Rezaei, S. S. Mortazavi, M. Razaz, and M. S. Ghazizadeh, "The statistical interval estimation of the mean and the hypothesis testing of population proportions for transformer tap position estimation," *Electric Power Systems Research*, vol. 164, pp. 212–219, Nov 2018.

[197] J. M. Cano, M. R. R. Mojumdar, and G. Alonso Orcajo, "Reconciling tap-changing transformer models," *IEEE Transactions on Power Delivery*, vol. 34, no. 6, pp. 2266–2268, Dec. 2019.

[198] P. A. Pegoraro, C. Sitzia, A. V. Solinas, and S. Sulis, "Estimation of line parameters, tap changer ratios, and systematic measurement errors based on synchronized measurements and a general model of tap-changing transformers," *IEEE Open Journal of Instrumentation and Measurement*, vol. 1, pp. 1–11, 2022.

[199] B. Vicol, "On-line overhead transmission line and transformer parameters identification based on PMU measurements," in *2014 International Conference and Exposition on Electrical and Power Engineering (EPE)*, 2014, pp. 1045–1050.

[200] D. Deka, S. Backhaus, and M. Chertkov, "Structure learning in power distribution networks," *IEEE Transactions on Control of Network Systems*, vol. 5, no. 3, pp. 1061–1074, 2017.

[201] K. Karaarslan and E. M. Yegin, "Determination of transmission line parameters by utilizing synchrophasor measurements," *Journal of Engineering Research and Applied Science*, vol. 13, no. 1, pp. 2515–2520, 2024.

[202] L. Chen, J. Liu, Z. Pan, and Z. Zhang, "Static parameter estimation and testability analysis of distribution lines based on multi-source measurement information," *Frontiers in Energy Research*, vol. 11, Sept. 2023.

[203] G. H. Golub and C. F. Van Loan, "An analysis of the total least squares problem," *SIAM journal on numerical analysis*, vol. 17, no. 6, pp. 883–893, 1980.

[204] R. K. Gupta, F. Sossan, J. Y. Le Boudec, and M. Paolone, "Compound admittance matrix estimation of three-phase untransposed power distribution grids using synchrophasor measurements," *IEEE Transactions on Instrumentation and Measurement*, vol. 70, 2021.

[205] L. Hofmann, "Series expansions for line series impedances considering different specific resistances, magnetic permeabilities, and dielectric permittivities of conductors, air, and ground," *IEEE Transactions on Power Delivery*, vol. 18, no. 2, pp. 564–570, April 2003.

[206] H. Dommel, "Overhead line parameters from handbook formulas and computer programs," *IEEE Transactions on Power Apparatus and Systems*, vol. PAS-104, no. 2, pp. 366–372, Feb 1985.

[207] I. W. Slutsker, S. Mokhtari, and K. A. Clements, "Real time recursive parameter estimation in energy management systems," *IEEE Transactions on Power Systems*, vol. 11, no. 3, pp. 1393–1399, Aug 1996.

[208] Y. Wang and W. Xu, "Algorithms and field experiences for estimating transmission line parameters based on fault record data," *IET. Gener. Transm. Distrib*, vol. 9, no. 13, pp. 1773–1781, 2015.

[209] Y. Liao and M. Kezunovic, "Online optimal transmission line parameter estimation for relaying applications," *IEEE Transactions on Power Delivery*, vol. 24, no. 1, pp. 96–102, Jan 2009.

[210] S. Mousavi-Seyedi, F. Aminifar, and S. Afsharnia, "Parameter estimation of multiterminal transmission lines using joint PMU and SCADA data," *IEEE Transactions on Power Delivery*, vol. 30, no. 3, pp. 1077–1085, June 2015.

[211] M. Asprou and E. Kyriakides, "Identification and estimation of erroneous transmission line parameters using PMU measurements," *IEEE Transactions on Power Delivery*, vol. PP, no. 99, pp. 1–1, 2017.

[212] X. Bian, X. Li, H. Chen, D. Gan, and J. Qiu, "Joint estimation of state and parameter with synchrophasors part I: State tracking," *IEEE Transactions on Power Systems*, vol. 26, no. 3, pp. 1196–1208, Aug 2011.

[213] ——, "Joint estimation of state and parameter with synchrophasors part II: Parameter tracking," *IEEE Transactions on Power Systems*, vol. 26, no. 3, pp. 1209–1220, Aug 2011.

[214] S. Gajare, A. K. Pradhan, and V. Terzija, "A method for accurate parameter estimation of series compensated transmission lines using synchronized data," *IEEE Transactions on Power Systems*, vol. PP, no. 99, pp. 1–1, 2017.

[215] S. S. Mousavi-Seyedi, F. Aminifar, and S. Afsharnia, "Parameter estimation of multiterminal transmission lines using joint pmu and scada data," *IEEE Transactions on Power Delivery*, vol. 30, no. 3, pp. 1077–1085, June 2015.

[216] C. Li, Y. Zhang, H. Zhang, Q. Wu, and V. Terzija, "Measurement-based transmission line parameter estimation with adaptive data selection scheme," *IEEE Transactions on Smart Grid*, vol. PP, no. 99, pp. 1–1, 2017.

[217] C. Rakpenthai and S. Uatrongjit, "Power system state and transmission line conductor temperature estimation," *IEEE Transactions on Power Systems*, vol. 32, no. 3, pp. 1818–1827, May 2017.

[218] Y. Wang, W. Xu, and J. Shen, "Online tracking of transmission-line parameters using scada data," *IEEE Transactions on Power Delivery*, vol. 31, no. 2, pp. 674–682, April 2016.

[219] S. Kurokawa, J. Pissolato, M. Tavares, C. Portela, and A. Prado, "A new procedure to derive transmission-line parameters: applications and restrictions," *IEEE Transactions on Power Delivery*, vol. 21, no. 1, pp. 492–498, Jan 2006.

[220] C.-S. Chen, C.-W. Liu, and J.-A. Jiang, "A new adaptive PMU based protection scheme for transposed/untransposed parallel transmission lines," *IEEE Transactions on Power Delivery*, vol. 17, no. 2, pp. 395–404, Apr 2002.

[221] R. Schulze and P. Schegner, "Parameter identification of unsymmetrical transmission lines," in *Porc. IEEE Bucharest PowerTech Conf.*, June 2009, pp. 1–7.

[222] M. Kato, T. Hisakado, H. Takani, H. Umezaki, and K. Sekiguchi, "Live line measurement of untransposed three phase transmission line parameters for relay settings," in *Proc. IEEE Power Eng. Soc. Gen. Meet.*, July 2010, pp. 1–8.

[223] R. Schulze, P. Schegner, and R. Zivanovic, "Parameter identification of unsymmetrical transmission lines using fault records obtained from protective relays," *IEEE Transactions on Power Delivery*, vol. 26, no. 2, pp. 1265–1272, April 2011.

[224] D. Ritzmann, J. Rens, P. S. Wright, W. Holderbaum, and B. Potter, "A novel approach to noninvasive measurement of overhead line impedance parameters," *IEEE Transactions on Instrumentation and Measurement*, vol. PP, no. 99, pp. 1–9, 2017.

[225] P. Ren, H. Lev-Ari, and A. Abur, "Tracking three-phase untransposed transmission line parameters using synchronized measurements," *IEEE Transactions on Power Systems*, vol. 33, no. 4, pp. 4155–4163, 2018.

[226] Y. G. Kononov, O. S. Rybasova, and K. A. Sidirov, "Identification of overhead-line parameters from pmu data with compensation of systematic measurement errors," in *2018 International Conference on Industrial Engineering, Applications and Manufacturing (ICIEAM)*, Moscow, Russia, May 2018, pp. 1–5.

[227] P. A. Pegoraro, C. Sitzia, A. V. Solinas, and S. Sulis, "Transmission line parameters estimation in the presence of realistic PMU measurement error models," *Measurement*, vol. 218, p. 113175, 2023.

[228] A. M. Kettner and M. Paolone, "On the properties of the compound nodal admittance matrix of polyphase power systems," *IEEE Transactions on Power Systems*, vol. 34, no. 1, pp. 444–453, 2019.

[229] D. Turizo and D. K. Molzahn, "Invertibility conditions for the admittance matrices of balanced power systems," *IEEE Transactions on Power Systems*, pp. 1–12, 2022.

[230] K. Moffat, M. Bariya, and A. Von Meier, "Unsupervised impedance and topology estimation of distribution networks—limitations and tools," *IEEE Transactions on Smart Grid*, vol. 11, no. 1, pp. 846–856, 2020.

[231] O. Lateef, R. G. Harley, and T. G. Habetler, "Bus admittance matrix estimation using phasor measurements," in *2019 IEEE Power & Energy Society Innovative Smart Grid Technologies Conference (ISGT)*, 2019, pp. 1–5.

[232] Y. Yuan, S. H. Low, O. Ardakanian, and C. J. Tomlin, "Inverse power flow problem," *IEEE Transactions on Control of Network Systems*, pp. 1–12, 2022.

[233] E. Fabbiani, P. Nahata, G. De Nicolao, and G. Ferrari-Trecate, "Identification of AC distribution networks with recursive least squares and optimal design of experiment," *IEEE Transactions on Control Systems Technology*, vol. 30, no. 4, pp. 1750–1757, 2022.

[234] O. Ardakanian, V. W. S. Wong, R. Dobbe, S. H. Low, A. von Meier, C. J. Tomlin, and Y. Yuan, "On identification of distribution grids," *IEEE Transactions on Control of Network Systems*, vol. 6, no. 3, pp. 950–960, 2019.

[235] J.-S. Brouillon, E. Fabbiani, P. Nahata, F. Dörfler, and G. Ferrari-Trecate, "Bayesian methods for the identification of distribution networks," in *Proceedings of the IEEE Conference on Decision and Control*, 2021, pp. 3646–3651.

[236] J.-S. Brouillon, E. Fabbiani, P. Nahata, K. Moffat, F. Dörfler, and G. Ferrari-Trecate, "Bayesian error-in-variables models for the identification of distribution grids," *IEEE Transactions on Smart Grid*, pp. 1–1, 2022.

[237] G. Cavraro, A. Bernstein, V. Kekatos, and Y. Zhang, "Real-time identifiability of power distribution network topologies with limited monitoring," *IEEE Control Systems Letters*, vol. 4, no. 2, pp. 325–330, 2019.

[238] J. Yu, Y. Weng, and R. Rajagopal, "PaToPa: A data-driven parameter and topology joint estimation framework in distribution grids," *IEEE Transactions on Power Systems*, vol. 33, no. 4, pp. 4335–4347, 2018.

[239] M. Halihal and T. Routtenberg, "Estimation of the admittance matrix in power systems under laplacian and physical constraints," in *ICASSP 2022-2022 IEEE International Conference on Acoustics, Speech and Signal Processing (ICASSP)*. IEEE, 2022, pp. 5972–5976.

[240] A. Mingotti, L. Peretto, and R. Tinarelli, "Calibration procedure to test the effects of multiple influence quantities on low-power voltage transformers," *Sensors*, vol. 20, no. 4, 2020.

[241] ——, "Effects of multiple influence quantities on rogowski-coil-type current transformers," *IEEE Transactions on Instrumentation and Measurement*, vol. 69, no. 7, pp. 4827–4834, 2020.

[242] R. A. Jabr, "High-order approximate power flow solutions and circular arithmetic applications," *IEEE Transactions on Power Systems*, vol. 34, no. 6, pp. 5053–5062, 2019.

[243] A. Bernstein, C. Wang, E. Dall'Anese, J.-Y. Le Boudec, and C. Zhao, "Load flow in multiphase distribution networks: Existence, uniqueness,

non-singularity and linear models," *IEEE Transactions on Power Systems*, vol. 33, no. 6, pp. 5832–5843, 2018.
[244] K. Christakou, D.-C. Tomozei, J.-Y. Le Boudec, and M. Paolone, "Gecn: Primary voltage control for active distribution networks via real-time demand-response," *IEEE Transactions on Smart Grid*, vol. 5, no. 2, pp. 622–631, 2013.
[245] R. Gupta, F. Sossan, and M. Paolone, "Grid-aware distributed model predictive control of heterogeneous resources in a distribution network: Theory and experimental validation," *IEEE Transactions on Energy Conversion*, vol. 36, no. 2, pp. 1392–1402, 2020.
[246] H. Su, P. Li, X. Fu, L. Yu, and C. Wang, "Augmented sensitivity estimation based voltage control strategy of active distribution networks with pmu measurement," *IEEE Access*, vol. 7, pp. 44 987–44 997, 2019.
[247] K. Christakou, J.-Y. LeBoudec, M. Paolone, and D.-C. Tomozei, "Efficient computation of sensitivity coefficients of node voltages and line currents in unbalanced radial electrical distribution networks," *IEEE Transactions on Smart Grid*, vol. 4, no. 2, pp. 741–750, 2013.
[248] R. Gupta, S. Fahmy, and M. Paolone, "Coordinated day-ahead dispatch of multiple power distribution grids hosting stochastic resources: An admm-based framework," *Electric Power Systems Research*, vol. 212, p. 108555, 2022.
[249] S. Bolognani and S. Zampieri, "On the existence and linear approximation of the power flow solution in power distribution networks," *IEEE Transactions on Power Systems*, vol. 31, no. 1, pp. 163–172, 2015.
[250] F. Tamp and P. Ciufo, "A sensitivity analysis toolkit for the simplification of mv distribution network voltage management," *IEEE Transactions on Smart Grid*, vol. 5, no. 2, pp. 559–568, 2014.
[251] G. De Carne, M. Liserre, and C. Vournas, "On-line load sensitivity identification in lv distribution grids," *IEEE Transactions on Power Systems*, vol. 32, no. 2, pp. 1570–1571, 2016.
[252] P. Li, W. Wu, X. Wang, and B. Xu, "A data-driven linear optimal power flow model for distribution networks," *IEEE Transactions on Power Systems*, vol. 38, no. 1, pp. 956–959, 2022.
[253] W. F. Massy, "Principal components regression in exploratory statistical research," *Journal of the American Statistical Association*, vol. 60, no. 309, pp. 234–256, 1965.
[254] Y. Liu, N. Zhang, Y. Wang, J. Yang, and C. Kang, "Data-driven power flow linearization: A regression approach," *IEEE Transactions on Smart Grid*, vol. 10, no. 3, pp. 2569–2580, 2018.
[255] S. Nowak, Y. C. Chen, and L. Wang, "Measurement-based optimal der dispatch with a recursively estimated sensitivity model," *IEEE Transactions on Power Systems*, vol. 35, no. 6, pp. 4792–4802, 2020.
[256] Y. Tan, Y. Chen, Y. Li, and Y. Cao, "Linearizing power flow model: A hybrid physical model-driven and data-driven approach," *IEEE Transactions on Power Systems*, vol. 35, no. 3, pp. 2475–2478, 2020.
[257] G. Jain, S. Sidar, and D. Kiran, "Alternative regression approach for data-driven power flow linearization methods," in *2021 9th IEEE International Conference on Power Systems (ICPS)*. IEEE, 2021, pp. 1–6.
[258] R. Rosipal and N. Krämer, "Overview and recent advances in partial least squares," in *International Statistical and Optimization Perspectives Workshop" Subspace, Latent Structure and Feature Selection"*. Springer, 2005, pp. 34–51.
[259] H. Wold, "Path models with latent variables: The nipals approach," in *Quantitative sociology*. Elsevier, 1975, pp. 307–357.
[260] G. E. Box and G. C. Tiao, *Bayesian inference in statistical analysis*. John Wiley & Sons, 2011.
[261] J. Zhang, C. Chung, and L. Guan, "Noise effect and noise-assisted ensemble regression in power system online sensitivity identification," *IEEE Transactions on Industrial Informatics*, vol. 13, no. 5, pp. 2302–2310, 2017.
[262] J. Chen, W. Wu, and L. A. Roald, "Data-driven piecewise linearization for distribution three-phase stochastic power flow," *IEEE Transactions on Smart Grid*, vol. 13, no. 2, pp. 1035–1048, 2021.
[263] Y. Chen, C. Wu, and J. Qi, "Data-driven power flow method based on exact linear regression equations," *Journal of Modern Power Systems and Clean Energy*, vol. 10, no. 3, pp. 800–804, 2021.
[264] D. W. Marquardt and R. D. Snee, "Ridge regression in practice," *The American Statistician*, vol. 29, no. 1, pp. 3–20, 1975.
[265] J. Zhang, X. Zheng, Z. Wang, L. Guan, and C. Chung, "Power system sensitivity identification—inherent system properties and data quality," *IEEE Transactions on Power Systems*, vol. 32, no. 4, pp. 2756–2766, 2016.
[266] S. Weckx, R. D'Hulst, and J. Driesen, "Voltage sensitivity analysis of a laboratory distribution grid with incomplete data," *IEEE Transactions on Smart Grid*, vol. 6, no. 3, pp. 1271–1280, 2014.
[267] Y. Liu, Y. Wang, N. Zhang, D. Lu, and C. Kang, "A data-driven approach to linearize power flow equations considering measurement noise," *IEEE Transactions on Smart Grid*, vol. 11, no. 3, pp. 2576–2587, 2019.
[268] Y. C. Chen, A. D. Domínguez-García, and P. W. Sauer, "Measurement-based estimation of linear sensitivity distribution factors and applications," *IEEE Transactions on Power Systems*, vol. 29, no. 3, pp. 1372–1382, 2013.
[269] Y. C. Chen, J. Wang, A. D. Domínguez-García, and P. W. Sauer, "Measurement-based estimation of the power flow jacobian matrix," *IEEE Transactions on Smart Grid*, vol. 7, no. 5, pp. 2507–2515, 2015.
[270] E. L. da Silva, A. M. N. Lima, M. B. de Rossiter Corrêa, M. A. Vitorino, and L. T. Barbosa, "Data-driven sensitivity coefficients estimation for cooperative control of pv inverters," *IEEE Transactions on Power Delivery*, vol. 35, no. 1, pp. 278–287, 2019.
[271] R. Gupta, F. Sossan, and M. Paolone, "Model-less robust voltage control in active distribution networks using sensitivity coefficients estimated from measurements," *Electric Power Systems Research*, vol. 212, p. 108547, 2022.
[272] R. Gupta and M. Paolone, "Experimental validation of model-less robust voltage control using measurement-based estimated voltage sensitivity coefficients," in *2023 IEEE Belgrade PowerTech*, 2023, pp. 1–8.
[273] J. Chen, W. Li, W. Wu, T. Zhu, Z. Wang, and C. Zhao, "Robust data-driven linearization for distribution three-phase power flow," in *2020 IEEE 4th Conference on Energy Internet and Energy System Integration (EI2)*. IEEE, 2020, pp. 1527–1532.
[274] J. Yu, Y. Weng, and R. Rajagopal, "Robust mapping rule estimation for power flow analysis in distribution grids," in *2017 North American Power Symposium (NAPS)*. IEEE, 2017, pp. 1–6.

Rahul K. Gupta earned his M.Sc. and Ph.D. degrees in Electrical Engineering from the Swiss Federal Institute of Technology Lausanne (EPFL), Switzerland in 2018 and 2023, respectively. His doctoral research was awarded the EPFL PhD Thesis Distinction in Electrical Engineering in 2023. From Oct. 2023 to Dec. 2024, he was a postdoctoral scholar at the School of Electrical and Computer Engineering, Georgia Institute of Technology, Atlanta, USA, supported by a grant from the Swiss National Science Foundation (SNSF). Since 2025, he has been an Assistant Professor at the School of Electrical Engineering and Computer Science (EECS), Washington State University (WSU), Pullman, USA. His research focuses on the operation and planning of active distribution networks, addressing various kinds of uncertainties, measurement and model-less control schemes, power system parameter estimation, and synthetic network generation.

Paolo Attilio Pegoraro (M'06, SM'19) received the M.Sc. (*summa cum laude*) degree in telecommunication engineering and the Ph.D. degree in electronic and telecommunication engineering from the University of Padova, Padua, Italy, in 2001 and 2005, respectively. From 2015 to 2018 he was an Assistant Professor with the Department of Electrical and Electronic Engineering, University of Cagliari, Cagliari, Italy, where he is currently Associate Professor. He has authored or co-authored over 170 scientific papers. His current research interests include the design of new measurement techniques for modern power networks, with attention to synchronized measurements and state estimation. Dr. Pegoraro is a member of IEEE IMS TC 39 (Measurements in Power Systems) and of IEC TC 38/WG 47. He is also a member of IEEE EPPC WG on Energy. He is an Associate Editor in Chief of the IEEE Transactions on Instrumentation and Measurement and the General Chair of the IEEE International Workshop on Applied Measurements for Power Systems (AMPS).

Ognjen Stanojev (S'18) received the B.Sc. degree in Electrical and Computer Engineering with a major in power systems from the University of Novi Sad, Serbia, in 2017. He obtained the M.Sc. and Ph.D. degrees in Electrical Engineering and Information Technology in 2019 and 2024, respectively, from the Swiss Federal Institute of Technology, Zurich, Switzerland. He is currently working as a scientist in ABB Corporate Research Center in Switzerland. His research interests include control and optimization of converter-dominated power systems.

Ali Abur is currently a Professor in the Department of Electrical and Computer Engineering at Northeastern University, Boston. He obtained his B.S. degree from Orta Dogu Teknik Universitesi, Ankara, Turkey and his M.S. and Ph.D. degrees from The Ohio State University all in Electrical Engineering. After receiving his PhD degree, he joined Texas A&M University and worked a Professor in the Electrical Engineering Department until November 2005. Then, he was appointed as a Professor and Chair of the Electrical Computer Engineering Department at Northeastern University, Boston. His research and educational activities have been in the areas of electric power systems modeling, state estimation, detection and identification of errors in the network model and measurements, fault location and electromagnetic transients modeling and simulations. He completed close to 50 projects sponsored by Federal or State Agencies as well as energy industry. He was the Associate Editor for IEEE Transactions on Power Systems between 1999-2011 and also served as a guest editor for special issues. He organized and co-chaired 2011 North American Power Symposium held in Boston. He was elected a Fellow of the IEEE for his work on power system state estimation in 2003 and was the recipient of 2014 IEEE Power & Energy Society Outstanding Power Engineering Educator Award. He published the book "Power System State Estimation" with his co-author in 2004.

Carlo Muscas (M'98, SM'15) received the M.S. degree (cum laude) in electrical engineering from the University of Cagliari, Cagliari, Italy, in 1994. He was an Assistant Professor and an Associate Professor with the University of Cagliari from 1996 to 2001 and from 2001 to 2017, respectively, where he has been a Full Professor of electrical and electronic measurement since 2017. He has authored and coauthored more than 190 scientific papers. His current research interests include the measurement of synchronized phasors, the implementation of distributed measurement systems for a modern electric grid, and the study of power quality phenomena. Prof. Muscas is currently an Associate Editor of the IEEE Open Journal of Instrumentation and Measurement and the Chairman of the TC 39 Measurements in Power Systems of the IEEE Instrumentation and Measurement Society.

Gabriela Hug received the M.Sc. degree in information technology and electrical engineering in 2004 and the Ph.D. degree in electric power systems in 2008 from ETH Zurich. She also received the diploma in Higher Education Teaching in Electrical Engineering in 2007 from the same institution. After her PhD studies, she worked in the Special Studies Group of Hydro One in Toronto, Canada and from 2009 - 2015 she was Assistant Professor at Carnegie Mellon University in Pittsburgh, USA. Currently, she is Professor in the Power Systems Laboratory at ETH Zurich. Her research is dedicated to modeling, control and optimization of electric power systems.

Mario Paolone (M'07, SM'10, F'22) received his M.Sc. (Hons.) and Ph.D. degrees in electrical engineering from the University of Bologna, Italy, in 1998 and 2002, respectively. In 2005, he became an Assistant Professor in power systems at the University of Bologna, where he worked in the Power Systems Laboratory until 2011. Since 2011, he has been with the Swiss Federal Institute of Technology, Lausanne, Switzerland, where he is a Full Professor and the Chair of the Distributed Electrical Systems Laboratory. His research focuses on power systems, with particular emphasis on real-time monitoring, operational aspects, protection, dynamics, and transients. Dr. Paolone has made significant contributions in the field of PMU-based situational awareness for Active Distribution Networks (ADNs) and in developing exact, convex, and computationally efficient methods for the optimal planning and operation of ADNs. Dr. Paolone was the founding Editor-in-Chief of the Elsevier journal Sustainable Energy, Grids and Networks.